Institutional Repository - Research Portal
Dépôt Institutionnel - Portail de la Recherche
researchportal.unamur.be
University of Namur

THESIS / THÈSE

DOCTOR OF VETERINARY SCIENCES

Evaluation of shear wave elastography in assessing the biomechanical properties of the patellar tendon in an ovine model

KAYSER, Francoise

Award date:
2022

Awarding institution:
University of Namur

Link to publication

General rights
Copyright and moral rights for the publications made accessible in the public portal are retained by the authors and/or other copyright owners and it is a condition of accessing publications that users recognise and abide by the legal requirements associated with these rights.

- Users may download and print one copy of any publication from the public portal for the purpose of private study or research.
- You may not further distribute the material or use it for any profit-making activity or commercial gain
- You may freely distribute the URL identifying the publication in the public portal ?

Take down policy
If you believe that this document breaches copyright please contact us providing details, and we will remove access to the work immediately and investigate your claim.

Download date: 04. May. 2026

University of Namur
Faculty of Sciences
Department of Veterinary Medicine

Evaluation of shear wave elastography in assessing the biomechanical properties of the patellar tendon in an ovine model

A dissertation submitted by Françoise KAYSER
in partial fulfillment of the requirements
for the degree of PhD in Veterinary Sciences

March 2022

Supervisors:
Prof. Jean-Michel Vandeweerd
Prof. Bernardo Innocenti
Prof. Ivo Lambrichts
Prof. Peter Clegg

Jury:

Prof. Jean-Michel Vandeweerd, University of Namur, Namur, Belgium, secretary
Prof. Bernardo Innocenti, BEAMS Department- ULB-Ecole Polytechnique de Bruxelles, Belgium
Prof. Ivo Lambrichts, Hasselt University, Diepenbeek, Belgium
Prof. Peter Clegg, University of Liverpool, Liverpool, UK
Prof. Fanny Hontoir, University of Namur, Namur, Belgium
Prof. Charles Nicaise, University of Namur, Namur, Belgium
Prof. Yves Boutsen, CHU UCL NAMUR site Godinne, Yvoir, Belgium
Prof. Frédéric Lecouvet, Cliniques Universitaires St Luc, Brussels, Belgium

President of the jury:

Prof. Benoît Muylkens, University of Namur, Namur, Belgium, jury president

TABLE OF CONTENTS

LIST OF ABBREVIATIONS 9
LIST OF FIGURES AND TABLES 11
1.GENERAL INTRODUCTION 13
1.1. Tendon Structure 13
1.2. Tendon Diseases in Humans 16
Definitions 16
Epidemiology 16
Risk factors 17
Pathology 18
Diagnosis 20
Treatment 21
Healing 22
Conclusion 22
2.RESEARCH QUESTIONS 23
3. WHAT IS THE NORMAL ANATOMY OF THE OVINE KNEE (STIFLE) BY CONVENTIONAL ULTRASOUND? 25
3.1. Introduction 25
3.2. Material and Methods 26
Animals 26
Ultrasonography and Gross Anatomy 26
3.3. Results 27
Cranial Approach 30
Lateral Approach 38
Medial Approach 39
3.4. Discussion 39
4. HOW DOES THE STIFFNESS OF THE PATELLAR TENDON VARY IN A POPULATION OF HEALTHY RESEARCH SHEEP? 43
4.1. Introduction 43

4.2. Material and Methods 46
Animals 46
Gross Anatomy 46
Histopathology of Cartilage 48
Biomechanical Tests 50
Statistical Analysis 51
4.3. Results 51
Cartilage Histopathology 51
Tendon Stiffness 52
4.4. Discussion 53
Effect of Age 53
Effect of Weight 54
Conclusion 55
5. DOES SHEAR WAVE VELOCITY ASSESSED BY ELASTOGRAPHY CORRELATE WITH STIFFNESS GIVEN BY TENSILE TEST IN THE OVINE PATELLAR TENDON? 57
5.1. Introduction 57
Strain Elastography 58
Shear Wave Elastography 58
5.2. Material and Methods 62
Animals 62
Ultrasound Examination 63
2D Ultrasound 63
Color Doppler Ultrasound 63
Shear Wave Elastography 64
Gross Anatomy 65
Biomechanical Tests 66
Statistical Analysis 67
5.3. Results 68
5.4. Discussion 69
6. Conclusions-Discussion-Perspectives 73

Could we use the sheep as a model for patellar tendon disorders? 73
Could we use biomechanical tests in an ovine model of patellar tendinopathy? 75
How could we use SWV assessed by elastography as a surrogate of stiffness given by tensile test in an ovine model of patellar tendon tendinopathy? 77
7. REFERENCES 79
ACKNOWLEDGEMENTS 101
ADDENDUM: PUBLISHED and SUBMITTED PAPERS 103

ABSTRACT

Tendons connect bone to muscle and are responsible for transmitting muscle contractile forces to the skeleton and for generating joint motion. Tendon injuries are very common in the general population as well as in occupational and professional athletes. The healing process is slow and incomplete and the available treatment options are unsatisfactory. Tendon injuries are associated with abnormal joint movement, clinical signs of inflammation, pain, and disability. Tendinopathies and subsequent tendon ruptures present a major clinical and financial challenge. There is therefore a need to develop new treatment strategies and new imaging techniques to detect it at an early stage and to assess its progress overtime accurately.

The aim of this PhD thesis was to assess, in an ovine model, whether shear wave elastography (SWE) can be used to evaluate the biomechanical properties of the patellar tendon, a tendon that is commonly affected in man. Three different questions were asked.

Firstly, what is the normal anatomy of the knee (stifle) by conventional ultrasound? We compared gross anatomy images to ultrasound scans. This study identified the structures that are easily accessible by ultrasound, including the patellar tendon due to its superficial location. It provided reference ultrasound images of the ovine stifle that are relevant for musculoskeletal research and showed that the ovine US anatomy was rather similar to that in man.

Secondly, how does the stiffness, one of the most important biomechanical parameters in tendons, vary in the patellar tendon in a population of healthy research sheep? We performed *ex vivo* load-displacement tests and assessed whether the stiffness of the patellar tendon varied with age and weight. We also collected stiffness reference values for future research studies. Our tests confirmed that the patellar tendon had a typical non-linear behavior. There was a significant positive correlation between body weight and the histological scores reflecting degenerative changes of the stifle (OARSI score) ($r=0.51$; $p=0.002$), and between age and OARSI score ($r= 0.67$; $p<0.0001$). We found a positive but not significant correlation between stiffness and age ($r=0.22$, $p=0.27$), and a statistically significant positive correlation between body weight and tendon stiffness ($r=0.39$, $p=0.04$) and between OARSI scores and tendon stiffness ($r=0.47$, $p=0.02$). We concluded that the most appropriate sheep population for future studies would be young (1 to 6 years old), non-overweight adults.

Thirdly, as SWE, an ultrasound based noninvasive imaging technique, has not been used on the ovine patellar tendon, we answered the question whether SWE measures were a relevant surrogate of biomechanical properties of tendons? We measured the shear wave velocity (SWV) in living sheep and correlated the results to measures obtained by *ex vivo* biomechanical tests. We found a statistically not significant positive correlation between SWV and age. Our data showed a significant positive correlation ($r=0.87$; $p=0.02$) between stiffness and SWV. We concluded that, in future research studies, SWE could be a promising tool to evaluate the biomechanical properties of the tendons. The SWV values obtained in our study could be considered as reference values.

In conclusion, the current PhD thesis, provided useful data in the context of tendon research with an ovine model. SWE is a promising imaging technique that could be used more extensively in other species including man.

LIST OF ABBREVIATIONS

CDUS: Color Doppler Ultrasound
MRI: Magnetic Resonance Imaging
OA: Osteoarthritis
OARSI: OsteoArthritis Research Society International
ROI: Region of Interest
SE: Strain Elastography
SWE: Shear Wave Elastography
SWV: Shear Wave Velocity
US: Conventional Ultrasound

LIST OF FIGURES AND TABLES

Figure 1: Hierarchical structure of the tendon
Figure 2: Histological images of tendinosis
Figure 3: MRI image in a sagittal plane comparing human knee with ovine stifle
Figure 4: Description of the cranial approach (angle 95°) for US of the ovine stifle
Figure 5: Cranio-sagittal US scan (panoramic reconstruction) and corresponding gross anatomic section (angle 95°)
Figure 6: Description of the cranio-lateral approach (angle 95°)
Figure 7: Cranio-lateral sagittal and transverse US scans and corresponding gross anatomic sections (angle 95°)
Figure 8: Description of the cranial approach (angle 75°)
Figure 9: Cranio-transverse US scans and corresponding gross anatomic sections (angle 75°)
Figure 10: Cranio-sagittal US scans and corresponding gross anatomic section (angle 75°)
Figure 11: Description of the approach to scan synovial recesses (angle 95°)
Figure 12: Cranio-sagittal, cranio-transverse and latero-transverse US scans of synovial recesses (angle 95°)
Figure 13: Description of the lateral approach
Figure 14: Latero-coronal US scans and corresponding gross anatomic section (110°)
Figure 15: Load-displacement curve of a tendon during an uniaxial tensile test
Figure 16: Cartilage histology
Figure 17: Patella-patellar tendon-tibial tuberosity unit placed on a metal frame
Figure 18: Load-deformation test showing the stiffness curve
Figure 19: Correlation plot between age and stiffness and weight and stiffness
Figure 20: Functioning of SWE
Figure 21: Position of the sheep during SWE
Figure 22: SWE of the patellar tendon
Figure 23: Patella-patellar tendon-tibial tuberosity unit placed on a metal frame at two different time points during the test
Figure 24: Force-diplacement test relating the stiffness curve
Figure 25: Correlation plot between shear wave velocity (m/s) and stiffness (N/mm)
Table 1: Legend: US and gross anatomy
Table 2: Weight, histological scores and stiffness related to three different age groups

1.GENERAL INTRODUCTION

1.1. Tendon Structure

Tendons connect bone to muscle and are responsible for transmitting muscle contractile forces to the skeleton and generate joint motion (Benjamin et al., 2006). Tendons must be stiff and strong.

They are made of cells (tenoblasts and tenocytes) and extracellular matrix. Type I, II and III collagens represent most of the tendon collagen secreted into extracellular space, with type I collagen accounting for 70-80% of the tendons dry weight (Fratzl, 2003). Proteoglycans, the most abundant class of glycoprotein, account for 1 to 20% of the dry weight. Elastin accounts for less than 1%. Water constitutes 60 to 70% of the tendon complex (Kannus, 2000).

Tenocytes secrete procollagen, a precursor molecule, that is cleaved to form tropocollagen. Tropocollagen molecules form cross-links to create the typical triple helix collagen molecules formed of two strands of collagen α1 chain and one strand of collagen α2 chain, which aggregate progressively into microfibrils and then in collagen fibrils. The triple helical structure provides the elasticity to type I collagen (Franchi et al., 2010). The tendon has a typical hierarchical structure, as depicted in Figure 1.

The hierarchical nature of tendon and the electrostatic cross-linking of the proteoglycan-rich matrix contribute to the elastic nature of the tendon. The complex tendon superstructure contributes to the high mechanical load that tendons can support (Franchi et al., 2010). During various phases of movements, the tendons are exposed not only to longitudinal but also to transversal and rotational forces. Additionally, tendons must be prepared to withstand direct contusions and pressures. The three-dimensional internal structure of the fibers forms a buffer against external forces.

The collagen fibrils are arranged in bundles parallel to the long axis of the tendon. These bundles are buckled into an undulating pattern, called crimp, in relaxed tendons. Unbuckling of the crimped collagen bundles during longitudinal loading acts as a natural shock-absorber on initial loading (Diamant et al., 1972), stretched out under strain (Franchi et al. 2007) and is important in elastic recoil.

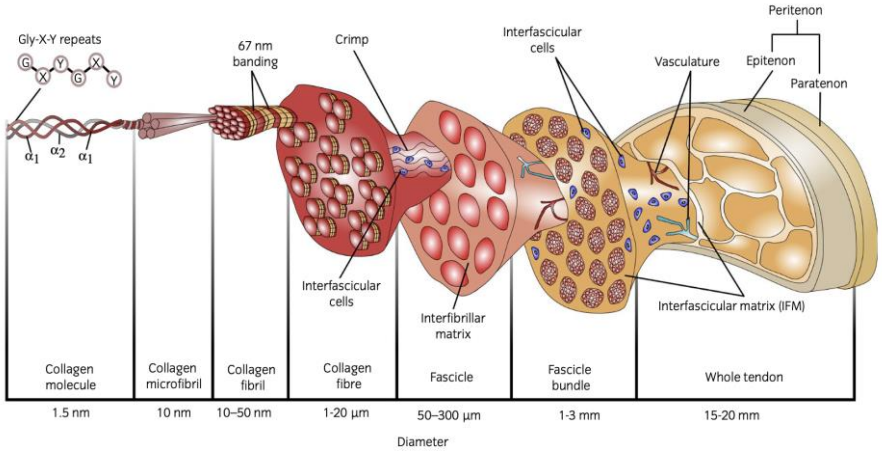


Figure 1: Hierarchical structure of the tendon. The typical triple helix collagen molecules aggregate together to form a microfibril. The microfibrils combine progressively into fibrils, the collagen fibrils are grouped into fibers. A bunch of collagen fibers forms a subfascicle, the subfascicles group together to form a fascicle and finally a group of fascicles makes up the tendon. The longitudinal fibers run parallel but also cross each other, forming spirals. Some of the individual fibrils and fibril groups form spiral-type plaits (reproduced from O'Brien et al., 2021, along with the relevant length scales).

The endotenon, a fine sheath of connective tissue, surrounds each collagen fiber, subfascicle and fascicle and binds the different fiber, subfascicle and fascicle bundles together. The endotenon has two roles: it helps the sliding of collagen fibrils, fibers and fascicles and provides a space for blood and lymphatic vessels and nerves (Schneider and Docheva, 2017; Docheva et al., 2015; Elliott, 1965). For example, in the superficial digital flexor tendon and the common digital extensor tendon in horses, interfascicular sliding provides high strain capacity (i.e., the maximum tensile strain that tendon can withstand before microtear or tear forming) (Thorpe et al., 2015).

The epitenon is in continuity with the endotenon and surrounds the tendon preventing adhesion to adjacent tissues. The epitenon contains the vascular, lymphatic, and nerve supplies of the tendon. Endotenon and epitenon prevent the separation of collagen fibers, subfascicles and fascicles under mechanical stress (Schneider and Docheva, 2017; Docheva et al., 2015). Some tendons, like the patellar tendon, present a paratenon, a structure of connective tissue, which covers the epitenon (Kvist et al., 1985) and reduces frictions between the tendon and nearby tissues (Schneider and Docheva, 2017; Docheva et al., 2015). Lubricin, a type of glycoprotein, located between tendon and paratenon, enables tendon sliding.

Tendons have a low blood supply compared to muscles, and a lower regenerative capacity. Tendons have 3 main streams to receive blood. There are two intrinsic systems, at the osteotendinous and myotendinous junction, and one extrinsic system, between the paratenon and the synovial sheath (Carr and Norris, 1989; Kvist and al.,

1995). The ratio between intrinsic and extrinsic systems varies among tendons. In particular, the patellar tendon is supplied by three arteries and by the anastomotic arch from the Hoffa fat pad (Pang et al., 2009).

The vascularization tends to decrease with the increase of mechanical load and age (Aström, 2000). A study performed in the tendon of the superficial digital flexor muscle in immature postnatal sheep demonstrated an important decline in vessel density (Meller et al. 2009). In tendinopathy, neovascularization, as shown by Color Doppler-ultrasound, is commonly encountered (Ohberg et al. 2001; Zanetti et al., 2003). Eccentric loading, a conservative treatment of tendinopathy, reduces neovascularization and improves recovery (Ohberg and Alfredson, 2004). Hence the exact role of neovascularization is not yet clear, but a balanced angiogenic response seems necessary in tendon healing.

Tendons contain lymphatic vessels. They play an important role in tissue repair mechanisms and proliferate during inflammation. Achilles tendons in rats are void of lymphatic vessels but they start to grow into the tendon repair tissue after injury (Tempfer et al., 2015). However, more investigations are needed to clarify the role of the lymphatic vessels.

Tendon innervation has different origins, from cutaneous, muscular and peritendinous nerve trunks. The nerve fibers form plexuses in the paratenon, from which branches penetrate the epitenon. However, most nerve fibers do not enter the main tendon body but terminate as nerve endings on the tendon's surface. At the myotendinous junction, nerve fibers cross and enter the endotenon septa. There are myelinated fibers with a mechanical-receptor function, detecting pressure and tension changes, and unmyelinated fibers, with nociceptors, detecting and transmitting pain (Lephart et al., 1997; Fitzgerald, 1992).

Tendons represent a connective tissue with high resistance to tensile loading. Previous studies showed that during daily activities the maximal patellar tendon force can range from 2.5 to 6 times the body weight (Kuster et al., 1997; Collins, 1995). It is a very organized tissue, designed to sustain biomechanical loads. However, its capacities are not unlimited and injuries can occur.

1.2. Tendon Diseases in Humans

Definitions

Tendinopathies are subdivided in three groups i.e., tendinitis, tendinosis and tenosynovitis. Any painful acute or chronic tendon impairment associated with inflammation has been originally identified as tendinitis (Landis et al., 1977). In contrast, tendinosis describes preferentially chronic degenerative conditions of the tendon due to an accumulation of micro-trauma (i.e., small tears) over time, mostly without inflammation, induced by physiological but stressful and repetitious activities, such as lifting or jumping. Tendinosis represents the most frequent pathological disorder affecting tendons (Landis et al., 1977). Tenosynovitis, also called paratendinitis or peritendinitis, refers to inflammation of a tendon sheath, often in combination with tendinosis (Ray et al., 2021). The inflammation causes swelling of the synovial sheath associated to hypervascularisation of the tendon sheath and fibrous exudate. These entities can cause tendon compression of the tendon, impeding its movement. Classically tenosynovitis is not associated to tendon degeneration.

In clinical practice, it is impossible to distinguish between these three different pathologies and therefore the general term "tendinopathy" is proposed to designate these three painful tendon conditions. In order to have a more accurate diagnosis, ultrasound (US) or magnetic resonance imaging (MRI) is required.

Spontaneous tendon tears and ruptures without any prior symptoms are called tendon injuries.

Epidemiology

Tendon disorders are common among the general population as well as in occupational or professional athletes during sports activities. They often occur in the context of sport activities, but may be due sometimes to simple daily activities in non-athletes. Tendon disorders represent approximately 50% of all sports injuries (Maffulli et al., 2003; Andarawis-Puri et al., 2015). In professional athletes, the incidence of tendon disorders is the highest in basketball, followed by roller hockey and futsal, the most commonly affected tendons being the patellar and Achilles tendons (Florit et al., 2019). The patellar tendon, also known as patellar ligament, the Achilles tendon, and the rotator cuff tendons (supraspinatus, infraspinatus) are often involved (Abat et al., 2017). Tendon disorders are usually associated with abnormal joint movement, clinical signs of inflammation and significant pain (Paavola et al., 2002). Disability may last for several months and even years despite treatment (Almekinders and Almekinders, 1994).

An observational registry-based study performed in a danish general practice population, extracting data from the electronic patient files (n=8836) from 2016, showed an annual incidence rate of tendinopathy of 7.9 per 1000 registered patients. They considered a diagnosis of tendinopathy in patients consulting with lower-extremity tendinopathy i.e., plantar heel pain; Achilles tendinopathy; patellar

tendinopathy; greater trochanteric pain syndrome or adductor tendinopathy (Riel et al., 2019).

Rotator cuff tendinopathies are present in around 30% of the general population, being the most common form of shoulder pain (Abat et al., 2017). A systemic review in children (under the age of 18 years) showed a prevalence of 8.2 to 33.3% for lower limb tendinopathies (Simpson et al., 2016). A retrospective study performed by Varlot and Martinot in a population of children presenting with pain in the anterior aspect of the knee and/or posterior aspect of the ankle, showed that 69.4% had at least one tendinopathy (Varlot and Martinot, 2020). More precisely, they found 66.4% of patellar tendinopathies (41.2% of which were associated with an apophysosis (Osgood Schlatter and/or Sinding Larsen)), and 70.3% of calcaneal tendinopathies (62.5% of which were associated with Sever's disease).

Tendinosis affects millions of people, in occupational athletes and professional athletes (Järvinen et al., 2001; Maffulli et al., 2003). Around 30% of all runners exhibit Achilles tendinopathy, with an annual incidence of 7% to 9% (Ackermann and Renström, 2012). Athletes, people over 40, as well as people with certain medical conditions such as tendonitis have a much greater probability of developing a tendon injury (Health Information-Mayo Clinic, 2010). However, tendinopathy may be related to age, without relation to any overuse activity. This age-related tendinopathy may be due to atrophic changes in response to the lack of tensile load, leading to degenerative lesions in the tendon (Almekinders et al., 2002; Almekinders et al., 2003).

Acute injuries like spontaneous rupture of tendons are common especially in rotator cuff tendons and Achilles tendon (Kannus and Natri, 1997). A rotator cuff tear, where the tendon detaches from the humerus bone in the shoulder, occurs with a frequency of about 4 people per 100,000 individuals (Doschanck and Zernicke, 2005). Similarly, Achilles tendon injury occurs in 12-18 per 100,000 individuals (Doschanck and Zernicke, 2005). Patellar tendon tears are relatively uncommon occurring in only about 0.7 per 100,000 individuals (Doschanck and Zernicke, 2005). Patellar tendon presents a high incidence of injuries, such as “jumper’s knee” in athletes (Zhang et al., 2015; Zhang et al., 2014).

Risk factors

A wide range of potential risk factors have been described, subdivided in mechanical overuse, intrinsic factors and extrinsic factors.

Mechanical overuse is exacerbated by muscle imbalance, malalignment of bones, or training errors (Dean et al., 2017; Sharma et Maffulli, 2008; Benjamin et al., 2008). Overuse and increased training may result in increased tendon thickness, stiffness, changes in histological architecture and eventually in inflammatory lesions and degeneration (American College of Sports Medicine, 2009; Lieber et al., 2017; Galloway et al., 2013).

Intrinsic risk factors include increased age (>30 years), female gender, heavy body weight, genetic predisposition, hormonal background (menopause), pre-existing disorders (diabetes mellitus, obesity, adiposity, hyperlipidemia, hypercholesterolemia and chronic gout arthritis) and prior tendon injuries (Leblanc et al., 2017; Kjaer et al., 2006; Kjaer et al., 2009).

Extrinsic risk factors include sustained sporting activity, pharmacological agents (fluoroquinolone and quinolone antibiotics, corticosteroids, aromatase inhibitors and statins), environmental factors like cold weather, unsuitable footwear and equipment, and unhealthy lifestyle habits i.e., smoking, alcohol consumption, low activity level, poor nutritional habits (leading to obesity, hyperlipidemia, hypercholesterolemia, diabetes mellitus) (Hess, 2010; Knobloch, 2016; Van der Linden et al., 2002). Those factors increase the risk of microtrauma (Shearn et al., 2011; Cook and Purdam, 2009). Another extrinsic factor known for the patellar tendon rupture (Delee and Craviotto, 1991; Marumoto et al., 1996; Miller et al., 1999) is the surgical injury due to bone-patellar tendon-bone graft harvesting for anterior cruciate ligament reconstruction (Francis et al., 2001).

The main biomechanical function of the patella is to improve the quadriceps efficiency by increasing the lever arm of the extensor mechanism. Patellar tendonitis happens when pushing knee tendon tissues too far, or too fast, repetitively. Thus, repeated jumping, sprinting and abrupt movements at fast speeds stress and strain the patellar tendon tissues. A term frequently used for patellar tendinopathy is Jumper's knee. The most risky types of sport are volleyball, basketball, football, running, dance, high and long jump, gymnastics and figure skating. This injury happens slowly over a long time, lots of minor strains and tiny tears making the tendon tissues weak and sore. Sudden, sizeable increase in activity, returning to play at full strength after a break instead of slowly getting back into a regular routine may initiate acute injuries as partial or complete tendon tear.

Pathology

Several terms are used to define tendon damage: tendinitis, tendinosis, tendinopathy. Apart from acute condition with peritendinitis, it is very rare to find evidence of microscopic inflammatory character in tendon lesions. The term tendinitis is therefore most often misused, and should be preferred to tendinopathy. The term tendinosis is reserved for degenerative lesions of the tendon body. Different histologic images are shown in figure 2.

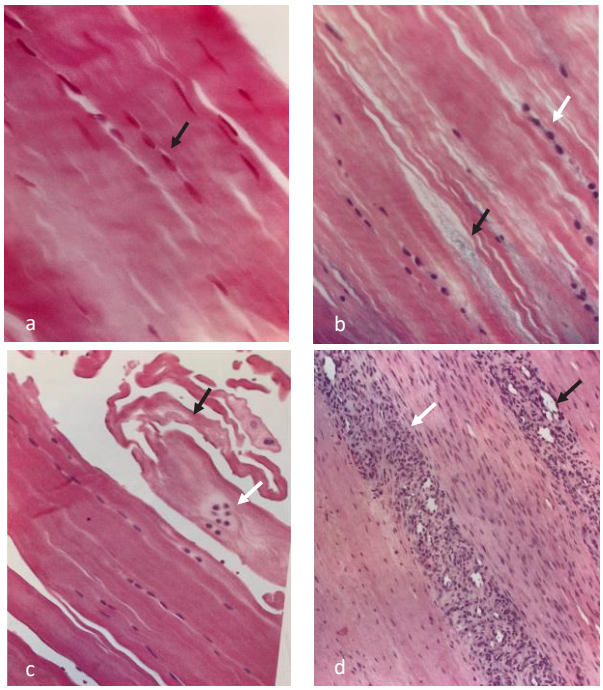


Figure 2: Histological images of tendinosis. (a) early tendinosis: the tenocytes in the central part of the image present a rounder shape (black arrow). (b): increased amount of proteoglycans separating collagen fibers (black arrow). Rounded tenocytes run between the collagen fibers (white arrow). (c): tenocytes with a chondroid appearance (white arrow) lie within collagen that exhibits fibrinoid degeneration with fragmentation (black arrow). (d): clusters of capillaries (black arrow) extend between the collagen fibers. Fibroblastic proliferation oriented parallel to the collagen bundles is shown (white arrow) (reproduced from Atlas of NonTumor Pathology-Non-Neoplastic Diseases of Bones and Joints, American Registry of Pathology, Armed Forces Institute of Pathology, 2011).

Cook referred to tendon pathology as a continuum (Cook and Purdam, 2009). The first phase of this continuum is a **reactive tendon** or **reactive tendinopathy** and is equivalent to a non-inflammatory proliferative cell response in the cell matrix resulting from a compressive or tensile overload. The cells change their shape and have more cytoplasmic organelles for increased protein production (collagen and proteogycans). Although some elongation/separation of collagen fiber bundles has been shown, the collagen integrity is usually maintained. The tendon thickens to reduce stress and increases its stiffness. On imaging, the tendon is thickened and swollen. This phase corresponds to a relatively short-term adaptation and can occur after sudden increased stress or direct impact to the tendon. This stage is reversible.

The second phase of the continuum is the **tendon disrepair**. This is due to the progression of the reactive tendinopathy occurring if the tendon is not offloaded and therefore not allowed to regress back to the normal state. The increased protein production (collagen and proteoglycans) continues, resulting in a separation of the collagen fibers and disorganisation within the cell matrix. There may be increased vascularity and neural ingrowth within the tendon. The most accurate method for diagnosis is imaging (US and MRI). This phase of tendinopathy may develop by frequent overloading of the tendon. It progresses much more quickly in the older stiffer tendon as there is less flexibility and adaptivity readily available in the tissues.

The third phase of the continuum is the **degenerative tendinopathy** suggesting a poor prognosis for healing and an irreversible stage. A general disorganisation of the cell matrix and areas of cell death are observed. By US and MRI areas of degeneration can be identified scattered throughout the tendon, interspersed with parts of the tendon that are in the disrepair phase and normal sections of tendon. Clinically the tendon can be thickened and present with nodular sections on palpations. This phase may be encountered in the older individual who has had ongoing tendinopathy as well as in the younger individual who has continued to overload the tendon.

Diagnosis

To date, there is no reliable method for detecting early tendinopathy. Tendons have mainly been evaluated clinically, by conventional US, Color Doppler-Ultrasound (CDUS) and MRI. The clinical examination is unable to distinguish among the different entities included under the term tendinopathy. Partial or even complete tendon tears may be misdiagnosed. US presents many advantages that are its low-cost, easy accessibility, repeatability, rapidity, X-Ray absence and dynamic examination possibility. The superficial location of tendons makes US a suitable tool for analysis. Morphological characteristics in tendon as echogenicity, homogeneity or thickness are well described by US (Davies et al., 1991). Tendon thickening, hypoechogenic areas and a loss of homogeneity are signs of tendinopathy. Neovascularization in chronic tendinopathies is documented by CDUS (Weinberg et al., 1998). MRI shows tendon thickening and an increased signal in T1 and T2 sequences. MRI may also show abnormalities in adjacent tissues. Inconveniently neither US and CDUS nor MRI provide mechanical properties of tendons, whereas biomechanical properties are the most reliable data to evaluate tendon recovery. Initially, the assessment of the mechanical properties through calculation was made using US and MRI combined to dynamometry (Hansen et al., 2006; Onambele et al., 2007; Seynnes et al., 2009; Svensson et al., 2012). Ultrasound elastography, a more recent non-invasive technique, allows the investigation of the mechanical properties of tendons requiring a manually (strain elastography) (Berko et al., 2015; Porta et al., 2014) or mechanically (transient elastography) applied force. Moreover, external compression, especially when made manually without any pressure determination device, may alter mechanical properties of the testing structure (Kot et al., 2012) and may impair reproducibility (Bercoff et al., 2004). Shear wave elastography (SWE) represents one of the transient elastography techniques. Developed almost three decades ago (Ophir et al., 1991), SWE has been used to directly determine patellar tendon elasticity in vivo since 2012 (Kot et al., 2012). Its real-time imaging can

estimate in vivo tissue strain distribution. Early diagnosis of tendon changes seen on US and biomechanical properties seen on elastography, in particular SWE, may improve the management of ongoing tendon injuries and thus prevent tendon degeneration.

Treatment

To date, none of the therapeutic options is satisfactory and repaired tendons do not regain their initial complete functionality and strength (Frankewycz et al., 2018).

Treatment may be conservative or non-conservative i.e., operative. The conservative treatment consists in activity modification, relative rest, oral Non-Steroidal Anti-Inflammatory Drugs (NSAID), corticosteroid injections and cryotherapy (Riley, 2008; Chimenti et al., 2017). However, the use of NSAID or corticosteroids for pain relief and inflammatory suppression, in the form of local or systemic drug delivery, is controversial due to a high risk of spontaneous tendon ruptures. Traditional physiotherapy combined to myofascial therapy, ultrasound, iono-and phonophoresis and acupuncture showed clinically good results (Riley, 2008; Chimenti et al., 2017). Conservative strategies include ultrasound treatment and shock wave therapy, eccentric exercises and low-intensity laser treatment (Chimenti et al., 2017). Even if promising, platelet rich plasma (PRP) still lacks consistent results. The autologous tenocyte implantation (Ortho-ATI) (Chen et al., 2007) seems a strong cell-based strategy for the treatment of chronic degenerative tendon disease. For this treatment the patient's tenocytes are extracted via a biopsy from his own healthy patellar tendon, expanded and delivered to the diseased tendon site through US guided injection under local anesthesia in order to stimulate tendon regeneration (Wang et al., 2015; Wang et al., 2013). Unfortunately, conservative treatment is less successful in degenerative tendinopathy and end stage tendon rupture; only 60% of the rehabilitated tendons are functional. Depending on the anatomic location of the tendinopathy, 10%–30% of patients need to be treated by surgery after conservative therapy failure (Aicale et al., 2018).

Tendon tissue engineering, based on the application of stem cells injected directly into the site of the tendon lesion or on the delivery of cells seeded on a carrier, such as hydrogel or dense matrix in order to accelerate the restorative process, is a new strategy being experimentally and pre-clinically explored (Kaux et al., 2015; Ma et al., 2019; Hsiao et al., 2019; Qiu et al., 2011). Up to date, there is little to no evidence of therapeutic effectiveness especially in the long term in most cases. Eventually, in order to offer a tailored treatment strategy, factors such as age and comorbidities must be considered.

A literature review from Steinmann et al. revealed that tendinopathy management is still restricted to symptomatic therapy despite significant progress in tendon research. Due to the incomplete understanding of underlying molecular and cellular mechanisms and risk factors, tendon-specific treatment options are yet unavailable (Steinmann et al., 2020).

Treatment is not satisfactory also because healing is difficult.

Healing

The oxygen consumption of tendons is 7.5 times lower than that of skeletal muscles (Vailas et al., 1978). Anaerobic energy-production capacity is essential for carrying loads as for maintaining tension during long periods, allowing to reduce the risk of ischemia and subsequent necrosis. However, due to the limited blood supply and a low metabolic rate (Williams, 1986; Fenwick et al., 2002; Kannus and Natri, 1997), tendon healing is prolonged and may result in the formation of a dysfunctional scar and tissue defect. Based on previous animal studies, tendon healing may be subdivided into 3 overlapping phases: the inflammatory phase, the repairing phase and the remodeling phase. After injury, the inflammatory phase lasts about 24 hours, followed by the repairing phase, which may last from a few days to 6 weeks after injury. Finally, during the remodeling phase, the repaired tissue changes to fibrous tissue, which again changes to scar-like tendon tissue after 10 weeks. During the later remodeling phase, covalent binding between collagen fibers increases, which results in higher stiffness and tensile strength of the repaired tissue (Wang, 2006). During tendon healing, altered collagen content, crosslinking, and alignment may also increase tissue stiffness.

Animal studies demonstrated that disuse of a limb or injury to the tendon alter the mechanical properties of tendons. This may be due to the reduction of the total area of collagen fibrils in the tendon cross-section and an increase in the numbers of thin and immature fibrils (Linder et al., 1994; Yasuda and Hayashi, 1999).

The ultimate outcome of tendon healing is the recovery of biomechanical properties. Tendon stiffness and Young's modulus are the most common parameters describing the biomechanical properties of a tendon under loading conditions, often highly correlated with the tensile failure load and strength of the tissue (Muraoka et al., 2005). Several studies suggested that the tendon mechanical properties provide an indication of the functional properties of a tendon as well as the recovery level of the internal tissue material (Atkinson et al., 1998; Kasperczyk et al., 1991; Kasperczyk et al., 1993).

Conclusion

Tendon disorders are common. They are difficult to treat or manage. Obviously early detection of structural changes and better diagnosis of biomechanical properties would help in improving management strategies.

2.RESEARCH QUESTIONS

Knowing that tendon disease is very frequent and slow to heal, and in the absence of effective treatment options and inadequate healing monitoring techniques, the aim of this PhD thesis was to improve knowledge in diagnostic imaging of biomechanical properties of the patellar tendon in the sheep, the most commonly used large animal species for research in musculo-skeletal diseases.

We focused on the patellar tendon for its ease of access due to its superficial location. Using the patellar tendon tear as a basic model for all tendon injuries and natural healing is an established academic practice. Many experimental surgical techniques developed for tendon injury repair have been studied in the patellar tendon (Doschank and Zernicke, 2005). The patellar tendon, being part of the knee extensor mechanism, transmits the quadriceps force to the tibia to generate knee extension. It is of fundamental importance in gait, orthostatism and joint stability. Due to its fundamental function for walking, running and standing in upright position, the mechanical properties of the patellar tendon have been extensively studied in man (Couppé et al., 2013; Grosset et al., 2014; Kot et al., 2012; Pearson et al., 2007; Zhang et al., 2015).

There are several advantages in using a sheep model to assess new imaging modalities. First, the knee of the sheep (also called stifle) is very similar to that in man (Doschanck and Zernicke, 2005) (Figure 3). The ovine knee sustains throughout the entire gait cycle similar strains than those imposed upon the human knee (Shearn et al., 2011). Shearn et al. showed that the morphology and physiology, bone geometry and soft tissue mechanics, are similar enough to produce stress-strain curves similar in sheep and man. Moreover, the stress-strain curves of the forces applied during walking to the stifle have a similar shape in sheep and man (Shearn et al., 2011). One of the advantages of the sheep over other large animal models is the humanlike size of joints such as the knee (Little and Smith, 2008). The anatomy of the ovine stifle has been well characterized (Proffen et al., 2012). CT and MRI anatomy of the stifle have been described (Vandeweerd et al., 2012; Vandeweerd et al., 2013a).

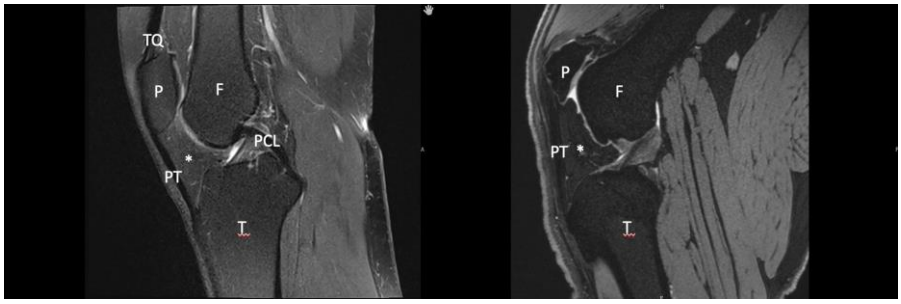


Figure 3: MRI image in a sagittal plane comparing human knee with ovine stifle. The human knee (left) is quite similar to the ovine stifle (right). Femur (F); tibia (T); patella (P); patellar tendon (PT); tendon of quadriceps muscle (TQ); infrapatellar fat pad (*).

More precisely, three research questions were answered.

Firstly, what is the normal anatomy of the knee (stifle) by conventional ultrasound? Secondly, how does the stiffness, one of the most important biomechanical parameters in tendons, vary in the patellar tendon in a population of healthy research sheep? Thirdly, as SWE has not been used on the ovine patellar tendon, we questioned whether SWE measures were a relevant surrogate of biomechanical properties of tendons?

3. WHAT IS THE NORMAL ANATOMY OF THE OVINE KNEE (STIFLE) BY CONVENTIONAL ULTRASOUND?

Adapted from

Kayser F, Hontoir F, Clegg P, Kirschvink N, Dugdale A, Vandeweerd JM. 2019. Ultrasound anatomy of the normal stifle in the sheep. Published in Anatomia Histologia Embryologia. Anat Histol Embryol. 2019; 00:1–10. doi :10.1111/ahe.12414

3.1. Introduction

Skeletally mature sheep are commonly used as large animal models in musculoskeletal research. The ovine stifle has often been the joint of choice to evaluate surgical and medical therapeutics for osteoarthritis (OA) (Aigner et al., 2010; Appleyard et al., 1999; Ghosh et al., 1991; Little et al., 1997; Oakley et al., 2004), meniscal injuries (Chevrier et al., 2009; Kohn et al., 1997; McNickle et al., 2009), cruciate ligaments (Amis et al., 1992; Hunt et al., 2005) and collateral ligaments (Allen et al., 1998). Knowledge of the anatomy of the joint is useful to plan surgical access and to assess the progress of the disease in research studies.

The anatomy of the ovine stifle has been described using radiography (Allen et al., 1998), computed tomography (Vandeweerd et al., 2012) and MRI (Vandeweerd et al., 2013a). US is another useful imaging modality that is time- and cost-effective, non-invasive and dynamic (Alves et al., 2016; Bianchi et al., 2002). Moreover, US is a useful tool for guiding injections and monitoring treatment effectiveness (Alves et al., 2016; Craig, 1999; Oo and Bo, 2016). High-frequency US is considered as an excellent modality to image normal ligaments, tendons, muscles and peripheral nerves as well as to diagnose a wide variety of pathological conditions affecting these structures. The US anatomy of the stifle has been described in horses (Hoegaerts et al., 2005) and cattle (Kofler, 1999). However, it has not been described so far in the sheep. US reference images are lacking and would be useful in research studies.

One objective of the current PhD thesis was to describe the US anatomy of the ovine stifle and provide reference images that would be useful for veterinarians and researchers.

3.2. Material and Methods

Animals

The hindlimbs of nine Île-de-France ewes (n = 18), euthanized for reasons other than musculoskeletal diseases (mastitis), were disarticulated at the coxofemoral joint and collected within 12 hours of death. Sheep were 6–8 years old, weighed 50–85 kg and came from the Sheep Centre of the University of Namur. The experimental protocol (KI 10/148) was approved by the local ethical committee for animal welfare. Limb specimens were moistened, wrapped in gauze, sealed in plastic bags and stored at −20°C. Each limb was identified by a number. For all investigations, limbs were thawed to room temperature, clipped and cleaned.

Ultrasonography and Gross Anatomy

Four pairs of limbs (n = 8) were scanned using an ultrasound iU22 machine (Philips, Eindhoven). Acoustic gel was used to improve transmission of US. Relevant scans were identified for optimal visualization of anatomical structures of clinical interest: articular surfaces and margins, ligaments, articular capsule, synovial cavity, menisci and their attachments, and tendons. A 17–5 MHz linear transducer was used for all structures except for the cruciate ligaments that were scanned with a 5–1 MHz convex transducer. After scanning, all limbs were dissected, and relevant anatomical structures were identified.

In addition, four other pairs of limbs (n = 8) were frozen in the positions that had been used for scanning. Then, the stifle joints were cut into 3-mm slab sections in sagittal, parasagittal, coronal, transverse and oblique planes. Each gross section was photographed and compared to the corresponding US images for identification of anatomical structures.

One other pair of fresh limbs (n = 2) was used to visualize synovial compartments. Twenty milliliters of water were injected into the femoro-tibial joint with a paraligamentous technique (Vandeweerd et al., 2012). A 21 G 38 mm (11/2 in.) needle was inserted along the lateral aspect of the patellar tendon at mid-distance between its distal and proximal insertions. Immediately after injection, the joint was flexed and extended 30 times.

3.3. Results

Four approaches were tested to image the stifle by US: cranial, medial, lateral and caudal. Cranial scans were made with the tibia and femur forming an angle of 95°. An angle of 75° was used to better visualize cruciate ligaments. Medial and lateral scans were obtained with the tibia and femur forming an angle of 95° and of 110° to better straighten collateral ligaments.

We described the US scans obtained with each approach in the sagittal, transverse and coronal planes. An oblique plane was used for the cruciate ligaments. Images were captured on a left limb. Scanning planes and positions of the probe are shown in Figures 4, 6, 8, 11 and 13. Figure annotations are detailed in Table 1.

***Table 1*: Legend: US and Gross Anatomy**

1.Femur
- *a. Lateral femoral condyle*
- *b. Medial femoral condyle*
- *c. Trochlea*

2.Tibia
- *a. Lateral plateau*
- *b. Medial plateau*

3.Patella

4.*Tendon of the m. quadriceps femoris*

5.Patellar tendon

6. Common tendon of peroneus tertius-extensor longus digitorum-extensor digiti III proprius

7. Tendon of the m. gluteobiceps

8. Medial meniscus
- *a.Cranial horn*
- *b.Middle segment*

9. Lateral meniscus
- *a.Cranial horn*
- *b.Middle segment*

10. Cranial cruciate ligament

11. Caudal cruciate ligament

12. Synovial Recesses
- *a. Suprapatellar*
- *b.Medial femoro-tibial*
- *c.Lateral femoro-tibial*
- *d.Tendinous*
- *e.Subpopliteus*

13. Lateral collateral ligament

14. Medial collateral ligament

15. Tendon of the m. popliteus

16. Adnexa
- *a. Skin*
- *b.Fat*
- *c.Infrapatellar fat pad*

Cranial Approach

The examination started with a 17–5 MHz linear transducer in the sagittal plane (Figure 4), proximally to the patella, progressing distally, then in a transverse plane progressing proximally. The tendon of m. quadriceps, the patellar tendon and the infrapatellar fat pad were consistently visualized in both planes. The tendon of m. quadriceps and the patellar tendon were hyperechoic to muscle, with a fibrillar yet homogeneous pattern (Figure 5). The infrapatellar fat pad appeared isoechoic to muscle.

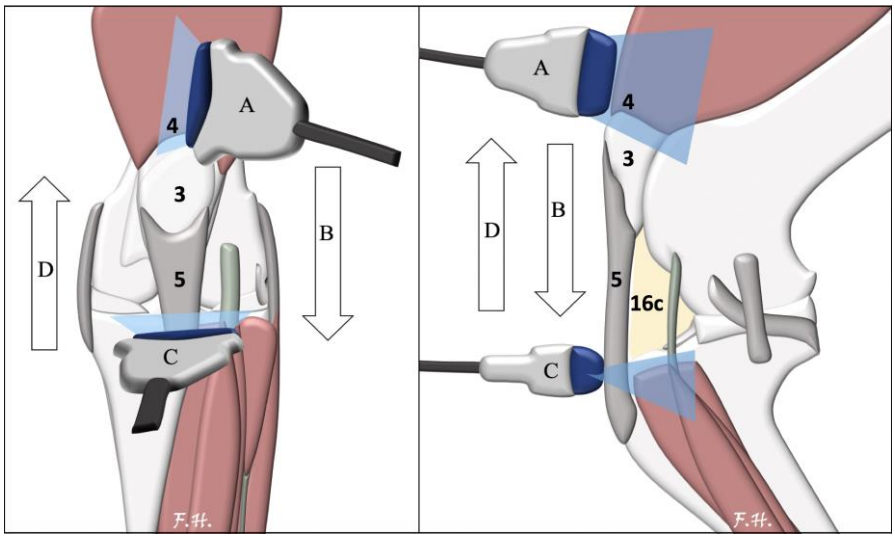


Figure 4: Description of the cranial approach (angle 95°) for US of the ovine stifle. The examination started in the sagittal plane, proximally to the patella (3) (A). The 17.5 MHz linear transducer was placed longitudinally on the tendon of m. quadriceps (4), and the tendon was scanned from the musculotendinous junction to its attachment on the patella. The transducer was then moved further distally (B) to visualize the patellar tendon (5) from its patellar attachment to its tibial attachment. The transducer was then rotated through 90° (C), and moved proximally to scan the patellar tendon and the tendon of m. quadriceps in a transverse plane (D). The infrapatellar fat pad (16c) was identified in sagittal and transverse planes. For key, see Table 1.

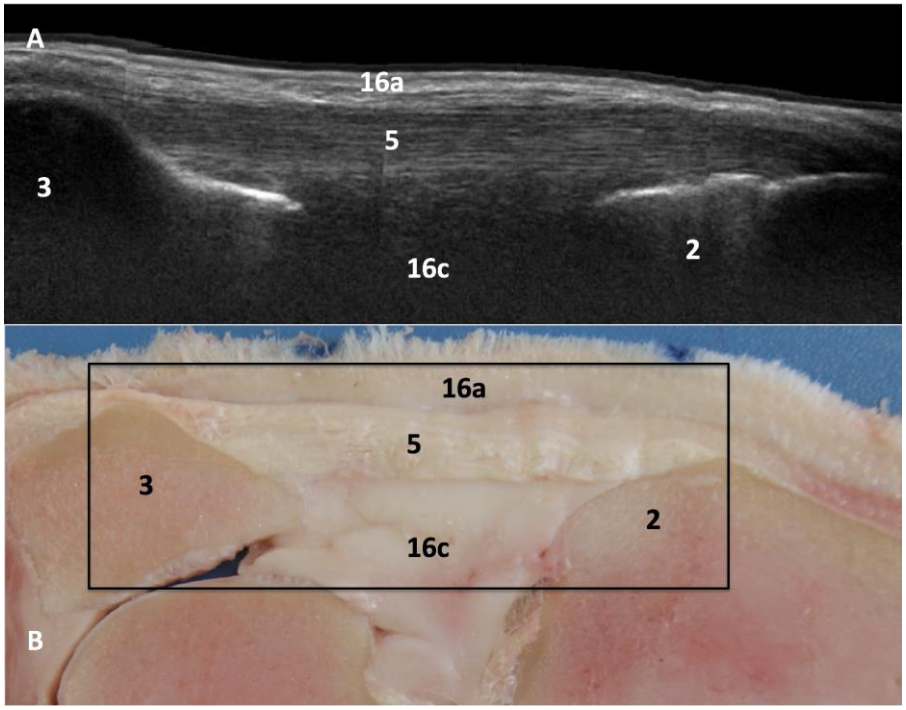


Figure 5: Cranio-sagittal US scan (panoramic reconstruction) (A) and corresponding gross anatomic section (angle 95°) (B). The black rectangle shows the scanning field. Note that the infrapatellar fat pad is not visualized on this US scan due to the reconstruction of the image for the manuscript. Tibia (2), patella (3), patellar tendon (5), skin (16a), infrapatellar fat pad (16c).

Then, the transducer was placed laterally to the patellar tendon, on the cranio-lateral aspect of the joint, to scan, in sagittal and transverse planes, the common tendon of m. peroneus tertius-extensor longus digitorum-extensor digiti III proprius and the tendon of m. gluteobiceps (Figure 6). Both tendons were hypoechoic, fibrillar, homogeneous and fully visualized (Figure 7).

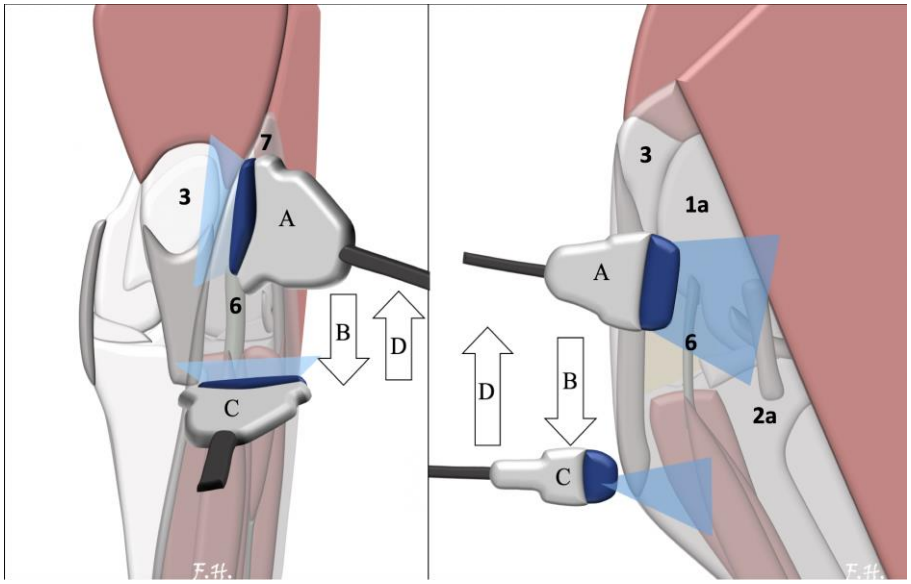


Figure 6: Description of the cranio-lateral approach (angle 95°). The transducer was placed on the cranio-lateral aspect of the joint (A) and moved distally (B), to scan the common tendon of m. peroneus tertius–extensor longus digitorum–extensor digiti III proprius (6) in a sagittal plane, from its femoral attachment, along the extensor groove, to 2 cm below the tibial plateau. Then, the structures were scanned in a transverse plane (C) from distal to proximal (D). The tendon of m. gluteobiceps (7) was also identified. Lateral femoral condyle (1a), lateral tibial plateau (2a), patella (3).

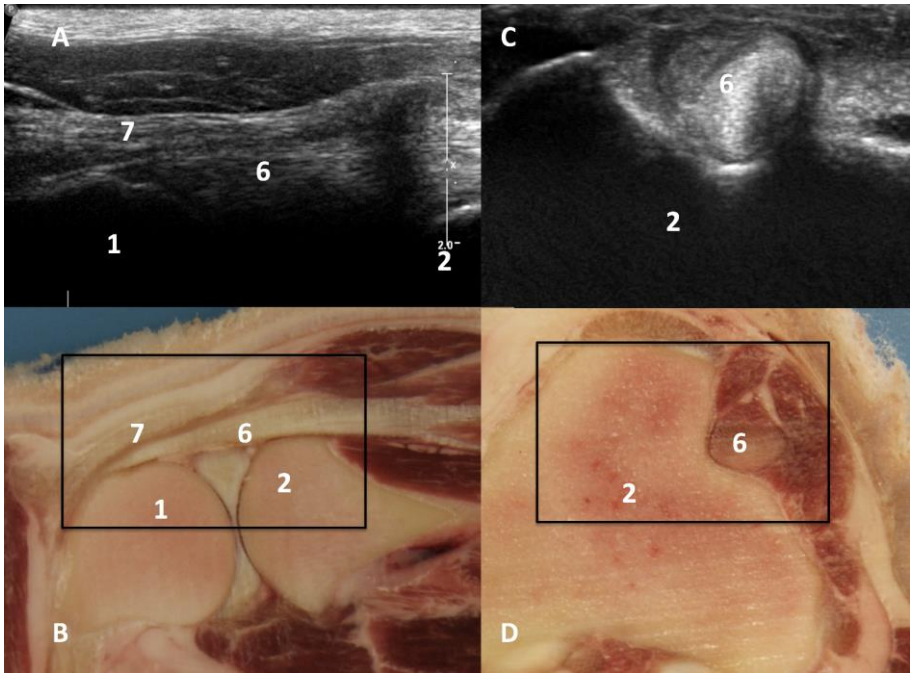


Figure 7: Cranio-lateral sagittal (A) and transverse (C) US scans and corresponding gross anatomic sections (B, D) (angle 95°). The black rectangle shows the scanning field. Femur (1), tibia (2), common tendon of m. peroneus tertius–extensor longus digitorum–extensor digiti III proprius (6), tendon of m. gluteobiceps (7).

The joint was then flexed (75°), and transverse scans of the articular surface of the trochlea of the femur were made proximally to the patella (Figure 8). Cartilage was seen on the whole surface of the trochlea, being somewhat thicker on the medial aspect. It was hypoechoic to muscle whilst the cortical bone was hyperechoic (Figure 9). Then, the transducer was moved distally and placed in medial and lateral parasagittal planes to visualize the surfaces of the femoral condyles. Only the abaxial part of the cartilage surface could be scanned. The margins of the tibial plateau and the cranial horns of the medial and lateral menisci were identified. However, the meniscus was less well visualized laterally than medially due to the interposition of the tendon of m. popliteus. Femoral cartilage was hypoechoic, with the cortical bone being hyperechoic, to muscle. The medial meniscus was hyperechoic to muscle. The lateral meniscus was mostly isoechoic to muscle, but its echogenicity varied due to the interposition of the tendon of m. popliteus. The cartilage of the medial and lateral tibial plateau was not visualized.

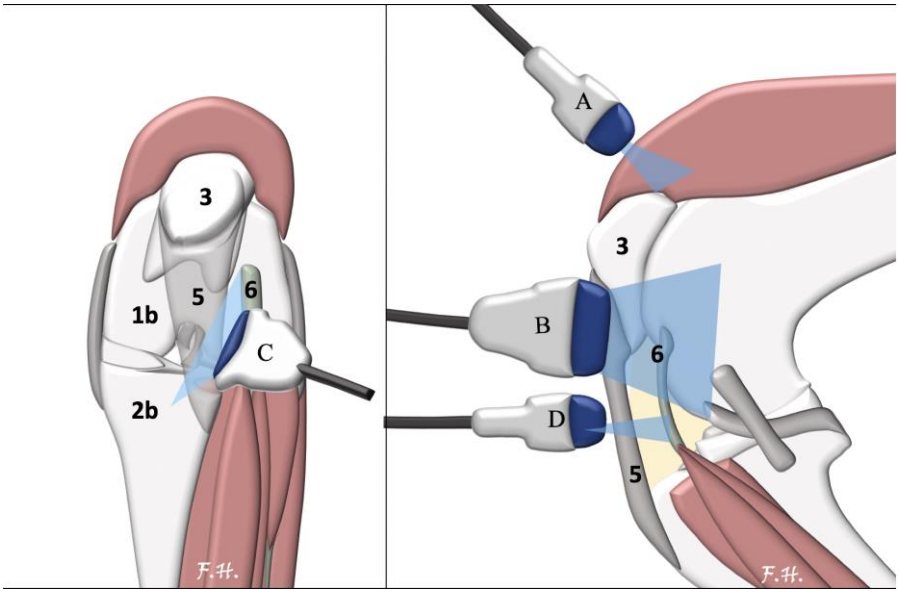


Figure 8: Description of the cranial approach (angle 75°). The transducer was placed proximally to the patella and moved distally, in a transverse plane (A), to visualize the trochlea of the femur and its overlying cartilage. Then, the transducer was rotated in parasagittal planes (B), medial and lateral, to visualize the femoral condyles and overlying cartilage, the margins of the tibial plateau, and the cranial horns of the medial and lateral menisci. A curvilinear 5–1 MHz transducer was then placed longitudinally on the patellar tendon and, from that landmark, rotated about 20° clockwise (for a left limb) (C) and anticlockwise (for a right limb), to visualize the cranial and caudal cruciate ligaments. The transducer was rotated further to a transverse plane, to identify the proximal attachment of the cranial cruciate ligament on the axial aspect of the lateral femoral condyle (D). Patella (3), patellar tendon (5), common tendon of m. peroneus tertius–extensor longus digitorum–extensor digiti III proprius (6).

A convex 1 MHz transducer was then used in sagittal, oblique and transverse planes to image cruciate ligaments (Figures 8 and 10).

The cranial and caudal cruciate ligaments were consistently but incompletely seen (Figure 10) due to their deep location and the necessity of using a 5–1 curvilinear transducer instead of a high-frequency linear transducer.

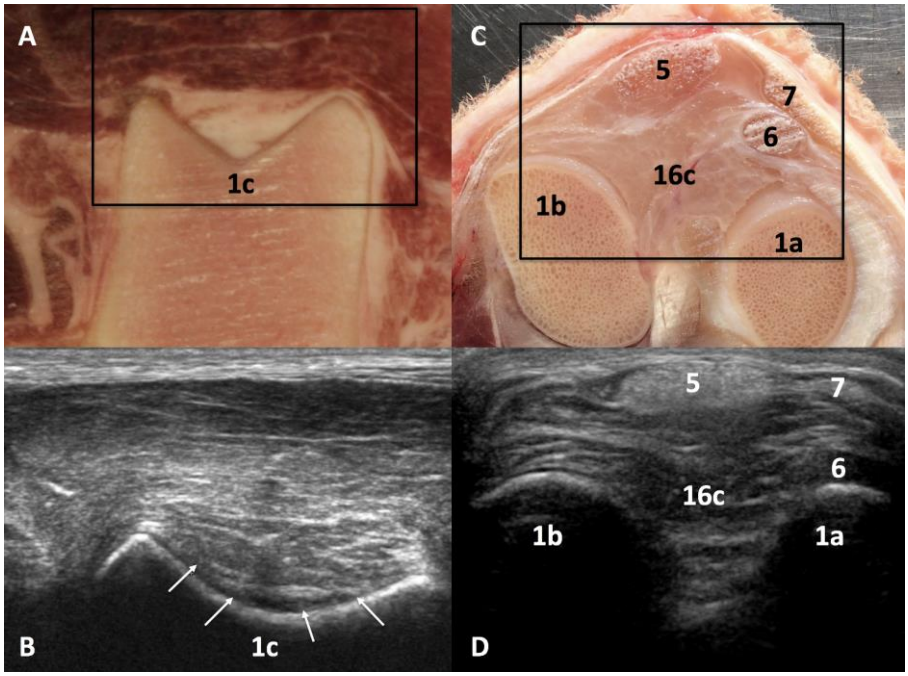


Figure 9: Cranio-transverse US scans (B, D) and corresponding gross anatomic sections (A, C) (angle 75°). The black rectangle shows the scanning field. Lateral femoral condyle (1a), medial femoral condyle (1b), trochlea (1c), patellar tendon (5), common tendon of m. peroneus tertius–extensor longus digitorum–extensor digiti III proprius (6), tendon of m. gluteobiceps (7), infrapatellar fat pad (16c).

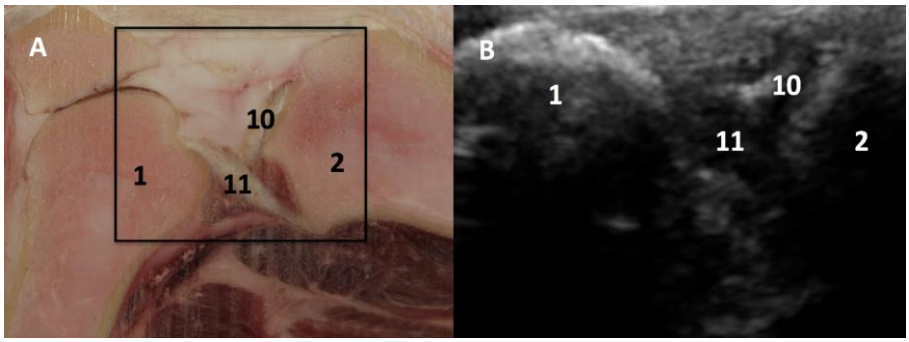


Figure 10: Cranio-sagittal US scans (B) and corresponding gross anatomic section (A) (angle 75°). The black rectangle shows the scanning field. Femur (1), tibia (2), cranial cruciate ligament (10), caudal cruciate ligament (11).

The cranial approach was suitable to scan several synovial recesses. After intraarticular injection of saline, the suprapatellar recess and the medial and lateral femoro-tibial compartments of the synovial cavity were consistently visualized cranially, respectively, sagittally and parasagittally (Figure 11). The tendinous recess extended distally on the cranio-lateral aspect of the proximal tibia in the extensor groove surrounding the common tendon of m. peroneus tertius–extensor longus digitorum–extensor digiti III proprius. All the recesses were anechoic due to the liquid content. The capsule appeared very thin and hyperechoic (Figure 12).

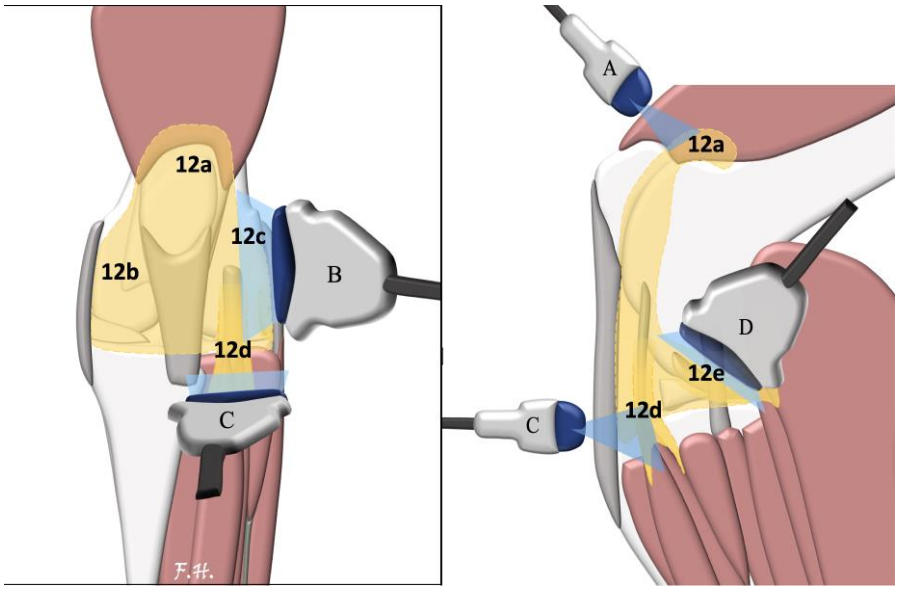


Figure 11: Description of the approach to scan synovial recesses (angle 95°). In a cranial approach, the transducer was placed proximally to the patella to identify the suprapatellar recess in a transverse plane (A). Then, it was turned in parasagittal planes to scan the femoro-tibial compartments, laterally and medially (B), and in a transverse plane to image the tendinous recess (C). In a lateral approach (D), the transducer was placed obliquely, in the same plane as the tendon of m. popliteus, to scan the subpopliteus recess. Suprapatellar recess (12a), medial femoro-tibial compartment (12b), lateral femoro-tibial compartment (12c), tendinous recess (12d), subpopliteus recess (12e).

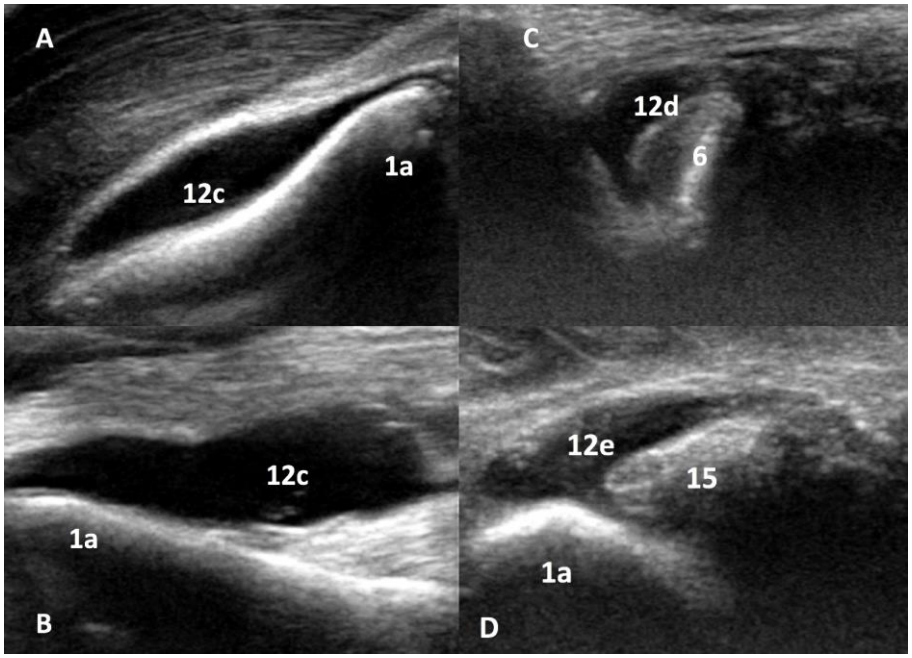


Figure 12: Cranio-sagittal(A), cranio-transverse (B, C) and latero-transverse (D) US scans of synovial recesses (angle 95°). Lateral femoral condyle (1a), common tendon of m. peroneus tertius– extensor longus digitorum–extensor digiti III proprius (6), lateral femoro-tibial compartment (12c), tendinous recess (12d), subpopliteus recess (12e), tendon of m. popliteus (15).

Lateral Approach

The lateral aspect of the stifle was evaluated with a linear 17–5 MHz transducer. The transducer was placed parallel to the lateral collateral ligament, the angle between femur and tibia being 110° (Figure 13). The lateral collateral ligament was identified with its attachments respectively on the lateral femoral tuberosity and the fibular head (Figure 14). The lateral collateral ligament was hyperechoic to muscle and fibrillar. The middle body of the lateral meniscus was isoechoic to muscle. The peripheral margin of the lateral femoral condyle and its overlying hypoechoic cartilage, and the margins of the lateral tibial plateau, were consistently visualized. With the joint in a more flexed position (95°), the tendon of m. popliteus was identified. It was hyperechoic to muscle, fibrillar and lying within the groove in the femoral condyle. This tendon was subject to anisotropy because of its curved course. In injected limbs, the subpopliteus recess was visualized, was anechoic and was of small volume.

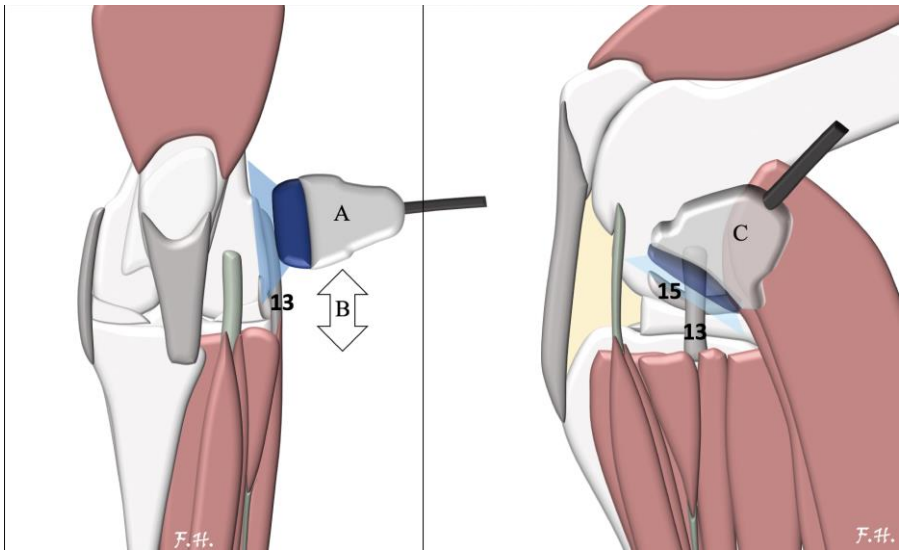


Figure 13: Description of the lateral approach. With an angle of 110° between femur and tibia, the transducer was placed longitudinally (A) on the lateral collateral ligament (13), and moved proximally and distally (B) to visualize its attachments on the lateral femoral tuberosity and the fibular head. The limb was slightly flexed (angle of 95°), and the transducer was placed obliquely, cranio-proximally to caudo-distally, parallel to the fibers of the tendon of m. popliteus (15) (C).

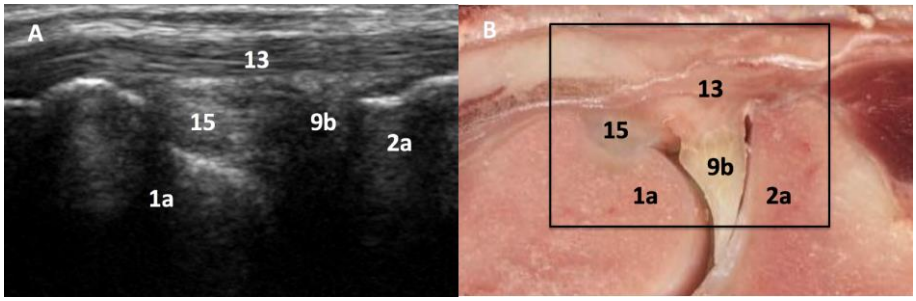


Figure 14: Latero-coronal US scans (A) and corresponding gross anatomic section (B) (110°). The black rectangle shows the scanning field. Lateral femoral condyle (1a), lateral tibial plateau (2a), middle segment of lateral meniscus (9b), lateral collateral ligament (13), tendon of m. popliteus (15).

Medial Approach

The medial aspect of the stifle was evaluated with a linear 17–5 MHz transducer in coronal and transverse planes similarly to the lateral approach. The medial collateral ligament and its attachments, the middle body of the medial meniscus, the articular margins of the medial femoral condyle and its overlying cartilage, and the abaxial part of the tibial plateau were visualized. The medial collateral ligament was hyperechoic and fibrillar. The medial meniscus was hyperechoic and better visualized than the lateral meniscus (via the lateral approach).

3.4. Discussion

This study demonstrated that US can be used to assess the ovine stifle. The caudal approach was not successful to identify caudal anatomical structures of the joint that might be relevant clinically, such as the caudal aspects of the articular surfaces of the femoral and tibial plateau, the caudal horns of the menisci and the supracondylar synovial recesses. Nevertheless, several other relevant anatomical structures could be identified with cranial, lateral and medial approaches. This is of clinical interest for several pathologies that occur in humans and are the object of research in ovine models.

In this study, the cranial and middle parts of the ovine menisci could be visualized, and especially well in the medial meniscus. Meniscal tear is a very common disease in humans. Different localizations of such tears within and between the menisci have been described (Beaufils and Pujol, 2018). Severe meniscal tears cause meniscal extrusion, mainly in the medial meniscus. Posterior tears are more common than middle or anterior tears (Chahla et al., 2016; Oei et al., 2010). Lesions of the posterior

part of the medial meniscus are described to occur generally in association with anterior cruciate ligament injuries (Seil et al., 2017). In humans, US has been reported to be a valid alternative to MRI in the assessment of meniscal extrusion (Papalia et al., 2017). Ovine mesenchymal stem cells/collagen scaffold was tested in a sheep meniscal cartilage tear model (Whitehouse et al., 2017); different repair techniques have also been tested (Scotti et al., 2013) such as stem cells seeded into scaffolds, cell-free scaffolds, gene therapy, intraarticular delivery of progenitor cells, biological glues, and partial and total tissue engineered meniscus replacement. Meniscectomy and induction of meniscal tears can be performed on medial (Gruchenberg et al., 2015) and lateral (Beveridge et al., 2011) meniscus in the sheep (Little et al., 2010). The current study suggested that, if US must be used to evaluate the efficacy of a treatment for meniscal tears, in a longitudinal research study using the ovine stifle, the initial lesion should be created in the cranial and middle body of the medial meniscus to optimize visualization. Laterally, menisci are also visible but cannot be assessed as accurately due to presence of the popliteus tendon. The echogenicity of the menisci appears similar to humans.

This study also demonstrated that US was able to identify the abaxial cortical surfaces of the femoral condyles and the abaxial overlying cartilage of the femur. The cartilage of the tibial plateau could not be identified, but the lateral, medial and cranial bony margins of the articular tibial surface could be visualized. In addition, the supra-patellar recess, the medial and lateral femoro-tibial compartments of the synovial cavity, the tendinous recess and the subpopliteus recess could be seen. All these anatomical structures can be useful to observe in an ovine model of induced OA. In sheep, OA is induced by medial (Cake et al., 2013) or lateral (Beveridge et al., 2014) meniscectomy or injuries to cranial cruciate ligament or medial collateral ligament (Beveridge et al., 2014). In OA, in humans, US is used to detect joint effusion, synovial hypertrophy and structural changes, including decrease in cartilage thickness, meniscus bulging and osteophyte formation (Oo and Bo, 2016). The current study indicated that those abnormalities are likely to be detected by US in the ovine stifle.

Cruciate ligament tears are frequent in humans (incidence of 68.6 per 100.000 person-years for the cranial cruciate ligament (Sanders et al., 2016); incidence unknown for caudal cruciate ligament). Caudal cruciate ligament tears are less common than cranial cruciate ligament tears and occur mainly in a multi-ligament-injured knee (Vaquero-Picado and Rodriguez-Merchan, 2017); it can be torn at its tibial or femoral attachments or more commonly through its substance. Isolated caudal cruciate ligament tears are uncommon and are often associated with meniscal tears and future symptomatic OA (Sanders et al., 2017). Research has been conducted in sheep with induced tears to test regeneration of cranial cruciate ligament, for example, after implantation of cell-seeded scaffold (Teuschl et al., 2016). Our study showed that the replacement of the linear transducer by a convex transducer made it possible to differentiate the cruciate ligaments, but a thorough examination of these structures by means of US remained difficult and would probably be not efficient in assessing healing in longitudinal trials.

This study also showed that the trochlea can be examined by US and is easily accessible by maximal flexion of the stifle. A trochlear defect repair method by allograft transplant has been described previously in the sheep (Cinque et al., 2017; Kitamura et al., 2016), and therefore, US could potentially be useful in such studies. The medial and lateral collateral ligaments were also well identified. In humans, the medial collateral ligament is the most common injured ligament in the knee; it is a major stabilizer of the knee joint (Frank et al., 2012). In research sheep, damage to the medial collateral ligament can be induced (Beveridge et al., 2014; Funakoshi et al., 2007), and it is likely that US could be used to follow up healing.

In the context of the current PhD thesis, this study interestingly demonstrated that the patellar tendon was perfectly visualized in our study, and that the anatomy of that tendon is rather similar than that in man. US was shown to be a good tool to assess the patellar tendon in humans (Miller, 2013). Again, US could be used in the sheep for the follow-up of induced lesions of the patellar tendon. The other tendons are less suited for US monitoring in longitudinal research studies in sheep. Though the quadriceps tendon is well identified by US in humans, it is less well visualized in sheep due to its shortness. The common tendon of m. peroneus tertius–extensor longus digitorum–extensor digiti III proprius is well visualized in sheep but does not exist in humans. Finally, our study showed that the ovine tendon of m. popliteus has a similar aspect as in humans, but is not well identified in its caudal part.

However, it is important to be aware of the limitations to the current study. It was performed in cadaveric limbs. We did not have to contend with animal movements and therefore probably obtained a higher image quality. Sedation or general anaesthesia would probably improve acquisition of images in live subjects.

4. HOW DOES THE STIFFNESS OF THE PATELLAR TENDON VARY IN A POPULATION OF HEALTHY RESEARCH SHEEP?

Adapted from

Françoise Kayser, Edoardo Bori, Sophie Fourny, Fanny Hontoir, Bernardo Innocenti, Peter Clegg, Alexandra Dugdale, Jean-Michel Vandeweerd. Ex vivo study correlating the stiffness of the ovine patellar tendon to age and weight.
Under revision in International Biomechanics.

4.1. Introduction

The ultimate outcome of tendon healing is the recovery of biomechanical properties. The mechanical behavior of the tendon depends on the fiber pattern and its viscoelastic characteristics when subjected to dynamic mechanical forces *in vivo*. The triple helical structure of type I collagen as well as the hierarchical nature of the tendon contribute to the elasticity of collagen (Franchi, 2010). The electrostatic cross-linking of the proteoglycan-rich matrix may contribute to the elastic nature of the tendon. The purpose of this particular tendon architecture is to withstand high tensile forces as well as guarantee force transmission (Kjaer, 2004). The main factors increasing the stiffness and strength of the tendon material are the content of collagen I, collagen alignment, and collagen cross-linking. The collagen fiber bundles running parallel to its long axis provide tensile strength to the tendon.

The mechanical properties of tendons can be studied ex vivo by a uniaxial tensile testing method in which isolated tendon specimens are stretched by an external force, eventually to failure, while both the specimen deformation and the applied force are recorded.

The uniaxial test enables to measure either the tendon stiffness, an extrinsic measurement of the tensile performance of the overall structure, or the Young's modulus, an intrinsic material property of the tendon.

Stiffness is the ratio between the force applied to the tendon and its change in length. Elasticity, or Young's modulus, is the ratio between the stress (ratio between the force applied and the cross-sectional area) and the strain (the ratio between the change in length and the initial length). With soft tissue structures, as they are quite irregular, the estimation of the cross-sectional area during the test may be quite difficult and could induce some estimation errors in the measurements that could lead to a reduced accuracy in the determination of the stress and therefore of the Elastic Modulus.

Hence, in the current study, we decided to measure the stiffness as our technique was quite accurate in evaluating force and displacement. Moreover, stiffness is a structural property, i.e., a property proper of the tendon as a whole, while elasticity is a material property (related to the material that constitutes a structure), meaning that it could change locally and it is not necessarily homogeneous along the tendon length.

The results are usually presented as a load-displacement curve (N/mm) for stiffness or a stress- strain curve for elasticity (N/mm^2). Four regions can be defined in this curve: the toe region, linear region, plastic region and failure region (Figure 15) (Butler and Awad, 1999).

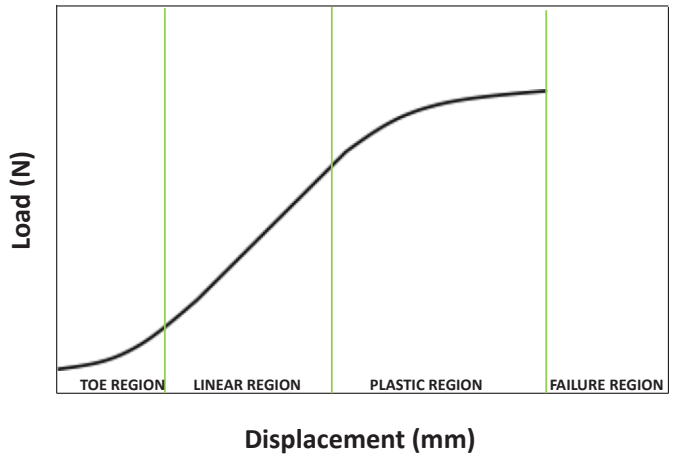


Figure 15: Load-displacement curve of a tendon during a uniaxial tensile test. The figure illustrates the different phases, corresponding to different mechanical behavior. The initial toe-region corresponds to the "un-crimping" of the crimped collagen fibrils. After this phase the collagen fibrils are aligned, and the trend force-displacement is linear (linear region). This linear region is an elastic region that is reversible, meaning that the tendon returns to its initial shape after load removal. In case of load maintenance, the tendon undergoes microscopic lesions (irreversibility). At this stage the tendon behaves in a plastic manner which means that a certain degree of deformation will persist after unloading. The end-stage corresponds to the macroscopic failure named the failure region.

The existence of the crimp explains the toe region of the tendon load-diplacement curve in which the tendon extends in length upon low levels of load. Once the crimp has been removed the load-displacement curve is linear, to a close approximation, until the tendon tissue fails.
The tendon stiffness is defined as the linear region of the load-displacement curve, which is a measure of its resistance to axial deformation. Stiffness is a structural

property of the tendon defined as the ratio of force (N) to displacement (mm). A typical tendon load-displacement curve has an initial toe region, where the tendon is strained up to 2%. In the linear region of the curve where the tendon is lengthened less than 4%, collagen fibers lose their crimp pattern (Johnson et al., 1994). In the case of the stress-strain curve, the slope of this linear region is referred as the Young's modulus of the tendon, also known as elastic modulus. Young's modulus in tension (or compression) is a mechanical property that measures the tensile (or compressive) stiffness of a solid material when the force is applied lengthwise. The Young's modulus (E) is a property of the material that tells us how easily it can stretch and deform and is defined as the ratio of tensile stress (σ) to tensile strain (ε). Where stress is the amount of force applied per unit area ($\sigma = F/A$) and strain is extension per unit length ($\varepsilon = \Delta L/L_0$).

The formula of stiffness is

$$S = \frac{F}{\delta}$$

- S is stiffness
- F is the force exerted on an object under tension
- δ is the tissue displacement

The unit used for stiffness in the metric system is Newton per millimeter (N/mm). This means the higher the tissue stiffness, the more force is needed for an identical tissue displacement obtained with a lower force.

The formula of Young's modulus is

$$E = \frac{\sigma}{\varepsilon} = \frac{F/A}{\Delta L/L0} = \frac{FL0}{A\Delta L}$$

- is the Young's modulus (elastic modulus)
- is the force exerted on an object under tension
- is the actual cross-sectional area, which equals the area of the cross-section perpendicular to the applied force
- is the amount by which the length of the object changes (is positive if the material is stretched, and negative when the material is compressed)
- is the original length of the object

The unit used for the Young's modulus in the metric system is the MPa, Newton per square millimeter (N/mm^2).
A material with a very high Young's modulus is called rigid (rigidity, or stiffness, is the extent to which an object resists deformation in response to an applied external force). A tissue with a higher Young's modulus needs a higher force to obtain tissue lengthening.

Since the patellar tendon covers a key role in extension of the knee joint, the biomechanical characteristics of the patellar tendon, such as elasticity and stiffness, are of paramount importance and constitute major outcome measures in research studies. However, to date, these patellar tendon properties have not been described in sheep, and there is therefore a need to document them in a population of research animals.

The aim of this study was therefore to document the properties of the healthy patellar tendon in research sheep, assessing changes with age and weight; the result was sought in terms of stiffness, addressing in this way the whole tendon system and not only the material it is composed of.

4.2. Material and Methods

Animals

Thirty-four ewes (Île-de-France; n= 34), from the Ovine Research Center of the University of Namur, were used. Their age ranged from 2 to 10 years, and their weight from 65 to 95 kg. The experimental protocol 10150MU was approved by the local ethical committee for animal welfare. All animals had no history of hindlimb lameness. They were assessed by palpation and observation. No swelling or pain of the stifle was observed. Animals were not lame before euthanasia.

Animal were sorted into three categories of age (1-2yo, 3-5yo, 6-10yo).

Gross Anatomy

Animals were sacrificed by intravenous administration of pentobarbital (150 mg/kg). Both hind limbs were transected at the level of the mid-femur within 1 hour of death. Soft tissue, including skin and muscles were removed. The patellar tendon and its attachments on the patella and the tibial tuberosity were carefully dissected and observed to confirm the absence of lesions or abnormalities.

The joint capsule, collateral ligaments and cruciate ligaments were transected. The knee joint was disarticulated, and the tibial tuberosity and patella were transected at 1.5 cm from their respective tendon attachments. Bone attachments were preserved so as not to affect the tendon insertion areas that are fundamental for mechanical load transfer.

Each harvested specimen consisting of an intact “patella-patellar tendon-tibial tuberosity” unit was individually wrapped in moistened gauze (with 0.9 % w/v NaCl), sealed in plastic bags, individually identified by a number and stored at -20°C. Previous studies showed no alteration in biomechanical properties after several freeze-thaw cycles compared to fresh tendons (Arnout N et al., 2013), though Huang

and al. recommend less than five freeze-thaw cycles. They showed that repetitive freeze-thaw cycles (more than five) declines structural, mechanical and viscoelastic properties of the tendon (Huang et al., 2011).
Four-mm thick osteochondral slabs in a coronal plane were obtained (medial femoral condyle, lateral femoral condyle, medial tibial condyle, lateral tibial condyle), before being processed for histology.

Histopathology of Cartilage

Histology is used as the gold standard to assess the articular cartilage of a joint, joint deterioration and joint ageing (Little et al., 2010). Articular cartilage changes are associated with ageing and diseases such as osteoarthritis. In the current study, histology was performed to assess joint deterioration and confirm the sample was representative of a normal ageing population of sheep by comparison to results of previously published studies (Vandeweerd et al., 2013b).
The osteochondral slabs were fixed in a 10% w/v neutral buffered formalin for 48 hours. The specimens were decalcified in 10% w/v formic acid/ 5% w/v formalin during 8 to 10 days, depending on softening of the slabs. After paraffin embedding, 7µm sections were cut and mounted on Superfrost Ultraplus® slides that improve cartilage adhesion. The sections were thoroughly deparaffinized in several xylene washes and graded alcohols to 70% w/v ethanol, then stained in 0.04% w/v toluidine blue and counterstained in 0.1% w/v aqueous fast green FCF. Finally, the slides were dehydrated in two changes of 99% isopropyl alcohol and two changes of xylene before mounting in DPX (DPX mounting media for histology).

The OARSI recommendations were used for histologic scoring of the cartilage (Little and al., 2010). Histologic abnormalities included: structural defects (0-10), chondrocyte density (0-4), cell cloning (0-4), interterritorial Toluidine blue (0-4), tidemark (0-3), extent of the defect (0-5) with a total scoring of 0-30 (Figure 16). The histologic grade per limb was determined by the summation of the total scores of the 4 anatomical regions in that limb.

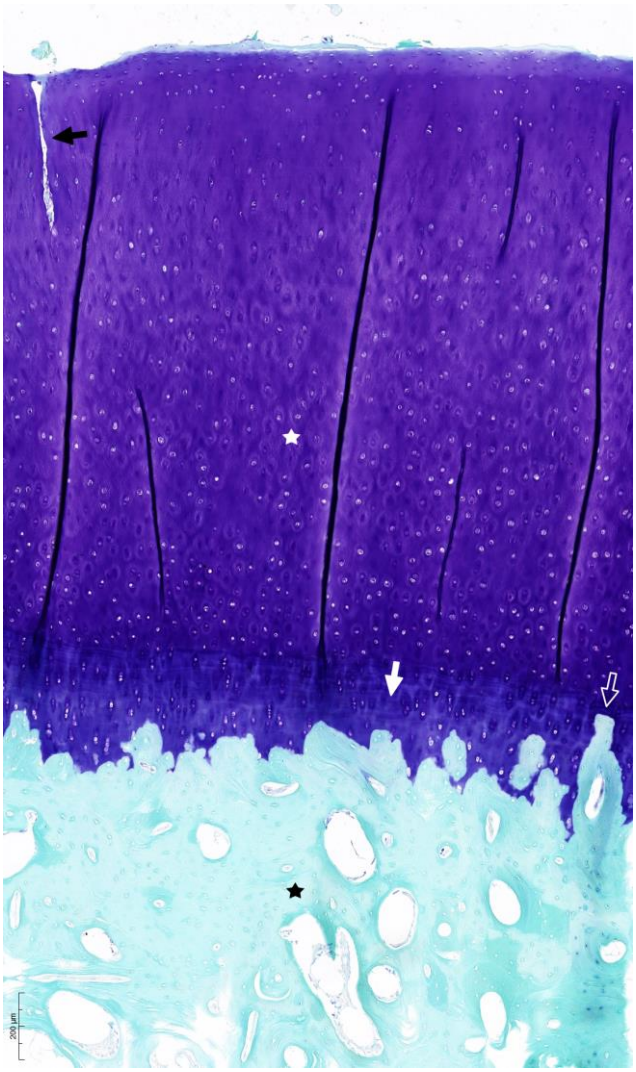


Figure 16: Cartilage histology. Toluidine blue/fast green stained section of cartilage scored as follows: Structure 4 (fissures to transitional zone 1/3 depth (black arrow)), Chondrocyte density 0, Cell cloning 0, Interterritorial toluidine blue 0, Tidemark 2 (duplicated tidemark (white arrow) with blood vessel penetrating through the subchondral bone plate (white open arrow)), with a total score of 6. Cartilage (white star). Subchondral bone (black star). Scale in lower left corner.

Biomechanical Tests

In thirty-four matched pairs of limbs (n=68), a uniaxial tensile test was performed on patellar tendons following an in-house validated procedure (Innocenti and al., 2018). For all investigations, frozen "patella-patellar tendon-tibial tuberosity" units were thawed to room temperature, cleaned thoroughly with 0.9 % w/v of NaCl and placed on a metal frame. The osseous parts of the specimen were cut with pliers to fit the clamp size. Four black ink dot markers were directly drawn onto each specimen in order to measure the displacement of the tendon tissue during the tensile test (Figure 17).

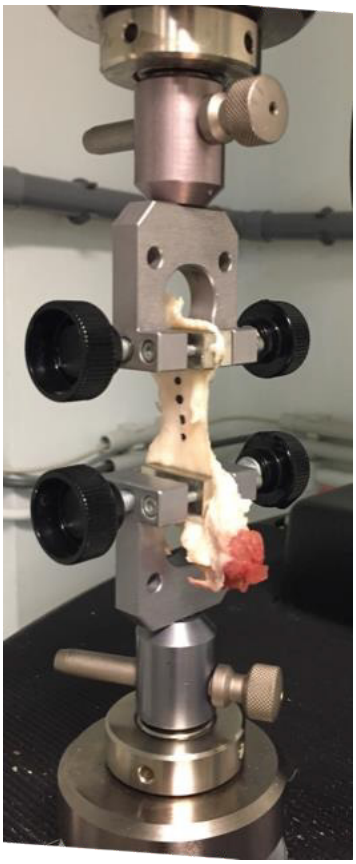


Figure 17: Patella-patellar tendon-tibial tuberosity unit placed on a metal frame. Patella-patellar tendon-tibial tuberosity unit fixed by two clamps. Four black ink dot markers were directly drawn onto the tendon specimen.

The camera was set to 100 fps. Force outputs were obtained via a dedicated 1 kN load cell (Lloyd Instruments Ltd). As the tendons had been manipulated and then stored at -20° C before the biomechanical tests, a series of 10 preconditioning stress-relaxation procedures was performed to ensure fibers alignment before the tensile testing. As recommended in the ASTM D638 standard (ASTM International, 2003), a crosshead speed of 5 mm/min was applied for the tensile test. The axial force was recorded and paired with the relative displacement during the tests. The tensile test was performed until failure and the resulting force-displacement curve was analyzed: after the initial toe region, the linear region of the curve (corresponding to the elastic region, i.e., the elongation of the helical structure of collagen (Kirkendall and Garrett, 1997)) was defined thanks to the dedicated software: a linear fitting process was used to determine the boundaries of the linear region and this latter was studied to obtain the relative stiffness of the tissue (obtained from the slope of the curve in the selected region).

Statistical Analysis

In order to examine the normality of data (patellar tendon stiffness and histologic scores of articular cartilage), Kolmogorov-Smirnov and Shapiro-Wilk tests were applied. Non-parametric tests were used, due to the non-normality of the data. The Wilcoxon signed-rank test was used to compare observations that were not independent (difference in patellar tendon stiffness between left and right hindlimbs). One limb was randomly chosen within each pair and data obtained from that limb (tendon stiffness, articular cartilage histologic grades) were used for analysis. Correlations between patellar tendon stiffness and other variables (age, weight, histological grades) were assessed by Spearman correlation coefficient. Data were collected in Microsoft Excel and analyzed using Graph Pad Prism 8. A p-value below 0.05 was considered to indicate a statistically significant difference.

4.3. Results

Cartilage Histopathology

Among the 272 (4x68) histologic slices, none presented artifacts or inadequate coloration that may have prevented correct interpretation. We found no significant difference in limb histologic total scores between left and right limbs ($p=0.93$).
The histologic scores (median, minimum, maximum) were, however, different between regions of interest: medial tibial condyle (7, 2, 17), lateral tibial condyle (6, 2, 18), medial femoral condyle (6, 2, 21) and lateral femoral condyle (5.5, 1, 13). Among the total number of lesions, we found 36.2% in the medial femoral condyle, 6.8% in the lateral femoral condyle, 37.9% in the medial tibial condyle and 15.5% in the lateral tibial condyle. Among the histologic abnormalities, beside the total score, structural defects and tidemark increased the most with age and weight.

There was a significant positive correlation between body weight and histologic score ($r=0.51$; $p=0.002$), and between age and histologic score ($r= 0.67$; $p<0.0001$).

Tendon Stiffness

Our tests confirmed that the patellar tendon has the typical "region" behavior, with a non-linear one (toe region) followed by a linear region preceding the eventual damaging of the fibers and consequent failure of the tendon (Figure 18).
The mean stiffness value of the 68 tendons was 52.44 N/mm (SD 35.62, SD = standard deviation).

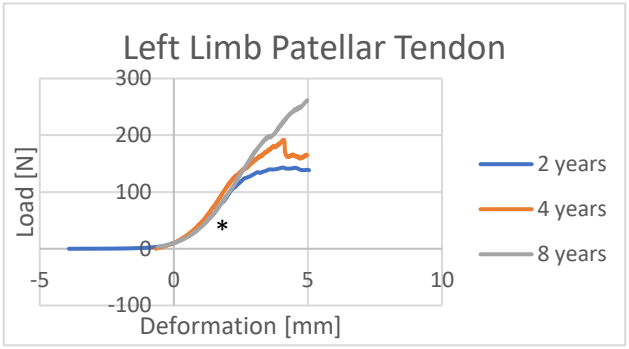


Figure 18: Load-deformation test showing the stiffness curve. Stiffness curve of the left patellar tendons related to three different age groups: 2 yo (year old), 4 yo) and 8 yo. * = linear region of the curve.

We found a positive but not significant correlation between stiffness and age (r=0.22, p=0.27). We also found a statistically significant positive correlation between body weight and tendon stiffness (r=0.39, p=0.04) (Figure 19) and between articular cartilage histologic scores and tendon stiffness (r=0.47, p=0.02) (Table 2).

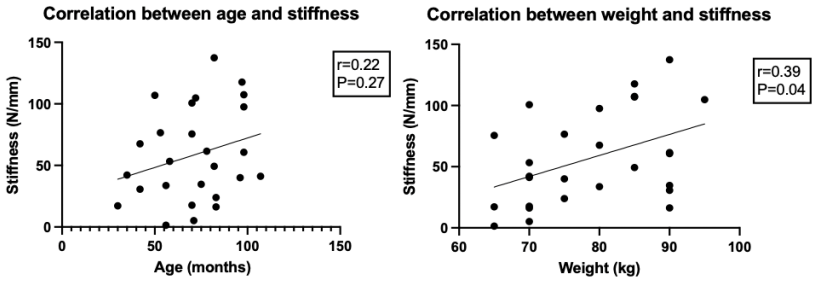


Figure 19: Correlation plot between age and stiffness and weight and stiffness. Correlation plot between age and stiffness (left) and between weight and stiffness (right). Correlation was positive but not significant between stiffness and age and statistically significant positive between stiffness and body weight.

	A1(1-2yo)	A2(3-5yo)	A3(6-10yo)
Weight (kg, mean+/-SD)	74.47+/-8.8	77.79+/-9.23	77.63+/-8 .44
Histologic score (median, minimum, maximum)	4(0,4)	9(4,47)	22.5(6,69)
Stiffness (N/mm, mean+/SD)	25.51+/-14.57	53.14+/-35.6	47.2+/-30.11

Table 2: Weight, histological scores and stiffness related to three different age groups: A1 (1-2 yo (year old)), A2 (3-5 yo) and A3 (6-10 yo).

4.4. Discussion

In research studies, the biomechanical characteristics of the tendon, like elasticity and stiffness, are major outcome measures. Due to the biomechanical similarity of the ovine stifle joint and the human knee (Herfat and al., 2012), the patellar tendon of the sheep can be adopted as a large animal model for human tendon disease investigation.

Our sample of sheep could be considered representative of a normal ageing ovine population. As previously described (Vandeweerd and al. 2013b), the histological changes of the stifle articular cartilage differed between anatomical regions of the joint, and the proportions of defects were around 30 % of lesions identified at the medial femoral condyle and 30 % at the medial tibial condyle. In addition, a significant positive correlation between age and histologic grade was identified. We also found a significant positive correlation between body weight and histologic grade of cartilage. The mean value of stiffness was 52.44 N/mm (SD35.62) in patellar tendons this sample of animals, a value quite similar to that found in a previous ex-vivo study (46-65-80 N/mm) on ovine patellar tendons (Kasperczyk and al., 1991).

Effect of Age

Our study showed a positive but not significant correlation between age and tendon stiffness. Other studies have investigated the effect of age. In canine patellar tendons there was a progressive stiffening of connective tissues with ageing (Haut and al., 1992). A study performed in rats showed that passive biomechanical properties of the muscle-tendon unit in Achilles tendons are altered with age, with a decreased relaxation response and increased stiffness in the tendons of middle-aged animals (Plate and al., 2013). On the other hand, a study conducted in New Zealand White rabbits showed no evidence of age-related changes in the biomechanical properties of healing tendons (Dressler and al., 2006).

The association between increased tendon stiffness and ageing may have different explanations. Tendons contain tenocytes that secrete matrix components such as elastin, proteoglycans and collagen.

It has been suggested that tensile stiffness changes in tissue are most likely due to changes in higher collagen structures rather than at the fibril level (Li and al., 2013; Fessel and al., 2014). Fascicle sliding has been described to decrease with ageing in horse (Thorpe et al., 2013). Even if no decrease in collagen content was noted in ageing Achilles tendons in mice, less organized collagen fibers containing an increased number of larger fibrils were observed (Gehwolf et al., 2016).

In a study in mice, older tendons were stiffer than young tendons. It was suggested that the consequences of ageing on mechanical properties could be due to advanced glycation end products (AGEs). The level of AGEs was higher in aged mice compared to younger ones (Wood and Brooks, 2016). Denaturation and crosslinking of collagen result from the formation of AGEs. These changes in collagen crosslinks limit fiber-fiber and fibril-fibril sliding, reduce the viscoelasticity of the tendon and increase the tendon stiffness. Similar changes were observed in another study conducted in rats (Gautieri et al., 2017). Some in vitro studies (Reddy, 2004) showed an association between AGEs and tendon mechanical properties. However, a clinical study conducted in vivo on the patellar tendon in man failed to associate tendon AGEs and changes in its mechanical properties (Eriksen and al., 2019).

Proteoglycans could also be involved in viscoelastic changes in aged tendons. Decorin is the most abundant proteoglycan in the small leucine-rich proteoglycan family (SLRP) in tendons. Decorin regulates the assembly of collagen I (Xu and al., 2018). The absence of decorin leads to an abnormal collagen fibrillogenesis, decreased tendon strength and stiffness (Danielson and al., 1997). Decorin and biglycan are essential regulators of collagen fibril and matrix assembly. A study, in a both decorin and biglycan gene expression knockout mouse model, showed changes in structural properties such as a shift to larger diameter fibrils with increased heterogeneity, and altered mechanical properties as decreased stiffness (Robinson and al., 2017). A study on old rats concluded that a decrease in proteoglycan 4 and elastin mRNA expression was responsible for the increased tendon stiffness observed with ageing, by reducing gliding properties of fascicular sheets (Kostrominova and Brooks, 2013).

An age-associated reduction in the functional fitness and metabolism of tendon stem cells may also be partially responsible for an ageing induced deterioration of the structure, composition and mechanical properties of tendon. Some authors described ageing as an “anarchy of stem cells”, with a decrease in the number and the functional fitness of tissue-specific stem cells (Fukada and al., 2014).

Effect of Weight

In the current study, we observed a significant positive correlation between tendon stiffness and increasing weight in sheep. In man, the incidence of tendon injury (Kelly and al., 2001; Savarese and al., 2010) and the patellar tendon stiffness (Tas and al., 2017a) were reported to be higher in overweight and obese human individuals. Another study showed that obesity was associated with a decrease in patellar tendon stiffness in females, whilst it was not the case in males (Tas and al., 2018). Another study reported instead that higher BMI was likely to be associated with greater tendon stiffness in young men (Tomlinson and al., 2021).

Strict comparison between species is complicated because lipid metabolism seems to be involved in tendon stiffness and this factor is different between omnivores and ruminants. A positive association between increased adiposity and tendinopathies was shown in man (Gaida and al., 2009). A study conducted in mice observed an accumulation of lipid droplets in aged Achilles and tail tendons, with an increased expression of adipogenic markers and reduced expression of beta-catenin, a regulator of adipogenesis (Gehwolf and al., 2016). Tendolipomatosis, may lead to tendinopathy by lipid cell deposition in the tendon tissue (Jozsa and al., 1984; Kannus and Jozsa, 1991). The lipid cells deposit in the tendon between the collagen fibers and may disrupt the cohesion of the collagen framework, thus weakening the tendon and increasing the risk of mechanical failure. Tendon-weakening is further exacerbated in overweight or obese individuals where the larger body mass increases the mechanical loading of the tendons.

Beside the effect of local lipid cells, the metabolic effects of increased adipose tissue might be responsible for lower tendon stiffness in man. The profile of adipokines (cytokines released by adipose tissue) expressed in obese individuals generally indicates a pro-inflammatory state (Battery and Maffulli, 2011). Cytokines may originate from the infrapatellar fat pad (Ushiyama and al., 2003). There is a relation between cytokines released by infrapatellar fat pad (Hoffa's fat pad) and knee osteoarthritis (Pottie and al., 2006). A larger infrapatellar fat pad (Culvenor and al., 2011) and systemic adiposity (Gaida and al., 2009) was associated with tendinopathy (Culvenor and al., 2011).

Those various and contradictory results indicate that different variables should be considered to assess the effect of weight in a species, such as the sheep. This should be considered in future studies.

Conclusion

In the scope of an ovine model of patellar tendon, this study showed that the stiffness of the healthy ovine patellar tendon increases significantly with weight. It also increases, but not significantly, with age. This study succeeded in the characterization of biomechanical properties of healthy tendons, providing useful reference values and establishing the basis for future biomechanical tests on patellar tendons in sheep. The most appropriate sheep population for those future studies would be young, non-overweight healthy adults.

5. DOES SHEAR WAVE VELOCITY ASSESSED BY ELASTOGRAPHY CORRELATE WITH STIFFNESS GIVEN BY TENSILE TEST IN THE OVINE PATELLAR TENDON?

Adapted from

Kayser F, Bori E, Armillotta N, Innocenti B, Hontoir F, Vandeweerd JM
Correlation between shear wave velocity assessed by elastography and stiffness given by tensile test in the ovine patellar tendon. Published in Archives of Clinical and Biomedical Research. Arch Clin Biomed Res. 2022; 6(1):905-916.
doi:10.26502/acbr.50170209

5.1. Introduction

To date, tendons are mainly evaluated clinically, by US, CDUS and MRI. Morphological changes of tendons such as echogenicity, homogeneity or thickness are well described by US (Davies et al., 1991). Neovascularization in chronic tendinopathies can be documented by CDUS (Weinberg et al., 1998). Inconveniently neither US and CDUS nor MRI inform on the mechanical properties of tendons. Unfortunately, these measures cannot be recorded *in vivo* due to the invasive nature of the available conventional biomechanical testing methods.

Traditionally assessed by manual palpation, tissue stiffness actually can be measured by ultrasound elastography. Ultrasound elastography, a more recent non-invasive technique, allows the investigation of those mechanical properties by applying a force either manually (strain elastography, SE) or mechanically by shear wave elastography (SWE). Unlike SE, SWE does not require a manual intervention by the ultrasonographer to produce strain, hence limiting operator biases (Hsiao et al., 2015; Zhang and Fu, 2013; Peltz et al., 2013; Kot et al., 2012). Patellar (Coombes et al., 2018), Achilles (Coombes et al., 2018) and rotator cuff tendons (Chiu et al., 2020) have been explored by SWE (Dirrichs et al., 2016). The technique was reported to be an accessible, non-invasive, easy-to-use, fast, cost-effective, reproducible and reliable tool in clinical and research work providing quantitative data, with a high level of inter-operator agreement (Hsiao et al., 2015; Payne et al., 2018) and minimal operator training. However, there is still a lack in standardization of SWE and there is no consensus about its application in tendon pathology.

To date, SWE has not been described in the sheep, and there is therefore a need to document them in a population of research animals. Moreover, before clinical acceptance, the validation of SWE requires correlation to tensile test values. It is therefore important to establish the SWV values in normal ovine patellar tendons

before using SWE in injured tendons, for example in models of induced tendinopathy or injury.
The aim of the third part of the thesis was to investigate whether SWV in healthy ovine patellar tendons, determined by SWE tested *in vivo*, was correlated to stiffness assessed by an *ex vivo* uniaxial tensile test considered as gold standard.

Strain Elastography

SE is a quasi-static operator-dependent technique (Klauser et al., 2014), depending on the application of a manual external light freehand transducer compression followed by the comparison of the images before and after the application of the compression, visualizing the tissue displacement. The tissue motion generated by cyclical manual compression and decompression using the transducer in SE is tracked to calculate the strain and reflect the tissue stiffness. In practice this means that a soft tissue will present a greater strain compared to hard tissue under the same external force. Thus, a larger strain value indicates a soft tissue and a lower strain indicates a hard tissue (the more the region is rigid the less it deforms). SE provides a semiquantitative measurement as an index of the relative elasticity between a chosen region of interest (ROI) in the examined tissue and a reference ROI located in the adjacent tissues. This technique enables only a qualitative analysis of the tissue (Ophir et al., 1991) and is ineffective in tissue stiffness quantification (Eby et al., 2013; Sarvazyan et al., 1998). Reproducibility of the measurements is poor due the operator-dependency, the manual compression being inconsistent.

Shear Wave Elastography

By contrast, SWE enables quantitative analysis of the tendon mechanical properties by measuring the shear elastic modulus and the shear wave velocity (SWV) related to tissue elasticity. In SWE an ultrasound induced acoustic radiation force, which is a time-varying force, is used to generate a micro-scale tissue movement (Figure 20). Whilst the initial layer resumes its original shape, the adjacent layers undergo shear, the shear wave propagating as a transverse shear wave, perpendicular to the initial direction of the force (Taljanovic et al., 2015). By analyzing the speed with which the shear waves propagate, the shear modulus (μ) of the tissue can be measured providing information about the tissue stiffness. Shear modulus is strongly correlated with the rigidity of the material, allowing its quantification. An ultrafast imaging enables the capture of the transient shear wave propagation. The shear wave velocity (c_s) is related to the shear modulus (G) of the tissue: $G=\rho c_s^2$, where ρ is the density of the tissue assumed to be a constant as 1000 kg/m^3. The Young's modulus, as measured by uniaxial tensile test, is approximately three times the shear wave modulus: $E=3G$. SWE is non-operator-dependant technique allowing a better reproducibility.

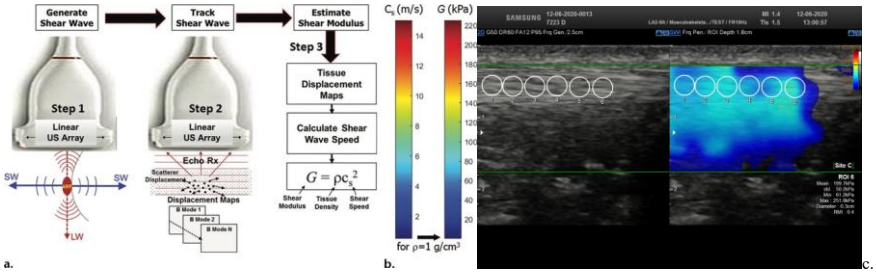


Figure 20: Functioning of SWE. (a) 3 steps of SWE functioning (Bercoff et al., 2004; Li and Snedeker, 2011): In step 1, a focused acoustic radiation force, from a linear US probe, generates shear waves which by itself provides a local stress that cause local displacement of the tissue. These generated shear waves propagate through the adjacent tissues in a transverse plane, perpendicular to the primary wave, at a much slower velocity, causing shear displacements of the tissue. In step 2, the transducer captures the vibration of the tissue created by the shear wave propagation and tracks the tissue displacement and shear wave velocities (SWV). In step 3, tissue displacement maps are used to calculate SWV (c_S), frequently expressed in meters per second. The distribution of SWV at each pixel is directly related to the shear modulus μ or G, which is calculated by a mathematical equation and expresses the tissue elasticity in units of pressure, expressed in kilopascals (kPa). The shear modulus is defined as the ratio of stress to strain that is given by $G = \rho c_S^2$, where ρ is the material density (Taljanovic et al., 2017). (b) color-coded elastogram. (c) shear wave elastography image as shown on the screen of the ultrasound device (reproduced from Taljanovic et al., 2017).

On the ultrasound screen (figure 20 b), quantitative shear modulus maps are represented in a color-coded elastogram. This elastogram displays SWV in meters per second (m/s) and/or tissue elasticity in kilopascals (kPa). On color elastogram, by agreement, red is usually defined for encoding hard consistency, green and yellow for intermediate consistency and blue for soft consistency, although these parameters may be changed by the user. In comparison to the previously described elastography techniques, SWE is considered to be more objective, reproducible and less operator-dependent because there is no need for external compression (Hsiao et al., 2015; Kot et al., 2012; Peltz et al., 2013; Zhang and Fu, 2013). This higher reproducibility and low operator-dependent influence is an advantage in clinical practice and in research as it ensures the comparison of results between studies and between assessments of the same specimen overtime. SWE allows direct assessment of tissue elasticity, with the possibility to obtain quantitative measurements without the need for manual compression.

In theory, SWE assumes a transverse homogeneous, isotropic and incompressible medium with a linear behavior, which does not apply to the complex tendon architecture (Brum et al., 2014). However, in tendons that are biological tissues, stress-strain ratio as well as load-displacement ratio have a non-linear behavior with four different regions: toe region, elastic region, plastic region and failure. This loading pattern makes the analysis of the tendon biomechanical properties far more

complicated. The shear modulus measurements have to be done in the plane parallel to the orientation of the fibers as tendons may be described as a unidirectional arrangement of collagen fibers within a supporting matrix (Gennisson et al., 2003). Therefore, the determination of tendon stiffness through shear wave analysis remains valid, as demonstrated by previous studies (Helfenstein-Didier et al., 2016; Le Sant et al., 2015). Previous studies also showed a strong positive correlation between patellar tendon shear modulus and longitudinal Young‘s Modulus, ultimate force to failure and resistance to tensile loading in *in vitro* models (Martin et al., 2015; Yeh et al., 2016). Royer et al. showed that μ (shear modulus) is approximately one third of the E (Young’s modulus) in incompressible media, including most biological tissues (Royer et al., 2011) (μ=E/3). Thus, assuming a purely elastic medium, the shear modulus μ can be used to obtain the Young’s modulus E according to E=3μ, which means that the values of the Young's modulus increase as the shear modulus increases (Royer et al., 2011). Hence, SWE enables indirectly the measurement of biomechanical properties like Young’s modulus. Shear waves propagate faster in stiffer and contracted tissues and along the long axis of the tendon. In a study performed in healthy individuals, Aubry and collaborators confirmed that Achilles tendon stiffness increases with stretching and that c_S values are higher when measured parallel to the tendon fibers, as opposed to perpendicular, due to tendon anisotropy (Aubry et al., 2013).

In practice, the probe has to be applied with a light pressure, perpendicular to the surface. A primary limitation of SWE is the depth of penetration. Shallow depths may be accommodated by applying a generous layer of coupling US gel or an intermediate gel cushion. Some ultrasound devices may limit the shape, size and possible localization of the ROI for post-analysis. Most devices require a timeout of a few seconds before the next acquisition, which prevent real-time dynamic imaging of structures in motion.

As shown by several studies, SWE is a relevant tool in patellar tendon evaluation (Hsiao et al., 2015; Kot et al., 2012; Peltz et al., 2013; Zhang et al., 2015; Zhang et al., 2014; Zhang and Fu, 2013). SWE enables the measurement of the elastic properties without need of further calculations (Jiang et al., 2015; Kot et al., 2012) offering a useful tool in either healthy or injured tendons as well as for different structures in small and large joints (Ooi et al., 2016; Zhang et al., 2014).

SWE can be used in clinical cases in man. By quantifying the mechanical properties, SWE is complementary to US and CDUS (Klauser et al., 2014; Drakonaki et al., 2012) in diagnostic practice. Ultrasound elastography is widely used in diagnosis and follow-up in breast neoplasms (Song et al., 2018; Pesce et al., 2020), thyroid neoplasms (Tuan et al., 2020) and liver fibrosis (Trebicka et al., 2021). SWE helps evaluating diverse musculoskeletal tissues in pathologic or traumatic conditions like rotator cuff tendon (Deng et al., 2021; Yoo et al., 2020), Achilles tendon (Coombes et al., 2018), patellar tendon (Coombes et al., 2018) as well as muscles (Shinohara et al., 2010; Wang et al., 2014; Lacourpaille et al., 2015; Brandenburg et al., 2015; Le Sant et al. 2015; Hirata et al., 2016; Guilhem et al., 2016; Kuo et al., 2013; Carpenter et al., 2015; Itoigawa et al., 2015; Rosskopf et al., 2016a; Eby et al., 2015), ligaments (Shen et al., 2013; Mhanna et al., 2016; Wu et al., 2016) and nerves (Kantarci et al., 2014;

Palmeri et al., 2009; Andrade et al., 2016). Due to the relationship between elastographic and clinical parameters, SWE enables the evaluation of spasticity after botulinum toxine injection in muscles in children with spastic cerebral palsy (Bertan et al., 2020). Spastic muscles appear stiffer than healthy muscles, the stiffness decreasing after botulinum toxine injection. SWE may also evaluate the muscle spasticity after stroke (Eby et al., 2017). Despite this, musculoskeletal use for SWE remains very basic in daily use in a clinical setting.

Most of the research studies performed in humans have been conducted *in vivo*. They involved the patellar tendon (Can et al., 2021 ; Kuervers et al., 2021; Breda et al., 2020 ; Quack et al., 2020 ; Zhang C et al., 2020 ; Laubach et al., 2020; Gulledge et al., 2019 ; Tas et al., 2017b ; Hardy et al., 2017 ; Gatz et al., 2017), Achilles tendon (Gatz et al., 2021; Gatz et al., 2020; Gatz et al., 2017; Ivanac et al., 2021; Nunes et al., 2021; Gonzales et al., 2021; Otter et al., 2020; Ciloglu et al., 2020; Dirrichs et al., 2019; Payne et al., 2018; Haen et al., 2017), supraspinatus tendon (Deng et al., 2021; Yoo et al., 2020; Baumer et al., 2017), infraspinatus tendon (Yu et al., 2021) common extensor tendon (lateral epicondylitis) (Zhu et al., 2020; Sendur et al., 2019), semitendinosus tendon (Itoigawa et al., 2018), and flexor pollicis longus tendon (Bai et al., 2021). Most of these studies were prospective.

Studies in man demonstrated an increased stiffness in healthy tendons (Yeh et al., 2016) compared to diseased tendon with a decreased SWV or shear modulus (Deng et al., 2021; Otter et al., 2020; Zhu et al., 2020; Gatz et al., 2020; Dewall et al., 2014; Ooi et al., 2016, Zhang et al., 2014). Deng et al. thought that SWE might identify the degree of supraspinatus tendon tear (Deng et al., 2021). Decreased SWV was also found postoperatively in the patellar tendon after total knee arthroplasty (Quack et al., 2020; Laubach et al., 2020) or high tibial osteotomy (Botanlioglu et al., 2016), in patients with Achilles tendon tear (Ivanac et al., 2021), and with lateral gastrocnemius tendon tear (Martin et al., 2015). Similarly, Bai et al. noted a lower Young's modulus, measured by SWE, when the tendon of the flexor pollicis longus was severed after volar plate fixation for distal radius fracture than when the tendon remained intact (Bai et al., 2021). During natural healing and after treatment, reduced SWE values increased during the course of time (Quack et al., 2020; Zhu et al., 2020; Ciloglu et al., 2020; Tamura et al, 2017a; Tamura et al., 2017b; Lustgarten et al., 2015). For example, in patients who have undergone anterior cruciate ligament reconstruction with a patellar tendon autograft, mean SWV increased overtime after the surgery (Gulledge et al., 2019). Whilst US and CDUS could not show significant alterations over time, SWE revealed a significant increase of elastic properties over time after extracorporeal shock wave therapy in Achilles tendon (Gatz et al., 2021). These authors also demonstrated that SWE is a more sensitive tool to describe symptom development than US or CDUS during conservative treatment (Gatz et al., 2017). In addition, Nunes et al. noted a lower shear modulus in symptomatic postoperative Achilles tendons than in asymptomatic specimens (Nunes et al., 2021). Several studies noted an increased shear elastic modulus or SWV in athletes versus nonathletes (Can et al., 2021; Gonzales et al., 2021; Dirrichs et al., 2019). Interestingly, an excellent intraobserver reliability and good interobserver reliability of SWE measurements was shown (Breda et al., 2020; Tas al., 2017b; Yu et al., 2021; Zhu et al., 2020; Sendur et al., 2019; Payne et al., 2018; Baumer et al., 2017; Tamura et al, 2017a; Tamura et al,

2017b; Zhang et al. 2013; Del Signore et al., 2021) as well as a good repeatability (Baumer et al., 2017; Piccionello et al. 2018; Zhang et al. 2013).

Possible influencing factors on SWE measures were also investigated. Gonzales et al. noted no significant differences between male and female athletes (Gonzales et al., 2021). A study by Yu et al. investigating infraspinatus tendon showed a lower value of shear modulus in the infraspinatus tendon in women compared to men (Yu et al., 2021). Itoigawa et al. also showed a higher stiffness in males than in females in the tendon of the semitendinosus muscle (Itoigawa et al., 2018). Hsiao et al. revealed a reduction in the shear modulus in patellar tendon with ageing (Hsiao et al., 2015). SWV was shown to be higher in the flexed knee (Kuervers et al., 2021; Hardy et al., 2017). As shown by Hardy et al., the lowest shear modulus was obtained at rest with the knee in a fully extended position (Hardy et al., 2017). Hence, the importance of defining the parameters well before any study in order to allow comparison of the results.

Obviously, comparisons between SWE and biomechanical tests remain scarce in man. A study performed *ex vivo* in human Achilles tendon demonstrated a statistical correlation between shear modulus given by SWE and elastic modulus given by tensile test (Haen et al., 2017).

In animals, research studies were conducted either *in vivo* or *ex vivo*. They involved the patellar tendon, Achilles tendon, superficial digital flexor tendon, and common digital extensor tendon. The animals were swine (Hsiao et al., 2020; Yeh et al., 2016; Dewall et al., 2014; Zhang et al. 2013), dogs (Del Signore et al., 2021; Piccionello et al. 2018), horses (Tamura et al, 2017a; Tamura et al, 2017b; Lustgarten et al., 2015), cattle (Rosskopf et al., 2016b) and rabbits (Martin et al., 2015). Several studies used sheep as a model. The sheep has been used to replicate aspects of rotator cuff injury and repair as well as the methods and materials employed in the surgical repair of rotator cuff tears (Baums et al., 2012; Jost et al., 2012; Maguire et al., 2011; Onay et al., 2013; Ostrander and McKinney, 2012<; Savage et al., 2013). Sheep have also been used to investigate the use of potential regenerative agents i.e., growth factors (Hee et al., 2011). An ovine model has been used to characterise flexor tendon injury and repair (Martinello et al., 2013). To date, no study on the correlation between SWE and biomechanical properties on the ovine patellar tendon has been published.

5.2. Material and Methods

Animals

Six ewes (Île-de-France; n= 6), from the Ovine Research Center of the University of Namur, were used. Their age ranged from 2 to 8 years. Previously to testing, the animals were kept free of movement in an outside paddock. Palpation of their stifle and locomotion were normal. No swelling, pain or lameness was observed. The experimental protocol 19006 VA was approved by the local ethical committee for animal welfare.

Ultrasound Examination

Animals were hold in a sitting position, in a chair specifically designed for sheep studies (Figure 21). Before ultrasound assessment, both left and right stifles were clipped, cleaned with water and soap, and shaved. The ultrasound examinations were performed with a high-resolution US scan (RS 85 Ultrasound System, Samsung Medison Co., Ltd Seoul Korea). A generous amount of coupling gel was used to improve transmission of US waves. The ultrasound transducer was hold manually for all examinations. All investigations were made at room temperature, with the tibia and femur forming an angle of approximately 95°. The examinations were performed by a radiologist with more than 20 years of experience in musculoskeletal ultrasound. All the data were acquired on the same day.

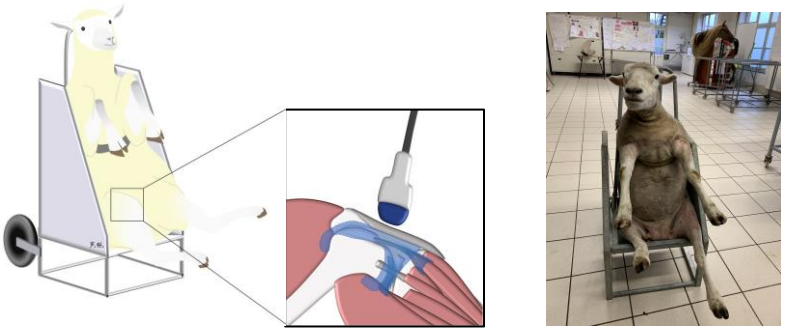


Figure 21: Position of the sheep during SWE. Study conducted with the sheep in a sitting position, hold by an abdominal strap in a dedicated chair.

2D Ultrasound

US examination included the evaluation of the entire patellar tendon, the patellar and tibial tuberosity attachments, the adjacent cranial soft tissues and the patellar fat pad using a L3-12A and LA4-18B linear-array transducer.
Tendon echogenicity and homogeneity were assessed in transverse and longitudinal planes. Abnormalities were searched and recorded if present.

Color Doppler Ultrasound

Potential neovascularization, that could be a sign of tendon disorder, was assessed by CDUS, using the LA4-18B linear-array transducer, in transverse and longitudinal planes. The entire patellar tendon and the adjacent soft tissues were explored.

Shear Wave Elastography

2D ultrasound was used to locate the patellar tendon and align the transducer longitudinally with the tendon fibers. When a correct image of the patellar tendon, without artifacts, was obtained, the shear wave mode was activated to obtain a color-coded elastogram. Through a dual display, the fiber-transducer alignment was constantly verified. The size of the rectangular acquisition box was defined previously to the data acquisition, to maximize the amount of tissue analyzed, avoiding the tendon extremities. The diameter of the circular ROI (region of interest) was held constant at 0.3 cm throughout the measurements in all the limbs. The ROI was set manually and was centered on the targeted patellar tendon.
SWE was assessed in a longitudinal plane, parallel to the fiber orientation, with light pressure on the skin, basically in the mid portion of the tendon, avoiding the tendon extremities, using a LA2-9A linear-array transducer. The transducer was kept motionless during 8-12 seconds to acquire the color-coded elastogram. When the color in the color-coded elastogram was uniform, the image was frozen enabling an off-line analysis through the captured images (Figure 22). Three images were captured, with 6 measurements on each. For each PT, the SWV was assessed, expressed in m/s, as well as the shear elastic modulus expressed in kPa. In our study, we considered the SWV for correlations.

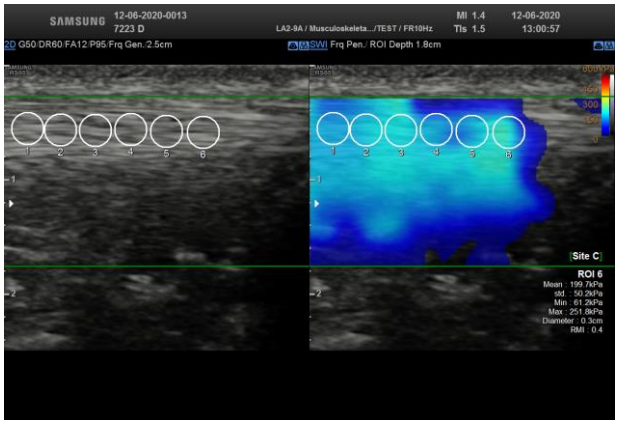


Figure 22: SWE of the patellar tendon. Dual display showing a 2D ultrasound image (left) used to locate the patellar tendon and align the tendon fibers longitudinally with the transducer. When a correct image of the patellar tendon was obtained, the shear wave mode was activated to obtain a color-coded elastogram. Three images were captured, with 6 measurements on each (right).

Gross Anatomy

Animals were sacrificed by intravenous administration of pentobarbital (150 mg/kg). Both hind limbs were transected at the level of the mid-femur, immediately after death. The patellar tendon and its attachments on the patella and the tibial tuberosity were carefully dissected. The patella and tibial tuberosity were sawed at 1.5 cm from their tendon attachment in order to not affect the tendon insertion areas that are fundamental for transferring loads.
Each harvested specimen consisting of an intact "patella-patellar tendon-tibial tuberosity" unit was individually wrapped in moistened gauze (with 0.9 % w/v NaCl), sealed in plastic bags, individually identified by a number and stored at -20°C until processed for biomechanical tests.

Biomechanical Tests

All specimens were submitted to biomechanical tests on a same day. In six matched pairs of limbs (n=12), a uniaxial tensile test was performed on patellar tendons following the procedure described in a former study (Innocenti et al., 2018). The frozen "patella-patellar tendon-proximal tibial" units were thawed to room temperature, cleaned thoroughly with 0.9 % w/v of NaCl solution and placed on a metal frame. The osseous parts of the specimen were cut with pliers to fit the clamp size (Figure 23).

The camera was set to 100 fps. Force outputs were obtained via a dedicated 1 kN load cell (Lloyd Instruments Ltd). A series of 10 preconditioning stress-relaxation procedures were performed to obtain a good alignment of fibers prior to tensile testing since tendons had been previously manipulated and then stored at -20° C. As suggested in the ASTM D638 standard (ASTM International, 2014), the tensile test was performed with a crosshead speed of 5 mm/min. The axial force was recorded and paired with the relative displacement during the tests. The tensile test was performed until failure. The resulting force-displacement curve was analyzed. The linear region of the curve, corresponding to the elastic region, i.e., the elongation of the helical structure of collagen (Kirkendall et Garrett, 1997), was determined thanks to a dedicated software: a linear fitting process was used to determine the boundaries of the linear region and this latter was studied to obtain the relative stiffness of the tissue (obtained from the slope of the curve in the selected region). Tendon stiffness, expressed in N/mm, is defined as the ratio between the force applied on the tendon and the change of the tendon length.

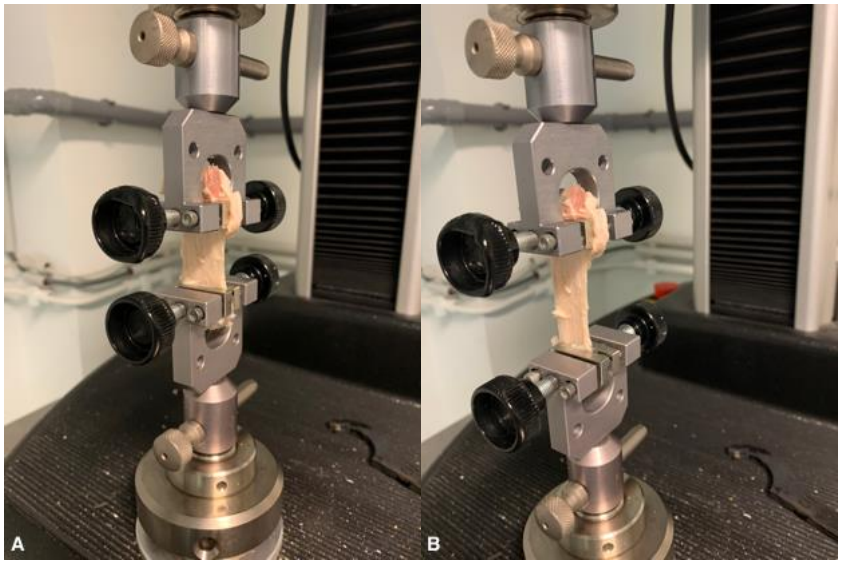


Figure 23: Patella-patellar tendon-tibial tuberosity unit placed on a metal frame at two different time points during the test. Patella-patellar tendon-tibial tuberosity unit fixed by two clamps. A: at the beginning of the uniaxial tensile test. B: at a more advanced phase of the uniaxial tensile test.

Statistical Analysis

Kolmogorov-Smirnov and Shapiro-Wilk tests were used to examine the normality of data (stiffness). Due to the normality of data, parametric tests were used. The Paired T test was used to compare observations that were not independent (difference in stiffness between left and right hindlimbs). Since there was no difference, one limb was randomly chosen within each pair and data obtained from that limb (SWV, tendon stiffness) was used for analysis. Correlations between mechanically measured SWV and tendon stiffness and age were assessed by Pearson correlation coefficient. Data were collected in Microsoft Excel and were analyzed using Graph Pad Prism 8. A p-value less than 0.05 was considered to indicate a statistically significant difference.

5.3. Results

On ultrasound all tendons presented a homogeneous fibrillar structure. We noted no focal or global abnormal thickening. We found no abnormalities in the patellar and tibial tuberosity attachments. The cranial soft tissues adjacent to the patellar tendon and the patellar fat pad were homogeneous in all cases. No neovascularization was observed by CDUS nor in the patellar tendon neither in the adjacent soft tissues.
The mean stiffness value of the 12 tendons was 45.69 N/mm (SD+/- 14.56). The tendon stiffness increased until failure.
Since there was no difference in patellar tendon stiffness between left and right hindlimbs, one limb was randomly chosen within each pair and data obtained from that limb (tendon stiffness) was used for analysis. Our tests confirmed that the patellar tendon had a typical non-linear behavior (Figure 24).

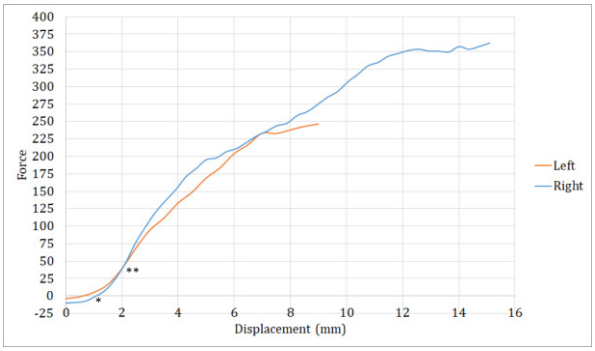


Figure 24: Force-diplacement test relating the stiffness curve. Force-Displacement curve in the corresponding left and right leg showing the initial toe region (*) and the linear region (**).

On SWE, the mean SWV value within the ROI was 6.27 m/s (SD+/-0.6).
We found a statistically not significant positive correlation between SWV and age (r=0.137, p=0.79).
Our data showed a significant positive correlation (r=0.87; p=0.02) between stiffness and SWV (Figure 25).

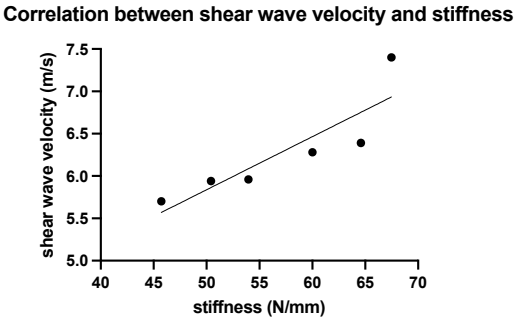


Figure 25: Correlation plot between shear wave velocity (m/s) and stiffness (N/mm). Correlation was significantly positive between shear wave velocity and stiffness.

5.4. Discussion

In this study the mean stiffness of patellar tendons was 45.69 N/mm (SD+/- 14.56). As previous studies were conducted in other animal models and reported only Young's modulus, our data constitute, to the best of our knowledge, the first reference values for patellar tendon stiffness in sheep.
With soft tissue structures, as they are quite irregular, the estimation of the cross-sectional area during the test may be quite difficult and could induce some measure errors in the determination of the stress (ratio between the force applied and the cross-sectional area) and therefore of the Elastic Modulus. For that reason, we decided to measure the stiffness as our technique is accurate in evaluating force and displacement.
Moreover, stiffness is a structural property, i.e., a property of the tendon as a whole, while elasticity is a material property (related to the material that constitutes a structure), meaning that it could change locally and not be homogeneous along the tendon length.
We found a statistically not significant positive correlation between SWV and age (r=0.137, p=0.79). This may be explained by progressive stiffening of connective tissues with ageing as shown in a study performed in canine patellar tendons (Haut and al., 1992). Similarly, a former study showed altered passive biomechanical properties of the muscle-tendon unit in normal ageing rats, with increased stiffness and decreased relaxation response in the Achilles tendons of middle-aged animals (Plate and al. 2013). The association between ageing and increased tendon stiffness

may have different explanations. Collagen crosslinks, resulting from the formation of advanced glycation end products, limit fiber-fiber and fibril-fibril sliding, reduce the viscoelasticity of the tendon and increase the tendon stiffness (Gautieri et al., 2017). Concomitantly fascicle sliding has been described to decrease with ageing (Thorpe et al., 2013). The reduced gliding properties of fascicular sheets may be explained by decreased proteoglycan 4 and elastin mRNA expression in tendons (Kostrominova and Brooks, 2013).

In the current study, a mean value of SWV of 6.27 m/s (SD+/-0.6) was found and there was a significant positive correlation (r=0.87; p=0.02) between stiffness and SWV. A former study performed *ex vivo* in human Achilles tendon by Haen et al. demonstrated a statistical correlation between shear modulus given by SWE and elastic modulus given by tensile test (Haen et al., 2017). Feng et al. showed a significant correlation between shear wave modulus and stiffness index obtained from a hand-held Myoton PRO device in healthy human Achilles tendon (Feng et al., 2018). Several *ex vivo* studies performed in swine (Hsiao et al., 2020; Zhang and Fu, 2013), New Zealand white rabbits (Martin et al., 2015) and bovines (Rosskopf et al., 2016b) showed a linear correlation between SWV measured by SWE and Young's modulus given by biomechanical tests.

Most studies have correlated *ex vivo* measurement of SWE to *ex vivo* biomechanical testing of dissected tendons (Haen et al., 2017; Feng et al., 2018; Martin et al., 2015; Hsiao et al., 2020; Zhang and Fu, 2013; Rosskopf et al., 2016b). The originality of our study was to investigate, *in vivo,* the patellar tendon biomechanical properties and to correlate them directly to the *ex vivo* biomechanical testing of dissected bone-tendon-bone units, creating a baseline database for further research use in testing therapeutics for tendon healing.

By connecting bone to bone, the patellar tendon is different from other tendons. A greater portion of the tendon is in proximity to bony insertion sites that may result in a tendon with a greater range of stiffness values. Therefore, the tendon may be more susceptible to subtle changes in the imaging area that occur between testing sessions or trials as pointed out by Peltz et al. (Peltz et al., 2013). In the present study, the ultrasonographer was aware of ultrasonography anatomy of the ovine stifle and dedicated time to adequately position the transducer at mid-tendon, to avoid bias in measurement of the tendon SWE.

However, our study has some limitations. First, though the position of the animal in the chair and the position of the limbs and instruments were held constant, since we performed the SWE in living non-sedated animal knee joint movement control was not always optimal and eventually muscle contracture may have changed slightly the flexion angle of the stifle and therefore the SWV values. Former studies reported variations of SWE measurements with knee flexion. Shear elastic modulus (Hardy et al., 2017) and shear wave velocity (Kuervers et al., 2021) were shown to be higher in the flexed knee. It is important to consider the conditions of measurement techniques well before any study in order to allow comparison of the results (Yu et al., 2021). In our study we controlled the testing position as much as possible to avoid this influence, but minimal limb movement cannot be excluded. In upcoming studies, a custom-designed mold with straps to keep the limb in a fixed position could be

developed. Unfortunately, all sheep do not support being constrained and sedation might be required, what could induce another bias.

Second, SWE was performed *in vivo*, in a relative static condition, opposed to the force-displacement test conducted *ex vivo*, in a non-static manner, with progressive force application. But that was precisely the objective of this study to compare non-invasive *in vivo* techniques to post-mortem *ex vivo* methods. We showed that SWV obtained in clinical condition i.e., in living animals, is correlated to SWV values obtained *ex vivo*. Similarly, Haen et al. reported that shear wave modulus in clinical-like condition was significantly correlated to shear modulus in harvested, not yet elongated Achilles tendon (Haen et al., 2017).

Third, although bone insertions were preserved for optimal tendon fixation during tensile test, a minimal slippage in the clamps may have occurred.

Fourth, our study included a small number of limbs. The known wide range of normal patellar tendon shear modulus (Zhang et al., 2015; Kot et al.; 2012, Mannarino et al., 2018), and hence SWV, may require a larger sample to be tested in order to obtain more reliable reference values.

To date, due to the subjective nature of the available common clinical evaluation methods, the success of conservative, non-conservative and rehabilitative treatments remains still controversial. Assessing healing as outcomes is important. The ovine patellar tendon could be used as a research model by creating injury either by surgery or by collagenase technique. SWE would allow a quantitative manner to track tendon stiffness changing in the healing process and assess the efficacy of novel therapies. The improved tendon mechanical properties, as measured by SWE, may be considered as an objective evaluation in tendon recovery.

Another future challenge for clinicians and researchers is the early detection of the disease that would allow effective strategies to attenuate the disease process before its chronic development. We can speculate that SWE may detect early changes in biomechanical properties related to tendinopathy, even before any changing may be diagnosed on US or CDUS. Currently, the effects of those novel management strategies on shortening or improving the healing process are based on some animal studies, as New Zealand white rabbits (Martin et al., 2015), but none have been conducted in sheep.

Even if our study showed that age does not seem to have a major impact on biomechanical results, the most appropriate sheep population for those future studies would be young adults since there are indications in the scientific literature that degradation of the biomechanical properties can occur with age (Gautieri et al. 2017).

In conclusion, by assessing tendon properties, SWE may be a promising technique to improve tendon disease diagnosis and to assess progress, tendon healing and efficacy of treatments or interventions. Shear wave modulus values obtained in our study could be considered as preliminary reference values in ovine patellar tendon for further research studies.

6. CONCLUSIONS-DISCUSSION-PERSPECTIVES

Could we use the sheep as a model for patellar tendon disorders?

We showed that the sheep is an appropriate animal model for the study of the patellar tendon. The ultrasound anatomy of the stifle is quite similar to that in man both in its superficial position, easy access, bone insertions and in its appearance on ultrasound i.e., echogenicity and homogeneity and absence of vascularization on CDU in normal tendons. Until now dogs, pigs, horses, rabbits, goats and sheep have been used as large animal model in musculoskeletal research. Proffen et al. compared the intra-articular knee anatomy i.e., anterior cruciate ligament, posterior cruciate ligament, medial meniscus, lateral meniscus, intercondylar notch in cow, sheep, goat, dog, pig and rabbit to that of human (Proffen et al., 2012). All the measurements were normalized by the width of tibial plateau for comparison between knees of different sizes. They found an overall conservation of the relative size but not the absolute size among the species. The sheep was the most suitable model for different intra-articular structures. Considering the results of that study as well as those from our study, the ovine stifle, in particular the patellar tendon, seems to be an appropriate large animal model for future research studies on tendon disorders and conventional US would be an essential imaging technique.

According to the theory of the continuum in tendon pathology, US may detect tendon thickening during reactive tendon phase, a reversible stage. At the tendon disrepair phase, there may be evidence of increased vascularity, accurately diagnosed by CDU. At the degenerative tendinopathy phase, US describes areas of degeneration scattered throughout the tendon and interspersed with parts of the tendon that are in the disrepair phase and normal sections of tendon. The tendon can be thickened and present with nodular sections at US. Hence high frequency US could be used to evaluate and quantify tendinopathy and monitor treatment. This may help to determine the onset of tendinopathic changes and aid the staging of tendinopathy. Early diagnosis of tendon changes by US may improve the management of ongoing tendon injuries and thus prevent tendon degeneration. However, this remains to be demonstrated in an ovine model of tendon disorder, for example after inducing the disease.

To date, patellar tendons of mice and rats have been used frequently as animal models in the development of an *in vivo* fatigue model by cyclic loading showing that the accumulation of microdamage leads to subsequent changings in biomechanical function (Sereysky JB et al., 2012).

Lesions can be induced chemically, by a collagenase injection (Williams et al., 1984). This chemically induced tendinopathy mimicks acute tendinitis. To obtain a more realistic animal model of overuse tendinopathy, chemically and mechanically jointly induced tendinopathy should be analyzed. Mechanical induced overuse tendinopathy may be obtained by either active muscle contraction using electrical stimulation or direct stretching of the tendon using an external device (Lee et al., 2006) or a

surgically created core lesion (Schramme et al., 2010). A fatigue load by applying a load to the patellar tendon as studied in rat may be attempted (Lee et al., 2006) in the ovine patellar tendon. To this purpose, after small incisions, clamps should be secured to the patella and tibia allowing a load to be applied to the patellar tendon. The patellar tendon is the only tendon enabling mechanical loading through bony attachment for clamping without inducing a compressive injury of the tendon. Sheep would be an appropriate animal model due to its larger size and subsequently bigger tendons enabling correct SWE examinations.

Those different techniques could be used in the sheep. Currently there is no real advantage of one method over the other. Both chemically and mechanically induced patellar tendinopathy should be prompted concurrently to reproduce a multifactorial etiology. Collagenase injection could be performed under ultrasound control, without anesthesia. Unlike the chemical technique, an issue in the use of the mechanical overloading techniques is the need for general anesthesia. A within-animal study could enable comparison between the diseased tendon and the contralateral healthy tendon used as a control.

The patellar tendon is an interesting tendon for studies because it experiences high-force cyclical loading, is often used for harvesting during anterior cruciate ligament repairs and is often involved in tendinopathy. Moreover, patellar tendon is easy to dissect due to its superficial localization, and portions of the tendon may be dissected mimicking clinically relevant injuries.

Could we use biomechanical tests in an ovine model of patellar tendinopathy?

We studied the mechanical properties of the patellar tendon by a uniaxial tensile testing method. This technique enables the measurement of either the tendon stiffness, an extrinsic structural property of the tendon, or the elastic modulus, an intrinsic material property of the tendon. In our study we decided to measure the stiffness as our technique was quite accurate in evaluating force and displacement. With irregular soft tissue structures such as the patellar tendon, the estimation of the cross-sectional area during the test may be quite difficult and could induce some estimation errors in the measurements that could lead to a reduced accuracy in the determination of the stress and therefore of the elastic modulus. Moreover, stiffness is a property of the tendon as a whole, while elasticity is related to the material that constitutes a structure, meaning that it could change locally and it is not necessarily homogeneous along the tendon length. By using a load-displacement test we addressed the whole tendon system and not only the material it is composed by. Our study provided reference values of stiffness in healthy tendons, providing useful baseline values.

This test should be used in future studies as a gold standard assessment. The contralateral healthy limb would be used for comparison. However, this will be possible only in euthanized animals. This is not possible when outcome measures must be obtained overtime in the same animal in longitudinal studies.

How could we use SWV assessed by elastography as a surrogate of stiffness given by tensile test in an ovine model of patellar tendon tendinopathy?

Tendon biomechanical parameters enable better quantifying the state of tissue healing over time, but inconveniently these measures cannot be recorded *in vivo* due to the invasive nature of the available conventional biomechanical testing methods. Our study showed that SWE can be a good surrogate to invasive tensile test by recording the elastic modulus and SWV *in vivo*.

Patellar tendon would be an accurate research model due to its easy accessibility and the fact that the anisotropy, typical of tendons, can be reduced by bending slightly the knee. To maintain the limb in a fixed position, with a constant knee flexion angle, a custom-made knee stabilizer with straps should be developed in order to improve the accuracy of measures. As shown in previous studies, two different structures with similar composition can present different shear modulus values on SWE if subjected to different tension/flexion during evaluation (Dubois et al., 2015; Fontenelle et al., 2018; Gennisson et al., 2010; Kot et al., 2012).

To get meaningful data in a research setting, standardization of various technical settings is required. Before examination, the knee would have to stay in the same position during at least 5 minutes to ensure that the tendon is in a resting phase. The probe has to be applied with a light pressure, perpendicular to the surface, and parallel to the orientation of the fibers. A generous layer of coupling US gel or an intermediate gel cushion should be applied. The ROI size should be slightly lower than the tendon diameter to avoid pollution by non-tendinous values. The acquisition time should not be too long (less than 20 seconds) in order to avoid transducer shifting that may be responsible for non-conforming SWV and elastic modulus values. Moreover, the injured tendon should be compared to the contralateral healthy tendon used as a baseline value. Finally, as the elastic modulus and SWV may vary among different SWE systems and machines, the user has to acquire the values proper to the specific machine in use (Rosskopf et al., 2016b; Kot et al., 2012). In a longitudinal study the same SWE system should be used. A limitation of our study was that all the SWE examinations were performed by one operator. Moreover, all examinations were done on the same day. In a future study, repeatability of SWE in ovine patellar tendon should be assessed. Optimally different operators should perform the SWE, on different days, allowing to test intraoperator and interoperator reproducibility. In a future study SWE should be acquired in different anatomical zones of the patellar tendon i.e., enthesis, pre-insertional area and mid-portion in order to obtain a range of values corresponding to the different areas. A former study performed in Achilles tendon showed an increasing stiffness from the musculo-tendinous junction to the enthesis area (Petitpierre et al., 2018). This may be explained by the presence of fibro-cartilage increasing the tendon stiffness. A reason for the delayed clinical implementation of SWE in musculoskeletal system is the difficulty to obtain reliable SWV measurements.

In an animal model, the improved tendon mechanical properties, as measured by SWE, may be considered as an objective evaluation in tendon recovery. SWE would

allow a quantitative manner to track tendon stiffness changing in the healing process, assessing the efficacy of novel therapies and improving the outcome. By quantifying the mechanical properties, SWE is complementary to US and CDUS (Klauser et al., 2014; Drakonaki et al., 2012). In a future research setting comparing two different treatments, we suggest to consider the comparative values rather than the absolute values, due to the variation of these values among the different tendons and species (Malliaras et al., 2013; Tardioli et al., 2012; Zhang et al., 2015; Zhang et al., 2014).

One of the future challenges for clinicians and researchers would be early detection of the disease that would allow effective strategies to attenuate the progress of the disease before its chronic installation. SWE may detect early changes in biomechanical properties related to tendinopathy, even before any changing may be diagnosed on US or CDUS. In the area of disease detection, innovative imaging techniques seem to be of great interest. In the area of prevention, tendon changing revealed by SWE may be interesting in follow-up of disease risk factor modification. However, in the ovine model, this remains to be demonstrated.

SWE could also be considered in other species. In horses for example, tendinopathy is common. The introduction of elastography, in particular SWE, shows promising results and might find wider use in equine practice as clinical development continues. The detection of subclinical tendon damage before clinical apparent tendinopathy promises individual rehabilitation and a decreased risk of re-injury. Finally, due to its non-invasive nature, SWE would limit animal sacrifice and be part of the 3R efforts requested in animal research.

7. REFERENCES

Abat F, Alfredson H, Cucchiarini M, Madry H, Marmotti A, Mouton C, Oliveira JM, Pereira H, Peretti GM, Romero-Rodriguez D, Spang C, Stephen, J, van Bergen CJA, de Girolamo L. Current trends in tendinopathy: consensus of the ESSKA basic science committee. Part I: biology, biomechanics, anatomy and an exercise-based approach. J Exp Orthop. 2017 Dec; 4:18. doi: 10.1186/s40634-017-0092-6

Ackermann PW, Renström P. Tendinopathy in Sport. Sports Health. 2012 May; 4(3): 193–201. doi:10.1177/1941738112440957

Aicale R, Tarantino D, Maffulli N. Surgery in Tendinopathies. Sports Med Arthrosc Rev. 2018 Dec; 26(4):200–202. doi: 10.1097/JSA.0000000000000214

Aigner T, Cook JL, Gerwin N, Glasson SS, Laverty S, Little CB, McIlwraith W, Kraus VB. Histopathology atlas of animal model systems - overview of guiding principles. Osteoarthritis Cartilage. 2010 Oct; 18 Suppl 3: S2–S6. doi: 10.1016/j.joca.2010.07.013

Allen MJ, Houlton JE, Adams SB, Rushton N. The surgical anatomy of the stifle joint in sheep. Vet Surg. 1998 Nov-Dec; 27(6):596–605. doi: 10.1111/j.1532-950X.1998.tb00536.x

Almekinders LC, Almekinders SV. Outcome in the treatment of chronic overuse sports injuries: a retrospective study. J Orthop Sports Phys Ther. 1994 Mar; 19(3):157-161. doi: 10.2519/jospt.1994.19.3.157

Almekinders LC, Vellema JH, Weinhold PS. Strain patterns in the patellar tendon and the implications for patellar tendinopathy. Knee Surg Sports Traumatol Arthrosc. 2002 Jan; 10(1):2-5. doi: 10.1007/s001670100224

Almekinders LC, Weinhold PS, Maffulli N. Compression etiology in tendinopathy. Clin Sports Med. 2003 Oct; 22(4):703-710. doi: 10.1016/s0278-5919(03)00067-x

Alves TI, Girish G, Kalume Brigido M, Jacobson JA. US of the Knee: Scanning techniques, pitfalls, and pathologic conditions. Radiographics. 2016 Oct; 36(6):1759–1775. doi: 10.1148 rg.2016160019

American College of Sports Medicine. American College of Sports Medicine position stand. Progression models in resistance training for healthy adults. Med Sci Sports Exerc. 2009 Mar; 41(3):687–708, 2009. doi: 10.1249/MSS.0b013e3181915670

Amis A, Camburn M, Kempson S, Radford W, Stead A. Anterior cruciate ligament replacement with polyester fibre. A long-term study of tissue reactions and joint stability in sheep. J Bone Joint Surg Br. 1992 Jul; 74(4): 605–613. doi :10.1302/0301-620X.74B4.1624524

Andarawis-Puri N, Flatow EL, Soslowsky LJ. Tendon basic science: Development, repair, regeneration, and healing. J Orthop Res. 2015 Jun; 33(6):780–784. doi:10.1002/jor.22869

Andrade RJ, Nordez A, Hug F, Ates F, Coppieters MW, Pezarat-Correia P, Freitas SR. Non-invasive assessment of sciatic nerve stiffness during human ankle motion using ultrasound shear wave elastography. J Biomech 2016 Feb;49(3):326–331. doi: 10.1016/j.jbiomech.2015.12.017

Appleyard RC, Ghosh P, Swain MV. Biomechanical, histological and immunohistological studies of patellar cartilage in an ovine model of osteoarthritis induced by lateral meniscectomy. Osteoarthritis Cartilage. 1999 May; 7(3):281–294. doi: 10.1053/ joca.1998.0202

Arnout N, Myncke J, Vanlauwe J, Labey L, Lismont D, Bellemans J. The influence of freezing on the tensile strength of tendon grafts: a biomechanical study. Acta Orthop Belg. 2013 Aug; 79(4):435-443

ASTM D638, "Standard Test Method for Tensile Properties of Plastics," ASTM Int. 2014, December 15

ASTM International. 2003. Standard test method for tensile properties of plastics. ASTM Int. 8: 46-58

Aström M. Laser Doppler flowmetry in the assessment of tendon blood flow. Scand J Med Sci Sports. 2000 Dec; 10(6):365-7. doi: 10.1034/j.1600-0838.2000.010006365.x

Atkinson TS, Atkinson PJ, Mendenhall HV, Haut RC. Patellar tendon and infrapatellar fat pad healing after harvest of an ACL graft. J Surg Res. 1998 Sep; 79(1):25-30. doi: 10.1006/jsre.1998.5387

Atlas of NonTumor Pathology-Non-Neoplastic Diseases of Bones and Joints, American Registry of Pathology, Armed Forces Institute of Pathology, First Series, Fascicle 9, 2011

Aubry S, Risson JR, Kastler A, Barbier-Brion B, Siliman G, Runge M, Kastler B. Biomechanical properties of the calcaneal tendon in vivo assessed by transient shear wave elastography. Skeletal Radiol. 2013 Aug; 42(8):1143–1150. doi: 10.1007/s00256-013-1649-9

Bai X, Liu Z, Wang B. Shear Wave Elastography (SWE) Evaluation of asymptomatic flexor pollicis longus tendon condition after volar plate fixation for distal radius fracture. Int J Gen Med. 2021 Jan; 14: 187–193. doi: 10.2147/IJGM.S290017

Battery L, Maffulli N. Inflammation in overuse tendon injuries. Sports Med Arthrosc Rev. 2011 Sep; 19(3):213-217. doi: 10.1097/JSA.0b013e31820e6a92

Baumer TG, Davis L, Dischler J, Siegal DS, van Holsbeeck M, Moutzouros V, Bey MJ. Shear wave elastography of the supraspinatus muscle and tendon: Repeatability and preliminary findings. J Biomech. 2017 Feb 28; 53:201-204. doi: 10.1016/j.jbiomech.2017.01.008

Baums MH, Spahn G, Buchhorn GH, Schultz W, Hofmann L, Klinger HM. Biomechanical and magnetic resonance imaging evaluation of a single- and double-row rotator cuff repair in an in vivo sheep model. Arthroscopy. 2012 Jun; 28(6):769-777. doi:10.1016/j.arthro.2011.11.019

Beaufils P, Pujol N. Meniscal repair: Technique. Orthop Traumatol Surg Res. 2018 Feb; 104(1S): S137–S145. doi: 10.1016/j.otsr.2017.04.016

Benjamin M, Kaiser E, Milz S. Structure-function relationships in tendons. A review. J Anat. 2008 Mar; 212(3):211-228. doi: 10.1111/j.1469-7580.2008.00864.x

Benjamin M, Toumi H, Ralphs JR, Bydder G, Best TM, Milz S. Where tendons and ligaments meet bone: Attachment sites ('entheses') in relation to exercise and/or mechanical load. J Anat. 2006 Apr; 208(4):471–490. doi: 10.1111/j.1469-7580.2006.00540.x

Bercoff J, Tanter M, Fink M. Supersonic shear imaging: a new technique for soft tissue elasticity mapping. IEEE Trans Ultrason Ferroelectr Freq Control. 2004 Apr; 51(4):396–409. doi: 10.1109/tuffc.2004.1295425

Berko NS, Mehta AK, Levin TL, Schulz JF. Effect of knee position on the ultrasound elastography appearance of the patellar tendon. Clin Radiol. 2015 Oct; 70(10):1083–1086. doi: 10.1016/j.crad.2015.06.100

Bertan H, Oncu J, Vanli E, Alptekin K, Sahillioglu A, Kuran B, Yilmaz F. Use of Shear Wave Elastography for quantitative assessment of muscle stiffness after botulinum toxin injection in children with cerebral palsy. J Ultrasound Med. 2020 Dec; 39(12):2327-2337. doi:10.1002/jum.15342

Beveridge JE, Heard BJ, Brown JJ, Shrive NG, Frank CB. A new measure of tibia femoral subchondral bone interactions that correlates with early cartilage damage in injured sheep. J Orthop Res. 2014 Oct; 32(10):1371–1380. doi: 10.1002/jor.22685

Beveridge JE, Shrive NG, Frank CB. Meniscectomy causes significant in vivo kinematic changes and mechanically induced focal chondral lesions in a sheep model. J Orthop Res. 2011 Sep; 29(9):1397–1405. doi: 10.1002/jor.21395

Bianchi S, Martinoli C, Bianchi-Zamorani MP, Valle M. Ultrasound of the joints. Eur Radiol. 2002 Jan; 12(1):56–61. doi: 10.1007/s00330-001-1162-8

Botanlioglu H, Kaynak G, Kantarci F, Guven MF, Zengin G, Aydingoz O. Length, thickness, and elasticity of the patellar tendon after closed wedge high tibial osteotomy: A shear wave elastographic study. J Orthop Surg 2016 Aug; 24(2):194–7. doi: 10.1177/1602400215

Brandenburg JE, Eby SF, Song P, Zhao H, Landry BW, Kingsley-Berg S, Bamlet WR, Chen S, Sieck GC, An KN. Feasibility and reliability of quantifying passive muscle stiffness in young children by using shear wave ultrasound elastography. J Ultrasound Med 2015 Apr; 34(4):663–670. doi: 10.7863/ultra.34.4.663

Breda SJ, van der Vlist A, de Vos RJ, Krestin GP, Oei EHG. The association between patellar tendon stiffness measured with shear-wave elastography and patellar tendinopathy: a case-control study. Eur Radiol. 2020 Nov; 30(11): 5942–5951. doi: 10.1007/s00330-020-06952-0

Brum J, Bernal M, Gennisson JL, Tanter M. In vivo evaluation of the elastic anisotropy of the human Achilles tendon using shear wave dispersion analysis. Phys Med Biol. 2014 Feb; 59(3):505-23. doi: 10.1088/0031-9155/59/3/505

Butler DL, Awad HA. Perspectives on cell and collagen composites for tendon repair. Clin Orthop Relat Res. 1999 Oct; (367 Suppl): S324-32. doi: 10.1097/00003086-199910001-00031

Cake MA, Read RA, Corfield G, Daniel A, Burkhardt D, Smith MM, Little CB. Comparison of gait and pathology out- comes of three meniscal procedures for induction of knee osteoarthritis in sheep. Osteoarthritis Cartilage. 2013 Jan; 21(1):226–236. doi: 10.1016/j.joca.2012.10.001

Can TS, Ozdemir S, Yilmaz BK. Shear-Wave Elastography of patellar ligament and Achilles tendon in semiprofessional athletes: Comparing with the nonexercising individuals. J Ultrasound Med. 2021 Dec. doi: 10.1002/jum.15908

Carpenter EL, Lau HA, Kolodny EH, Adler RS. Skeletal muscle in healthy subjects versus those with GNE-related myopathy: evaluation with shear-wave US-a pilot study. Radiology. 2015 Nov; 277(2):546–554. doi: 10.1148/radiol.2015142212

Carr AJ, Norris SH. The blood supply of the calcaneal tendon. J Bone Joint Surg Br. 1989 Jan; 71(1):100-1. doi: 10.1302/0301-620X.71B1.2914976

Chahla J, Dean C, Moatshe G, Mitchell J, Cram T, Yacuzzi C, LaPrade R. Meniscal ramp lesions. anatomy, incidence, diagnosis, and treatment. Orthop J Sports Med. 2016 Jul; 4(7):2325967116657815. doi: 10.1177/2325967116657815

Chen JM, Willers C, Xu J, Wang A, Zheng MH. Autologous tenocyte therapy using porcine-derived bioscaffolds for massive rotator cuff defect in rabbits. Tissue Eng. 2007 Jul; 13(7):1479–1491. doi: 10.1089/ten.2006.0266

Chevrier A, Nelea M, Hurtig M, Hoemann CD, Buschmann MD. Meniscus structure in human, sheep, and rabbit for animal models of meniscus repair. J Orthop Res. 2009 Sep; 27(9):1197–1203. doi: 10.1002/jor.20869

Chimenti RL, Cychosz CC, Hall MM, Phisitkul P. Current Concepts Review Update: Insertional Achilles Tendinopathy. Foot Ankle Int. 2017 Oct; 38(10):1160–1169. doi: 10.1177/1071100717723127

Chiu YH, Chang KV, Chen IJ, Wu WT, Ozçakar L. Utility of sonoelastography for the evaluation of rotator cuff tendon and pertinent disorders: a systematic review and meta-analysis. Eur Radiol. 2020 Dec; 30(12):6663-6672. doi:10.1007/s00330-020-07059-2

Ciloglu O, Görgülü FF. Evaluation of a torn Achilles tendon after surgical repair an Ultrasound and Elastographic study with 1-year follow-up. J Ultrasound Med. 2020 Jul; 39(7): 1263-1269. doi: 10.1002/jum.15214

Cinque M, Kennedy N, Moatshe G, Vinagre G, Chahla J, Hussain Z, LaPrade R. Osteochondral allograft transplants for large trochlear defects. Arthrosc Tech. 2017 Oct; 6(5): e1703–e1707. doi: 10.1016/j.eats.2017.06.027

Collins JJ. The redundant nature of locomotor optimization laws. J Biomech. 1995 Mar; 28(3):251-267. doi: 10.1016/0021-9290(94)00072-c

Cook JL, Purdam CR. Is tendon pathology a continuum? A pathology model to explain the clinical presentation of load-induced tendinopathy. Br J Sports Med. 2009 Jun; 43(6):409-416. doi: 10.1136/bjsm.2008.051193

Coombes BK, Tucker K, Vicenzino B, Vuvan V, Mellor R, Heales L, Nordez A, Hug F. Achilles and patellar tendinopathy display opposite changes in elastic properties: a shear wave elastography study. Scand J Med Sci Sports. 2018 Mar; 28(3): 1201-1208. doi: 10.1111/sms.12986

Couppé C, Kongsgaard M, Aagaard P, Vinther A, Boesen M, Kjaer M, Magnusson SP. Differences in tendon properties in elite badminton players with or without patellar tendinopathy. Scand J Med Sci Sports. 2013 Mar; 23(2):89–95. doi: 10.1111/sms.12023

Craig JG. Infection: Ultrasound-guided procedures. Radiol Clin North Am. 1999 Jul; 37(4):669–678. doi: 10.1016/ S0033-8389(05)70122-6

Culvenor AG, Cook JL, Warden SJ, Crossley KM. Infrapatellar fat pad size, but not patellar alignment, is associated with patellar tendinopathy. Scand J Med Sci Sports. 2011 Dec; 21(6): e405-411. doi: 10.1111/j.1600-0838.2011.01334.x

Danielson KG, Baribault H, Holmes DF, Graham H, Kadler KE, Iozzo RV. Targeted disruption of decorin leads to abnormal collagen fibril morphology and skin fragility. J Cell Biol. 1997 Feb; 136(3):729-743. doi: 10.1083/jcb.136.3.729

Davies SG, Baudouin CJ, King JB and Perry JD. Ultrasound, computed tomography and magnetic resonance imaging in patellar tendinitis. Clin Radiol. 1991 Jan; 43(1):52-56. doi:10.1016/s0009-9260(05)80355-1

Dean BJF, Dakin SG, Millar NL, Carr AJ. Review: Emerging concepts in the pathogenesis of tendinopathy. Surgeon. 2017 Dec; 15(6):349-354. doi: 10.1016/j.surge.2017.05.005

Del Signore F, De Dominicis S, Mastromatteo G, Simeoni F, Scapolo PA, Tamburro R, Vignoli M. Sonoelastography of normal canine common calcaneal tendon: Preliminary results. Vet Comp Orthop Traumatol. 2021 May; 34(3):200-205. doi: 10.1055/s-0040-1721660

Delee JC, Craviotto DF. Rupture of the Quadriceps Tendon After A Central 3rd Patellar Tendon Anterior Cruciate Ligament Reconstruction. American Journal of Sports Medicine. 1991 Jul; 19:415-416

Deng H, Mi Y, Lu B, Xu P. Application of virtual touch tissue imaging quantification in diagnosis of supraspinatus tendon injury. J Xray Sci Technol. 2021; 29(5):881-890. doi: 10.3233/XST-210865

Dewall RJ, Jiang J, Wilson JJ, Lee KS. Visualizing tendon elasticity in an ex vivo partial tear model. Ultrasound Med Biol. 2014 Jan; 40(1):158-67. doi: 10.1016/j.ultrasmedbio.2013.08.022

Diamant J, Keller A, Baer E, Litt M, Arridge RG. Collagen; ultrastructure and its relation to mechanical properties as a function of ageing. Proc R Soc Lond B Biol Sci. 1972 Mar; 180(1060):293–315

Dirrichs T, Quack V, Gatz M, Tingart M, Kuhl CK, Schrading S. Shear Wave Elastography (SWE) for the evaluation of patients with Tendinopathies. Acad Radiol. 2016 Oct; 23(10):1204-1213; doi: 10.1016/j.acra.2016.05.012

Dirrichs T, Schrading S, Gatz M, Tingart M, Kuhl CK, Quack V. Shear Wave Elastography (SWE) of asymptomatic Achilles tendons: A comparison between semiprofessional athletes and the nonathletic general population. Acad Radiol. 2019 Oct; 26(10):1345-1351. doi: 10.1016/j.acra.2018.12.014

Docheva D, Muller SA, Majewski M, Evans CH. Biologics for tendon repair. Adv Drug Deliv Rev. 2015 Apr; 84: 222–239. doi: 10.1016/j.addr.2014.11.015

Doschank MR, Zernicke RF. Structure, Function, and Adaptation of Bone-Tendon and Bone-Ligament Complexes. J Musculoskelet Neuronal Interact. 2005 Mar; 5(1): 35-40

Drakonaki EE, Allen GM, Wilson DJ. Ultrasound elastography for musculoskeletal applications. Br J Radiol. 2012 Nov; 85(1019):1435–1445. doi: 10.1259/bjr/93042867

Dressler MR, Butler DL, Boivin GP. Age-related changes in the biomechanics of healing patellar tendon. J Biomech. 2006; 39(12):2205-2212. doi: 10.1016/j.jbiomech.2005.07.003

Dubois G, Kheireddine W, Vergari C, Bonneau D, Thoreux P, Rouch P, Tanter M, Gennisson JL, Skalli W. Reliable Protocol for Shear Wave Elastography of Lower Limb Muscles at Rest and During Passive Stretching. Ultrasound Med Biol. 2015 Sep; 41(9):2284–2291. doi: 10.1016/j.ultrasmedbio.2015.04.020

Eby SF, Cloud BA, Brandenburg JE, Giambini H, Song P, Chen S, LeBrasseur NK, An KN. Shear wave elastography of passive skeletal muscle stiffness: influences of sex and age throughout adulthood. Clin Biomech. 2015 Jan; 30(1):22–27. doi: 10.1016/j.clinbiomech.2014.11.011

Eby SF, Song P, Chen S, Chen Q, Greenleaf JF, An KN. Validation of shear wave elastography in skeletal muscle. J Biomech. 2013 Sep; 46(14):2381-7. doi: 10.1016/j.jbiomech.2013.07.033

Eby SF, Zhao H, Song P, Vareberg BJ, Kinnick RR, Greenleaf JF, An KN, Brown AW, Chen S. Quantifying spasticity in individual muscles using shear wave elastography. Radiol Case Rep. 2017 Jun; 12(2):348-352. doi:10.1016/j.radcr.2017.01.004

Elliott DH. Structure and function of mammalian tendon. Biol Rev Camb Philos Soc. 1965 Aug; 40:392-421. doi: 10.1111/j.1469-185x.1965.tb00808.x

Eriksen CS, Svensson RB, Gylling AT, Couppé C, Magnusson SP, Kjaer M. Load magnitude affects patellar tendon mechanical properties but not collagen or collagen cross-linking after long-term strength training in older patients. BMC Geriatr. 2019 Jan; 19(1):30. doi: 10.1186/s12877-019-1043-0

Feng YN, Li YP, Liu CL, Zhang ZJ. Assessing the elastic properties of skeletal muscle and tendon using shearwave ultrasound elastography and MyotonPRO. Sci Rep. 2018 Nov; 8:17064. doi:10.1038/s41598-018-34719-7

Fenwick SA, Hazleman BL, Riley GP. The vasculature and its role in the damaged and healing tendon. Arthritis Res. 2002; 4(4):252-260. doi: 10.1186/ar416

Fessel G, Li Y, Diederich V, Guizar-Sicairos M, Schneider P, Sell DR, Monnier VM, Snedeker JG. Advanced glycation end-products reduce collagen molecular sliding to affect collagen fibril damage mechanisms but not stiffness. PLoS One. 2014 Nov; 9(11): e110948. doi: 10.1371/journal.pone.0110948

Fitzgerald MJT. Neuroanatomy: basic and clinical. 2nd ed. Philadelphia: Balliere Tindall; 1992

Florit D, Pedret C, Casals M, Malliaras P, Sugimoto D, Rodas G. Incidence of Tendinopathy in Team Sports in a Multidisciplinary Sports Club Over 8 Seasons. J Sports Sci Med. 2019 Dec; 18(4):780-788

Fontenelle CRC, Mannarino P, Ribeiro FBDO, Milito MA, Carvalho ACP, Menegaldo LL, Oliveira LF. Semitendinosus and patellar tendons shear modulus evaluation by supersonic shearwave imaging elastography. Clin Physiol Funct Imaging. 2018 Feb. doi: 10.1111/cpf.12506

Franchi M, Fini M, Quaranta M, De Pasquale V, Raspanti M, Giavaresi G, Ottani V, Ruggeri A. Crimp morphology in relaxed and stretched rat Achilles tendon. J Anat. 2007 Jan; 210(1):1–7. doi: 10.1111/j.1469-7580.2006.00666.x

Franchi M, Ottani V, Stagni R, Ruggeri A. Tendon and ligament fibrillar crimps give rise to left-handed helices of collagen fibrils in both planar and helical crimps. J Anat. 2010 Mar; 216(3):301-309. doi:10.1111/j.1469-7580.2009.01188.x

Francis A, Thomas RDM, McGregor TA. Anterior cruciate ligament rupture: reconstruction surgery and rehabilitation. A nation-wide survey of current practice. Knee. 2001 Mar; 8(1):13-18. doi: 10.1016/s0968-0160(00)00073-9

Frank CB, Beveridge JE, Huebner KD, Heard BJ, Tapper JE, O'Brien EJ, Shrive NG. Complete ACL/MCL deficiency induces variable degrees of instability in sheep with specific kinematic abnormalities correlating with degrees of early osteoarthritis. J Orthop Res. 2012 Mar; 30(3):384–392. doi: 10.1002/jor.21549

Frankewycz B, Penz A, Weber J, da Silva NP, Freimoser F, Bell R, Nerlich M, Jung EM, Docheva D, Pfeifer CG. Achilles tendon elastic properties remain decreased in long term after rupture. Knee Surg Sports Traumatol Arthrosc. 2018 Jul; 26(7)2080–2087.
doi: 10.1007/s00167-017-4791-4

Fratzl Peter. Cellulose and Collagen: From Fibres to tissues. Current Opinion in Colloid and Interface Science. 2003 Mar; 8(1): 32-39. doi: 10.1016/S1359-0294(03)00011-6

Fukada SI, Ma Y, Uezumi A. Adult stem cell and mesenchymal progenitor theories of aging. Front Cell Dev Biol. 2014 Mar; 2:10. doi: 10.3389/fcell.2014.00010

Funakoshi Y, Hariu M, Tapper JE, Marchuk LL, Shrive NG, Kanaya F, Rattner JB, Hart DA, Frank CB. Periarticular ligament changes following ACL/MCL transection in an ovine stifle joint model of osteoarthritis. J Orthop Res. 2007 Aug; 25(8): 997–1006. doi: 10.1002/jor.20370

Gaida JE, Ashe MC, Bass SL, Cook JL. Is adiposity an under-recognized risk factor for tendinopathy? A systematic review. Arthritis Rheum. 2009 Jun; 61(6):840–849.
doi: 10.1002/art.24518

Galloway MT, Lalley AL, Shearn JT. The Role of Mechanical Loading in Tendon Development, Maintenance, Injury, and Repair. J Bone Joint Surg Am. 2013 Sep; 95(17):1620–1628. doi: 10.2106/ JBJS.L.01004

Gatz M, Betsch M, Dirrichs T, Schrading S, Tingart M, MD, Michalik R, Quack V. Eccentric and isometric exercises in Achilles tendinopathy evaluated by the VISA-A Score and Shear Wave Elastography. Sports Health. 2020 Jul-Aug; 12(4): 373–381.
doi: 10.1177/1941738119893996

Gatz M, Schrading S, Dirrichs T, Betsch M, Tingart M, Rath B, Kuhl C, Quack V. Topical polidocanol application in combination with static stretching in tendinopathies: a prospective pilot study. Muscles Ligaments Tendons J. 2017 May 10; 7(1):88-97.
doi: 10.11138/mltj/2017.7.1.088

Gatz M, Schweda S, Betsch M, Dirrichs T, de la Fuente M, Reinhardt N, Quack V. Line- and point-focused extracorporeal shock wave therapy for Achilles tendinopathy: A placebo-controlled RCT study. Sports Health. Sep-Oct 2021; 13(5):511-518.
doi: 10.1177/1941738121991791

Gautieri A, Passini FS, Silvan U, Guizar-Sicairos M, Carimati G, Volpi P, Moretti M, Schoenhuber H, Redaelli A, Berli M, Snedeker JG. Advanced glycation end-products: Mechanics of aged collagen from molecule to tissue. Matrix Biol. 2017 May; 59:95-108.
doi: 10.1016/j.matbio.2016.09.001

Gehwolf R, Wagner A, Lehner C, Bradshaw AD, Scharler C, Niestrawska JA, Holzapfel GA, Bauer HC, Tempfer H, Traweger A. Pleiotropic roles of the matricellular protein Sparc in tendon maturation and ageing. Sci Rep. 2016 Sep; 6:32635. doi 10.1038/srep32635

Gennisson JL, Catheline S, Chaffaï S, Fink M. Transient elastography in anisotropic medium: Application to the measurement of slow and fast shear wave speeds in muscles. J Acoust Soc Am. 2003 Jul; 114(1):536-541. doi: 10.1121/1.1579008

Gennisson JL, Deffieux T, Macé E, Montaldo G, Fink M, Tanter M. Viscoelastic and anisotropic mechanical properties of in vivo muscle tissue assessed by supersonic shear imaging. Ultrasound Med Biol. 2010 May; 36(5):789-801.
doi: 10.1016/j.ultrasmedbio.2010.02.013

Ghosh P, Burkhardt D, Read R, Bellenger C. Recent advances in animal models for evaluating chondroprotective drugs. J Rheumatol Suppl. 1991 Feb; 27:143–146

Gonzalez FM, Gleason CA, Lee KS, Labid SA, Nazarian LN, Morrison WB, Reiter DA. Shear wave elastography assessment and comparison study of the Achilles tendons in optimally conditioned asymptomatic young collegiate athletes. Skeletal Radiol. 2021 Dec; 50(12):2381-2392. doi: 10.1007/s00256-021-03798-5.

Grosset JF, Breen L, Stewart CE, Burgess KE, Onambélé GL. Influence of exercise intensity on training-induced tendon mechanical properties changes in older individuals. Age. 2014 Jun; 36(3):9657, 2014. doi: 10.1007/s11357-014-9657-9

Gruchenberg K, Ignatius A, Friemert B, von Lübken F, Skaer N, Gellynck K, Kessler O, Dürselen L. In vivo performance of a novel silk fibroin scaffold for partial meniscal replacement in a sheep model. Knee Surg Sports Traumatol Arthrosc. 2015 Aug; 23(8):2218–2229. doi: 10.1007/s00167-014-3009-2

Guilhem G, Doguet V, Hauraix H, Lacourpaille L, Jubeau M, Nordez A, Dorel S. Muscle force loss and soreness subsequent to maximal eccentric contractions depend on the amount of fascicle strain in vivo. Acta Physiol. 2016 Jun; 217(2):152–163. doi: 10.1111/apha.12654

Gulledge CM, Baumer TG, Juliano L, Sweeney M, McGinnis M, Sherwood A, Moutzouros V, Bey MJ. Shear wave elastography of the healing human patellar tendon following ACL reconstruction. Knee. 2019 Mar; 26(2):347-354. doi: 10.1016/j.knee.2018.12.006

Haen TX, Roux A, Soubeyrand M, Laporte S. Shear waves elastography for assessment of human Achilles tendon's biomechanical properties: an experimental study. J Mech Behav Biomed Mater. 2017 May; 69:178-184. doi: 10.1016/j.jmbbm.2017.01.007

Hansen P, Bojsen-Moller J, Aagaard P, Kjaer M, Magnusson SP. Mechanical properties of the human patellar tendon, in vivo. Clin Biomech 2006 Jan; 21(1):54–58.
doi: 10.1016/j.clinbiomech.2005.07.008

Hardy A, Rodaix C, Vergari C, Vialle R. Normal range of patellar tendon elasticity using the sharewave elastography technique: an in vivo study in normal volunteers. Surg Technol Int. 2017 Dec; 31:227-230. hal-03156476

Haut RC, Lancaster RL, DeCamp CE. Mechanical properties of the canine patellar tendon: some correlations with age and the content of collagen. J Biomech. 1992 Feb; 25(2):163-173. doi:10.1016/0021-9290(92)90273-4

Health Information-Mayo Clinic. "Rotator Cuff Injury." Mayo Clinic, Aug. 21, 2010.
Web. 2021

Hee CK, Dines JS, Dines DM, Roden CM, Wisner-Lynch LA, Turner AS, McGilvray KC, Lyons AS, Puttlitz CM, Santoni BG. Augmentation of a rotator cuff suture repair using rhPDGF-BB and a type I bovine collagen matrix in an ovine model. Am J Sports Med. 2011 Aug; 39(8):1630-1639. doi:10.1177/0363546511404942

Helfenstein-Didier C, Andrade R J, Brum J, Hug F, Tanter M, Nordez A, Gennisson J-L. In vivo quantification of the shear modulus of the human Achilles tendon during passive loading using shear wave dispersion analysis. Phys Med Biol. 2016 Mar 21; 61(6):2485-2496. doi: 10.1088/0031-9155/61/6/2485

Herfat ST, Boguszewski DV, Shearn JT. Applying Simulated in vivo motions to measure human knee and ACL kinetics. Ann Biomed Eng. 2012 Jul; 40(7): 1545-1553. doi: 10.1007/s10439-011-0500-5

Hess GW. Achilles tendon rupture: A review of etiology, population, anatomy, risk factors, and injury prevention. Foot Ankle Spec. 2010 Feb; 3(1):29–32. doi: 10.1177/1938640009355191

Hirata K, Miyamoto-Mikami E, Kanehisa H, Miyamoto N. Muscle- specific acute changes in passive stiffness of human triceps surae after stretching. Eur J Appl Physiol. 2016 May; 116(5):911–918. doi: 10.1007/s00421-016-3349-3

Hoegaerts M, Nicaise M, Van Bree H, Saunders JH. Cross-sectional anatomy and comparative ultrasonography of the equine medial femorotibial joint and its related structures. Equine Vet J. 2005 Nov; 37(6):520–529. doi: 10.2746/042516405775314817

Hsiao MY, Chen YC, Lin CY, Chen WS, Wang TG. Reduced patellar tendon elasticity with aging: in vivo assessment by Shear Wave Elastography. Ultrasound Med Biol. 2015 Nov; 41(11):2899-2905. doi: 10.1016/j.ultrasmedbio.2015.07.008

Hsiao MY, Lin AC, Liao WH, Wang T.G, Hsu C.H, Chen WS, Lin FH. Drug-loaded hyaluronic acid hydrogel as a sustained-release regimen with dual effects in early intervention of tendinopathy. Sci Rep. 2019 Mar; 9(1):4784. doi: 10.1038/s41598-019-41410-y

Hsiao YY, Yang TH, Chen PY, Hsu HY, Kuo LC, Su FC, Huang CC. Characterization of the extensor digitorum communis tendon using high-frequency ultrasound shear wave elastography. Med Phys. 2020 Apr; 47(4):1609-1618. doi:10.1002/mp.14061

Huang H, Zhang J, Sun K, Zhang X, Tian S. Effects of repetitive multiple freeze-thaw cycles on the biomechanical properties of human flexor digitorum superficialis and flexor pollicis longus tendons. Clin Biomech. 2011 May; 26(4):419-423. doi:10.1016/j.clinbiomech.2010.12.006

Hunt P, Scheffler S, Unterhauser F, Weiler A. A model of soft-tissue graft anterior cruciate ligament reconstruction in sheep. Arch Orthop Trauma Surg. 2005 May; 125(4):238–248. doi: 10.1007/s00402-004-0643-z

Innocenti B, Larrieu JC, Lambert P, Pianigiani S. Automatic characterization of soft tissues material properties during mechanical tests. Muscles, Ligaments and Tendons J. 2018 Apr;7 (4):529-537. doi: 10.11138/mltj/2017.7.4.529

Itoigawa Y, Sperling JW, Steinmann SP, et al. Feasibility assessment of shear wave elastography to rotator cuff muscle. Clin Anat 2015 Mar;28(2):213–218

Itoigawa Y, Takazawa Y, Maruyama Y, Yoshida K, Sakai T, Ichimura K, Kaneko K. A new technique of surgical planning for anterior cruciate ligament reconstruction: Feasibility assessment of Shear Wave Elastography to tendon of Semitendinosus muscle. Clin Anat. 2018 Apr; 31(3):404-408. doi: 10.1002/ca.23000

Ivanac G, Lemac D, Kosovic V, Bojanic K, Cengic T, Dumic-Cule I, Pecina M, Brkljacic B. Importance of shear-wave elastography in prediction of Achilles tendon rupture. Int Orthop. 2021 Apr; 45(4):1043-1047. doi: 10.1007/s00264-020-04670-2

Järvinen TA, Kannus P, Paavola M, Järvinen TL, Jozsa L, Järvinen M. Achilles tendon injuries. Curr Opin Rheumatol. 2001 Mar; 13(2):150-155. doi: 10.1097/00002281-200103000-00009

Jiang Y, Li GY, Qian LX, Hu XD, Liu D, Liang S, Cao Y. Characterization of the nonlinear elastic properties of soft tissues using the supersonic shear imaging (SSI) technique: Inverse method, ex vivo and in vivo experiments. Med Image Anal. 2015 Feb; 20(1):97–111. doi: 10.1016/j.media.2014.10.010

Johnson GA, Tramaglini DM, Levine RE, Ohno K, Choi NY, Woo SLY. Tensile and Viscoelastic Properties of Human Patellar Tendon. J Orthop Res. 1994 Nov; 12(6)796-803. doi: 10.1002/jor.1100120607

Jost PW, Khair MM, Chen DX, Wright TM, Kelly AM, Rodeo SA. Suture number determines strength of rotator cuff repair. J Bone Joint Surg Am. 2012 Jul; 94(14):e100. doi:10.2106/JBJS.K.00117

Jozsa L, Réffy A, Bálint JB. 1984. The pathogenesis of tendolipomatosis: an electron microscopical study. Int Orthop. 1984 Jun; 7(4):251–255. doi: 10.1007/BF00266836

Kannus P, Jozsa L. Histopathological changes preceding spontaneous rupture of a tendon: a controlled study of 891 patients. J Bone Joint Surg Am. 1991 Dec; 73(10):1507–1525

Kannus P, Natri A. Etiology and pathophysiology of tendon ruptures in sports. Scand J Med Sci Sports. 1997 Apr; 7(2):107-112. doi: 10.1111/j.1600-0838.1997.tb00126.x

Kannus P. Structure of the tendon connective tissue. Scand J Med Sci Sports. 2000 Dec; 10(6):312-320. doi:10.1034/j.1600-0838.2000.010006312.x

Kantarci F, Ustabasioglu FE, Delil S, Olgun DC, Korkmazer B, Dikici AS, Tutar O, Nalbantoglu M, Uzun N, Mihmanli I. Median nerve stiffness measurement by shear wave elastography: a potential sonographic method in the diagnosis of carpal tunnel syndrome. Eur Radiol. 2014 Feb; 24(2):434–440. doi: 10.1007/s00330-013-3023-7

Kasperczyk W J, Bosch U, Oestern HJ, Tscherne H. Influence of immobilization on autograft healing in the knee joint: a preliminary study in a sheep knee PCL model. Arch Orthop Trauma Surg. 1991; 110:158-161

Kasperczyk WJ, Bosch U, Oestern HJ, Tscherne H. Staging of patellar tendon autograft healing after posterior cruciate ligament reconstruction. A biomechanical and histological study in a sheep model. Clin Orthop Relat Res. 1993 Jan; 286:271-82

Kaux JF, Croisier JL, Forthomme B, Crielaard JM. New conservative treatments of chronic tendinopathies. Rev Med Liege. 2015 Oct; 70(10):507–510

Kayser F, Bori E, Armillotta N, Innocenti B, Hontoir F, Vandeweerd JM. Correlation between shear wave velocity assessed by elastography and stiffness given by tensile test in the ovine patellar tendon. Published in Archives of Clinical and Biomedical Research. Arch Clin Biomed Res. 2022; 6(1):905-916. doi:10.26502/acbr.50170209

Kayser F, Hontoir F, Clegg P, Kirschvink N, Dugdale A, Vandeweerd JM. 2019. Ultrasound anatomy of the normal stifle in the sheep. Anat Histol Embryol. 2019 Jan; 48(1):87-96. doi: 10.1111/ahe.12414

Kelly BM, Rao N, Louis SS, Kostes BT, Smith RM. Bilateral, simultaneous, spontaneous rupture of quadriceps tendons without trauma in an obese patient: a case report. Arch Phys Med Rehabil. 2001 Mar;82(3):415-418. doi: 10.1053/apmr.2001.19784

Kirkendall DT, Garrett WE. Function and biomechanics of tendons. Scand J Med Sci Sports. 1997 Apr; 7:62-66. doi: 10.1111/j.1600-0838.1997.tb00120.x

Kitamura N, Yokota M, Kurokawa T, Gong JP, Yasuda K. In vivo cartilage regeneration induced by a double-network hydrogel: Evaluation of a novel therapeutic strategy for femoral articular cartilage defects in a sheep model. J Biomed Mater Res A. 2016 Sep; 104(9):2159–2165. doi.org/10.1002/ jbm.a.35745

Kjaer M, Langberg H, Heinemeier K, Bayer ML, Hansen M, Holm L, Doessing S, Kongsgaard M, Krogsgaard MR, Magnusson SP. From mechanical loading to collagen synthesis, structural changes and function in human tendon. Scand J Med Sci Sports. 2009 Aug; 19(4):500–510. doi: 10.1111/j.1600-0838.2009.00986.x

Kjaer M, Magnusson P, Krogsgaard M, Moller JB, Olesen J, Heinemeier K, Hansen M, Haraldsson B, Koskinen S, Esmarck B, Langberg H. Extracellular matrix adaptation of tendon and skeletal muscle to exercise. J. Anat. 2006 Apr; 208(4):445–450. doi: 10.1111/j.1469-7580.2006.00549.x

Kjaer M. Role of extracellular matrix in adaptation of tendon and skeletal muscle to mechanical loading. Physiol Rev. 2004 Apr; 84(2):649–698. doi: 10.1152/physrev.00031.2003

Klauser AS, Miyamoto H, Bellmann-Weiler R, Feuchtner GM, Wick MC, Jaschke WR. Sonoelastography: musculoskeletal applications. Radiology. 2014 Sep; 272(3):622–633. doi: 10.1148/radiol.14121765

Knobloch, K. Drug-Induced Tendon Disorders. Adv. Exp. Med. Biol. 2016 Aug; 920:229–238. doi: 10.1007/978-3-319-33943-6_22

Kofler, J. Ultrasonographic examination of the stifle region in cattle-normal appearance. Veterinary J. 1999 Jul; 158(1):21–32. doi: 10.1053/tvjl.1998.0329

Kohn D, Rudert M, Wirth C, Plitz W, Reiss G, Maschek H. Medial meniscus replacement by a fat pad autograft. An experimental study in sheep. Internal Orthopaedics. 1997 Feb;21(4):232–238. doi: 10.1007/s002640050157

Kostrominova T Y, Brooks S V. Age-related changes in structure and extracellular matrix protein expression levels in rat tendons. Age. 2013 Dec; 35(6): 2203-2214. doi: 10.1007/s11357-013-9514-2

Kot BCW, Zhang ZJ, Lee AWC, Leung VYF, Fu SN. Elastic modulus of muscle and tendon with shear wave ultrasound elastography: variations with different technical settings. PLoS One. 2012; 7(8): e44348. doi: 10.1371/journal.pone.0044348

Kuervers EJ, Firminger CR, Edwards WB. Effect of knee angle and Quadriceps muscle force on Shear-Wave Elastography measurements at the Patellar Tendon. Ultrasound Med Biol. 2021 Aug; 47(8):2167-2175. doi: 10.1016/j.ultrasmedbio.2021.03.031

Kuo WH, Jian DW, Wang TG, Wang YC. Neck muscle stiffness quantified by sonoelastography is correlated with body mass index and chronic neck pain symptoms. Ultrasound Med Biol. 2013 Aug;39(8):1356–1361. doi: 10.1016/j.ultrasmedbio.2012.11.015

Kuster MS, Wood GA, Stachowiak GW, Gachter A. Joint load considerations in total knee replacement. J Bone Joint Surg Br. 1997 Jan; 79(1): 109-113.
doi: 10.1302/0301-620x.79b1.6978

Kvist M, Hurme T, Kannus P, et al. Vascular density at the myotendinous junction of the rat gastrocnemius muscle after immobilization and remobilization. Am J Sports Med. 1995 May-June; 23(3):359-64. doi: 10.1177/036354659502300320

Kvist M, Jozsa L, Jarvinen M, et al. Fine structural alterations in chronic Achilles paratenonitis in athletes. Pathol Res Pract. 1985 Oct; 180(4):416-23. doi: 10.1016/S0344-0338(85)80115-1

Lacourpaille L, Hug F, Guével A, Péréon Y, Magot A, Hogrel JY, Nordez A. Non-invasive assessment of muscle stiffness in patients with Duchenne muscular dystrophy. Muscle Nerve. 2015 Feb; 51(2):284–286. doi: 10.1002/mus.24445

Landis WJ, Paine MC, Glimcher MJ. Electron microscopic observation of bone tIssue prepared anhydrously in oranganic solvents. J Ultrastruct Res. 1977 Apr; 59(1): 1-30.
doi: 10.1016/S0022-5320(77)80025-7

Laubach M, Hellmann JT, Dirrichs T, Gatz M, Quack V, Tingart M, Betsch M. Anterior knee pain after total knee arthroplasty: A multifactorial analysis. J Orthop Surg. 2020 Jan-Apr; 28(2):2309499020918947. doi: 10.1177/2309499020918947

Le Sant G, Ates F, Brasseur JL, Nordez A. Elastography study of hamstring behaviors during passive stretching. PLoS One. 2015 Sep; 10(9): e0139272. doi: 10.1371/journal.pone.0139272

Leblanc DR, Schneider M, Angele P, Vollmer G, Docheva D. The effect of estrogen on tendon and ligament metabolism and function. J. Steroid Biochem Mol Biol. 2017 Sep; 172:106–116

Lee H, Wang VM, Laudier DM, Schaffler MB, Flatow EL. A novel in vivo model of tendon fatigue damage accumulation. Trans Orthop Res Soc. 2006; 31:1058

Lephart SM, Pincivero DM, Giraldo JL, Fu FH. The role of proprioception in the management and rehabilitation of athletic injuries. Am J Sports Med. 1997 Jan-Feb;25(1):130-7.
doi: 10.1177/036354659702500126

Li Y, Fessel G, Georgiadis M, Snedeker JG. Advanced glycation end-products diminish tendon collagen fiber gliding. Matrix Biol. 2013 Apr; 32(3-4): 169-177.
doi: 10.1016/j.matbio.2013.01.003

Li Y, Snedeker JG. Elastography: modality-specific approaches, clinical applications, and research horizons. Skeletal Radiol. 2011 Apr; 40(4): 389–397.
doi:10.1007/s00256-010-0918-0

Lieber RL, Roberts TJ, Blemker SS, Lee SSM, Herzog W. Skeletal muscle mechanics, energetics and plasticity. J Neuroeng Rehabil 2017 Oct; 14(1):108.
doi: 10.1186/s12984-017- 0318-y

Linder LH, Sukin DL, Burks RT, Haut RC. Biomechanical and histologic properties of the canine patellar tendon after removal of its medial third. Am J Sports Med. 1994 Jan-Feb; 22(1):136-42. doi: 10.1177/036354659402200121

Little C, Smith S, Ghosh P, Bellenger C. Histomorphological and immunohistochemical evaluation of joint changes in a model of osteoarthritis induced by lateral meniscectomy in sheep. J Rheumatol. 1997 Nov; 24(11): 2199–2209

Little CB, Smith MM, Cake MA, Read RA, Murphy MJ, Barry FP. The OARSI histopathology initiative - recommendations for histologic assessments of osteoarthritis in sheep and goats. Osteoarthritis Cartilage. 2010 Oct; 18 Suppl 3:S80-92. doi: 10.1016/j.joca.2010.04.016

Little CB, Smith MM. Animal models of osteoarthritis. Current Rheumatology Reviews. 2008; 4(3):175-182. doi: 10.2174/157339708785133523

Lustgarten M, Redding WR, Labens R, Davis W, Daniel TM, Griffith E, Seiler GS. Elastographic evaluation of naturally occuring tendon and ligament injuries of the equine distal limb. Vet Radiol Ultrasound. 2015 Nov-Dec; 56(6):670-9. doi: 10.1111/vru.12284

Ma R, Schar M, Chen T, Wang H, Wada S, Ju X, Deng XH, Rodeo SA. Use of Human Placenta-Derived Cells in a Preclinical Model of Tendon Injury. J. Bone Joint Surg Am. 2019 Jul; 101(13): e61. doi: 10.2106/JBJS.15.01381

Maffulli N, Wong J, Almekinders LC. Types and epidemiology of tendinopathy. Clin Sports Med. 2003 Oct; 22(4):675–692. doi: 10.1016/S0278-5919(03)00004-8

Maguire M, Goldberg J, Bokor D, Bertollo N, Pelletier MH, Harper W, Walsh WR. Biomechanical evaluation of four different transosseous-equivalent/suture bridge rotator cuff repairs. Knee Surg Sports Traumatol Arthrosc. 2011 Sep; 19(9):1582-1587. doi:10.1007/s00167-011-1436-x

Malliaras P, Kamal B, Nowell A, Farley T, Dhamu H, Simpson V, Morrissey D, Langberg H, Maffulli N, Reeves ND. Patellar tendon adaptation in relation to load-intensity and contraction type. J Biomech. 2013 Jul; 46(11):1893–1899. doi: 10.1016/j.jbiomech.2013.04.022

Mannarino P, Lima KMM, Fontenelle CRC, Matta TT, de Salles BF, Simão R, Oliveira LF. Analysis of the correlation between knee extension torque and patellar tendon elastic property. Clin Physiol Funct Imaging. 2018 May; 38(3):378-383. doi: 10.1111/cpf.12424

Martin JA, Biedrzycki AH, Lee KS, DeWall RJ, Brounts SH, Murphy WL, Markel MD, Thelen DG. In vivo measures of shear wave speed as a predictor of tendon elasticity and strength. Ultrasound Med Biol. 2015 Oct; 41(10): 2722–2730. doi: 10.1016/j.ultrasmedbio.2015.06.008

Martinello T, Bronzini I, Perazzi A, Testoni S, De Benedictis GM, Negro A, Caporale G, Mascarello F, Iacopetti I, Patruno M. Effects of in vivo applications of peripheral blood-derived mesenchymal stromal cells (PB-MSCs) and platelet-rich plasma (PRP) on experimentally injured deep digital flexor tendons of sheep. J Orthop Res. 2013 Feb; 31(2):306-314. doi:10.1002/jor.22205

Marumoto JW, Mitsunaga MM, Richardson AB, Medoff RJ, Mayfield GW. Late patellar tendon ruptures after removal of the central third for anterior cruciate ligament reconstruction - A report of two cases. Am J Sports Med. 1996 Sep-Oct; 24(5):698-701

McNickle A, Wang V, Shewman E, Cole B, Williams J. Performance of a sterile meniscal allograft in an ovine model. Clin Orthop Relat Res. 2009 Jul; 467(7):1868–1876. doi: 10.1007/s11999-008-0567-y

Meller R, Schiborra F, Brandes G, Knobloch K, Tschernig T, Hankemeier S., Haasper C, Schmiedl A, Jagodzinski M, Krettek C, Willbold E. Postnatal maturation of tendon, cruciate ligament, meniscus and articular cartilage: a histological study in sheep. Ann Anat. 2009 Sep; 191(6):575-585. doi: 10.1016/j.aanat.2009.08.005

Mhanna C, Marquardt TL, Li ZM. Adaptation of the transverse carpal ligament associated with repetitive hand use in pianists. PLoS One. 2016; 11(3): e0150174. doi: 10.1371/journal.pone.0150174

Miller MD, Nichols T, Butler CA. Patella fracture and proximal patellar tendon rupture following arthroscopic anterior cruciate ligament reconstruction. Arthroscopy. 1999 Sep; 15(6):640-643. doi: 10.1053/ar.1999.v15.015064

Miller TT. The patellar tendon. Semin Musculoskelet Radiol. 2013 Feb; 17(1):56–59. doi: 10.1055/s-0033-1333915

Muraoka T, Muramatsu T, Fukunaga T, Kanehisa H. Elastic properties of human Achilles tendon are correlated to muscle strength. J Appl Physiol. 2005 Aug; 99(2):665-669. doi: 10.1152/japplphysiol.00624.2004

Nunes P, Betsch M, Fuss B, Dirrichs T, Tingart M, Quack V, Gatz M. Evaluation of Current Symptoms in Postoperative Achilles Tendons: A Multimodal Ultrasound Study. Healthcare. 2021 Mar; 9(3):288. doi: 10.3390/healthcare9030288

O'Brien C, Marr N, Thorpe C. Microdamage in the equine superficial digital flexor tendon. Equine Vet J. 2021 May; 53(3):417-430. doi: 10.1111/evj.13331

Oakley SP, Lassere MN, Portek I, Szomor Z, Gosh P, Kirkham BW, Murrell GAC, Wulf S, Appleyard RC. Biomechanical, histologic and macroscopic assessment of articular cartilage in a sheep model of os- teoarthritis. Osteoarthritis Cartilage. 2004 Aug;12(8):667–679. doi: 10.1016/j.joca.2004.05.006

Oei EHG, Koster IM, Hensen JHJ, Boks SS, Wagemakers HPA, Koes BW, Vroegindeweij D, Bierma-Zeinstra SMA, Hunink MGM. MRI follow-up of conservatively treated meniscal knee lesions in general practice. Eur Radiol. 2010;20(5): 1242–1250. doi: 10.1007/ s00330-009-1648-3

Ohberg L, Alfredson H. Effects on neovascularisation behind the good results with eccentric training in chronic mid-portion Achilles tendinosis? Knee Surg Sports Traumatol Arthrosc. 2004 Sep; 12(5):465-470. doi:10.1007/s00167-004-0494-8

Ohberg L, Lorentzon R, Alfredson H. Neovascularisation in Achilles tendons with painful tendinosis but not in normal tendons: an ultrasonographic investigation. Knee Surg Sports Traumatol Arthrosc. 2001 Jul; 9(4):233-238. doi:10.1007/s001670000189

Onambélé GN, Burgess K, Pearson SJ. Gender-specific in vivo measurement of the structural and mechanical properties of the human patellar tendon. J Orthop Res. 2007 Dec; 25(12):1635–1642. doi: 10.1002/jor.20404

Onay U, Akpinar S, Akgün RC, Balçik C, Tuncay IC. Comparison of repair techniques in small and medium-sized rotator cuff tears in cadaveric sheep shoulders. Acta Orthop Traumatol Turc. 2013; 47(3):179-183. doi:10.3944/aott.2013.2935

Oo WM, Bo MT. Role of Ultrasonography in Knee Osteoarthritis. J Clin Rheumatol. 2016 Sep; 22(6):324–329. doi: 10.1097/RHU.0000000000000436

Ooi CC, Richards PJ, Maffulli N, Ede D, Schneider ME, Connell D, Morrissey D, Malliaras P. A soft patellar tendon on ultrasound elastography is associated with pain and functional deficit in volleyball players. J Sci Med Sport 2016 May; 19(5):373–378.
doi: 10.1016/j.jsams.2015.06.003

Ophir J, Céspedes I, Ponnekanti H, Yazdi Y, Li X. Elastography: A quantitative method for imaging the elasticity of biological tissues. Ultrason Imaging. 1991 Apr;13(2):111–134.
doi: 10.1177/016173469101300201

Ostrander RV, McKinney BI. Evaluation of footprint contact area and pressure using a triple-row modification of the suture-bridge technique for rotator cuff repair. J Shoulder Elbow Surg. 2012 Oct; 21(10):1406-1412. doi:10.1016/j.jse.2011.10.027

Otter S, Payne C, Jones AM, Webborn N, Watt P. Differences in Achilles tendon stiffness in people with gout: a pilot study. BMC Musculoskelet Disord. 2020 Oct 7; 21(1):658.
doi: 10.1186/s12891-020-03598-3

Paavola M, Kannus P, Järvinen TAH, Khan K, Jozsa L, Järvinen M. Achilles tendinopathy. J Bone Joint Surg Am. 2002 Nov; 84(11):2062-2076. doi:10.2106/00004623-200211000-00024

Palmeri ML, Dahl JJ, MacLeod DB, Grant SA, Nightingale KR. On the feasibility of imaging peripheral nerves using acoustic radiation force impulse imaging. Ultrason Imaging. 2009 Jul;31(3):172–182. doi: 10.1177/016173460903100303

Pang J, Shen S, Pan WR, Jones IR, Rozen WM, Taylor GI. The arterial supply of the patellar tendon: anatomical study with clinical implications for knee surgery. Clin Anat. 2009 Apr; 22(3):371-376. doi: 10.1002/ca.20770

Papalia R, Papalia G, Russo F, Diaz LA, Bressi F, Sterzi S, Denaro V. Meniscal extrusion as booster of osteoarthritis. J Biol Regul Homeost Agents. 2017 Dec; 31(4 Suppl 2):33–44

Payne C, Watt P, Cercignani M, Webborn N. Reproducibility of shear wave elastography measures of the Achilles tendon. Skeletal Radiol. 2018 Jun; 47(6):779-784.
doi: 10.1007/s00256-017-2846-8

Pearson SJ, Burgess K, Onambele GNL. Creep and the in vivo assessment of human patellar tendon mechanical properties. Clin Biomech. 2007 Jul;22(6):712–717, 2007.
doi: 10.1016/j.clinbiomech.2007.02.006

Peltz CD, Haladik JA, Divine G, Siegal D, van Holbeeck M, Bey MJ. Shearwave elastography: repeatability for measurement of tendon stiffness. Skeletal Radiol. 2013 Aug; 42(8):1151-1156. doi:10.1007/s00256-013-1629-0

Pesce K, Binder F, Chico MJ, Swiecicki MP, Galindo DH, Terrasa S. Diagnostic performance of shear wave elastography in discriminating malignant and benign breast lesions: Our experience with QelaXtoTM software. J Ultrasound. 2020 Dec; 23(4):575-583. doi:10.1007/s40477-020-00481-8

Petitpierre F, Perez JT, Bise S, Fournier C, Hauger O, Dallaudière B. Quantitative elastography of Achilles tendon using Shear Wave Elastography (SWE): correlation with zonal anatomy. Muscles, Ligaments and Tendons J. 2018; 8(2): 229-237. doi:10.32098/mltj.02.2018.12

Piccionello AP, Serrani D, Busoni V, Salvaggio A, Bonazzi M, Bergamino C, Volta A. Sonoelastographic Features of the Patellar Ligament in clinically normal dogs. Vet Comp Orthop Traumatol. 2018 Jul; 31(4):279-284. doi: 10.1055/s-0038-1651499

Plate JF, Wiggins WF, Haubruck P, Scott AT, Smith TL, Saul KR, Mannava S. Normal aging alters in vivo passive biomechanical response of the rat gastrocnemius-Achilles muscle-tendon unit. J Biomech. 2013 Feb; 46(3):450-455. doi:10.1016/j.jbiomech.2012.11.007

Porta F, Damjanov N, Galluccio F, Iagnocco A, Matucci-Cerinic M. Ultrasound elastography is a reproducible and feasible tool for the evaluation of the patellar tendon in healthy subjects. Int J Rheum Dis. 2014 Sep; 17(7): 762–766. doi: 10.1111/1756-185X.12241

Pottie P, Presle N, Terlain B, Netter P, Mainard D, Berenbaum F. Obesity and osteoarthritis: more complex than predicted! Ann Rheum Dis. 2006 Nov; 65(11):1403-1405. doi: 10.1136/ard.2006.061994

Proffen BL, McElfresh M, Fleming BC, Murray MM. A comparative anatomical study of the human knee and six animal species. Knee. 2012 Aug; 19(4):493-499. doi: 10.1016/j.knee.2011.07.005

Qiu Y, Lim JJ, Scott L, Jr, Adams RC, Bui HT, Temenoff JS. PEG-based hydrogels with tunable degradation characteristics to control delivery of marrow stromal cells for tendon overuse injuries. Acta Biomater. 2011 Mar; 7(3):959–966. doi: 10.1016/j.actbio.2010.11.002

Quack V, Betsch M, Hellmann J, Eschweiler J, Schrading S, Gatz M, Rath B, Tingart M, Laubach M, Kuhl CK, Dirrichs T. Evaluation of Postoperative Changes in Patellar and Quadriceps Tendons after Total Knee Arthroplasty-A Comprehensive Analysis by Shear Wave Elastography, Power Doppler and B-mode Ultrasound. Acad Radiol. 2020 Jun; 27(6): e148-e157. doi: 10.1016/j.acra.2019.08.015

Ray G, Sandean DP, Tall MA. Tenosynovitis. StatPearls [Internet]. Last Update: July 26, 2021

Reddy GK. Cross-linking in collagen by nonenzymatic glycation increases the matrix stiffness in rabbit Achilles tendon. Exp Diabesity Res. 2004 Apr-Jun; 5(2):143-153. doi: 10.1080/15438600490277860

Riel H, Lindstrøm CF, Rathleff MS, Jensen MB, Olesen JL. Prevalence and incidence rate of lower-extremity tendinopathies in a Danish general practice: a registry-based study. BMC Musculoskelet Disord. 2019 May; 20(1): 239. doi: 10.1186/s12891-019-2629-6

Riley, G. Tendinopathy–from basic science to treatment. Nat Clin Pract Rheumatol. 2008 Feb; 4(2) 82–89. doi: 10.1038/ncprheum0700

Robinson KA, Sun M, Barnum CE, Weiss SN, Huegel J, Shetye SS, Lin L, Saez D, Adams SM, Iozzo RV, Soslowsky LJ, Birk DE. Decorin and biglycan are necessary for maintaining collagen fibril structure, fiber realignment and mechanical properties of mature tendons. Matrix Biol. 2017 Dec; 64:81-93. doi: 10.1016/j.matbio.2017.08.004

Rosskopf AB, Bachmann E, Snedeker JG, Pfirrmann CWA, Buck FM. Comparison of shear wave velocity measurements assessed with two different ultrasound systems in an ex-vivo tendon strain phantom. Skeletal Radiol. 2016b Nov; 45(11):1541-1551. doi:10.1007/s00256-016-2470-z

Rosskopf AB, Ehrmann C, Buck FM, Gerber C, Flück M, Pfirrmann CWA. Quantitative shear-wave US elastography of the supraspinatus muscle: reliability of the method and relation to tendon integrity and muscle quality. Radiology. 2016a Feb; 278(2):465–474. doi: 10.1148/radiol.2015150908

Royer D, Gennisson JL, Deffieux T, Tanter M. On the elasticity of transverse isotropic soft tissues (L). J Acoust Soc Am. 2011 May; 129(5):2757–2760. doi: 10.1121/1.3559681

Sanders TL, Kremers HM, Bryan AJ, Larson DR, Dahm DL, Levy BA, Stuart MJ, Krych AJ. Incidence of Anterior Cruciate Ligament Tears and Reconstruction: A 21-Year Population-Based Study. Am J Sports Med. 2016 Jun; 44(6):1502–1507. doi: 10.1177/0363546516629944

Sanders TL, Pareek A, Barrett IJ, Kremers HM, Bryan AJ, Stuart MJ, Levy BA, Krych AJ. Incidence and long-term follow- up of isolated posterior cruciate ligament tears. Knee Surg Sports Traumatol Arthrosc. 2017 Oct; 25(10): 3017–3023. doi: 10.1007/ s00167-016-4052-y

Sarvazyan AP, Rudenko OV, Swanson SD, Fowlkes JB, Emelianov SY. Shear wave elasticity imaging: a new ultrasonic technology of medical diagnostic. Ultrasound Med Biol. 1998 Nov; 24(9):1419–1435. doi: 10.1016/s0301-5629(98)00110-0

Savage AJ, Spruiell MD, Schwertz JM, McGwin G, Eberhardt A, Ponce BA. The effect of sliding knots on the suture-tendon interface strength: a biomechanical analysis comparing sliding and static arthroscopic knots. Am J Sports Med. 2013; 41(2):296-301. doi:10.1177/0363546512472168

Savarese E, Bisicchia S, Amendola A. Bilateral spontaneous concurrent rupture of the patellar tendon in a healthy man: case report and review of the literature. Musculoskelet Surg. 2010 Nov; 94(2):81-88. doi: 10.1007/s12306-010-0077-4

Schneider M, Docheva D. Mysteries Behind the Cellular Content of Tendon Tissues. J Am Acad Orthop Surg. 2017 Dec; 25(12): e289–e290. doi: 10.5435/JAAOS-D-17-00520

Schramme M, Hunter S, Campbell N, Blikslager A, Smith R. A surgical tendonitis model in horses: technique, clinical, ultrasonographic and histological characterisation. Vet Comp Orthop Traumatol. 2010; 23(4):231-239. doi: 10.3415/VCOT-09-10-0106

Scotti C, Hirschmann MT, Antinolfi P, Martin I, Peretti GM. Meniscus repair and regeneration: review on current methods and research potential. Europ Cell Mater. 2013 Sep; 26:150–170. doi: 10.22203/ecm.v026a11

Seil R, Hoffmann A, Scheffler S, Theisen D, Mouton C, Pape D. Ramp lesions: Tips and tricks in diagnostics and therapy. Orthopade. 2017 Oct; 46(10): 846–854. doi: 10.1007/ s00132-017-3461-z

Şendur HN, Cindil E, Cerit M, Demir NB, Şendur AB , Oktar SÖ. Interobserver variability and stiffness measurements of normal common extensor tendon in healthy volunteers using shear wave elastography. Skeletal Radiol. 2019 Jan; 48(1):137-141. doi: 10.1007/s00256-018-3021-6

Sereysky JB, Andarawis-Puri N, Jespen KJ, Flatow EL. Structural and mechanical effects of in vivo fatigue damage induction on murine tendon. J Orthop Res. 2012 Jun; 30(6):965-972. doi:10.1002/jor.22012

Seynnes OR, Erskine RM, Maganaris CN, Longo S, Simoneau EM, Grosset JF, Narici MV. Training-induced changes in structural and mechanical properties of the patellar tendon are related to muscle hypertrophy but not to strength gains. J Appl Physiol. 2009 Aug; 107(2):523–530. doi: 10.1152/japplphysiol.00213.2009

Sharma P, Maffulli N. Tendinopathy and tendon injury: the future. Disabil Rehabil. 2008; 30(20-22):1733-1745. doi: 10.1080/09638280701788274

Shearn JT, Kinneberg KRC, Dyment NA, Galloway MT, Kenter K, Wylie C, and Butler DL. "Tendon Tissue Engineering: Progress, Challenges and Translation to the clinic." Journal of Musculoskeletal&Neuronal interactions. 2011 Jun; 11(2): 163-173

Shen ZL, Vince DG, Li ZM. In vivo study of transverse carpal ligament stiffness using acoustic radiation force impulse (ARFI) imaging. PLoS One. 2013; 8(7): e68569.
doi: 10.1371/journal.pone.0068569

Shinohara M, Sabra K, Gennisson JL, Fink M, Tanter M. Real-time visualization of muscle stiffness distribution with ultrasound shear wave imaging during muscle contraction. Muscle Nerve. 2010 Sep;42(3):438–441. doi: 10.1002/mus.21723

Simpson M, Rio E, Cook J. At What Age Do Children and Adolescents Develop Lower Limb Tendon Pathology or Tendinopathy? A Systematic Review and Meta-analysis. Sports Med. 2016 Apr; 46(4):545-57. doi: 10.1007/s40279-015-0438-0

Song EJ, Sohn Y-M, Seo M. Tumor stiffness measured by quantitative and qualitative shear wave elastography of breast cancer. Br J Radiol. 2018 Jun; 91(1086):20170830. doi:10.1259/bjr.20170830

Steinmann S, Pfeifer CG, Brochhausen C, Docheva D. Spectrum of Tendon Pathologies: Triggers, Trails and End-State. Int J Mol Sci. 2020 Jan; 21(3): 844. doi:10.3390/ijms21030844

Svensson RB, Hansen P, Hassenkam T, Haraldsson BT, Aagaard P, Kovanen V, Krogsgaard M, Kjaer M, Magnusson SP. Mechanical properties of human patellar tendon at the hierarchical levels of tendon and fibril. J Appl Physiol. 2012 Feb; 112(3):419–426.
doi: 10.1152/japplphysiol.01172.2011

Taljanovic M, Gimber LH, Becker GW, Latt LD, Klauser AS, Melville DM, Gao L, Witte RS. Shear-Wave Elastography: Basic Physics and Musculoskeletal Applications. Radiographics. May-June 2017; 37(3):855-870. doi:10.1148/rg.2017160116

Taljanovic MS, Melville DM, Klauser AS, Latt LD, Arif-Tiwari H, Gao L, Witte RS. Advances in lower extremity ultrasound. Curr Radiol Rep. 2015;3(6):19.
doi: 10.1007/s40134-015-0100-5

Tamura N, Kuroda T, Kotoyori Y, Fukuda K, Nukada T, Kato T, Kuwano A, Kasashima Y. Application of sonoelastography for evaluating the stiffness of equine superficial digital flexor tendon during healing. Vet Rec. 2017b Feb; 180(5):120. doi: 10.1136/vr.103869

Tamura N, Nukada T, Kato T, Kuroda T, Kotoyori Y, Fukuda K, Kasashima Y. The use of sonoelastography to assess the recovery of stiffness after equine superficial digital flexor tendon injuries: A preliminary prospective longitudinal study of the healing process. Equine Vet J. 2017a Sep; 49(5):590-595. doi: 10.1111/evj.12665

Tardioli A, Malliaras P, Maffulli N. Immediate and short-term effects of exercise on tendon structure: biochemical, biomechanical and imaging responses. Br Med Bull. 2012 Sep; 103(1):169–202. doi: 10.1093/bmb/ldr052

Taş S, Onur MR, Yılmaz S, Soylu AR, Korkusuz F. Shear Wave Elastography Is a Reliable and Repeatable Method for Measuring the Elastic Modulus of the Rectus Femoris Muscle and Patellar Tendon. J Ultrasound Med. 2017b Mar; 36(3):565-570. doi: 10.7863/ultra.16.03032

Taş S, Yilmaz S, Onur MR, Korkusuz F. Obesity decreases patellar tendon stiffness in females but not males. Orthopaedic Proceedings. 2018; Vol. 99-B, No. SUPP_1

Taş S, Yılmaz S, Onur MR, Soylu AR, Altuntas O, Korkusuz F. Patellar tendon mechanical properties change with gender, body mass index and quadriceps femoris muscle strength. Acta Orthop Traumatol Turc. 2017a Jan; 51 (1): 54-59. doi: 10.1016/j.aott.2016.12.003

Tempfer H, Kaser-Eichberger A, Korntner S, Lehner C, Kunkel N, Traweger A Trost A, Strohmaier C, Bogner B, Runge C. Presence of lymphatics in a rat tendon lesion model. Histochem Cell Biol. 2015 Apr; 143:411-419. doi:10.1007/s00418-014-1287-x

Teuschl A, Heimel P, Nürnberger S, van Griensven M, Redl, H, Nau T. A Novel Silk Fiber-Based Scaffold for Regeneration of the Anterior Cruciate Ligament: Histological Results from a Study in Sheep. Am J Sports Med. 2016 Jun; 44(6):1547–1557.
doi: 10.1177/0363546516631954

Thorpe CT, Godinho MSC, Riley GP, Birch HL, Clegg PD, Screen HRC. The interfascicular matrix enables fascicle sliding and recovery in tendon, and behaves more elastically in energy storing tendons. J Mech Behav Biomed Mater. 2015 Dec; 52:85-94.
doi: 10.1016/j.jmbbm.2015.04.009

Thorpe CT, Udeze CP, Birch HL, Clegg PD, Screen HR. Capacity for sliding between tendon fascicles decreases with ageing in injury prone equine tendons: a possible mechanism for age-related tendinopathy? Eur Cell Mater. 2013 Jan; 25: 48-60. doi:10.22203/ecm.v025a04

Tomlinson DJ, Erskine RM, Morse CI, Pappachan JM, Sanderson-Gillard E, Onambélé-Pearson GL. The combined effects of obesity and ageing on skeletal muscle function and tendon properties in vivo in men. Endocrine. 2021 May; 72(2):411-422.
doi:10.1007/s12020-020-02601-0

Trebicka J, Gu W, de Ledinghen V, Aubé C, Krag A, Praktiknjo M, Castera L, Dumortier J, Bauer DJM, Friedrich-Rust M, Pol S, Grgurevic I, Zheng R, Francque S, Gottfriedovà H, Mustapic S, Sporea I, Berzigotti A, Uschner FE, Simbrunner B, Ronot M, Cassinotto C, Kjaergaard M, Andrade F, Schulz M, Semmler G, Drinkovic IT, Chang J, Brol MJ, Rautou PE, Vanwolleghem T, Strassburg CP, Boursier J, Ferstl PJ, Rasmussen DN, Reiberger T, Vilgrain V, Guibal A, Guillaud O, Zeuzem S, Vassord C, Lu X, Vonghia L, Senkerikova R, Popescu A, Margini C, Wang W, Thiele M, Jansen C. Two-dimensional shear wave elastography predicts survival in advanced chronic liver disease. Gut. 2021 Jan; gutjnl-2020-323419.
doi: 10.1136/gutjnl-2020-323419

Tuan PA, Duc NM, An M, Vien MV, Giang BV. The Role of Shear Wave Elastography in the Discrimination Between Malignant and Benign Thyroid Nodules. Acta Inform Med. 2020 Dec; 28(4):248-253. doi:10.5455/aim.2020.28.248-253

Ushiyama T, Chano T, Inoue K, Matsusue Y. Cytokine production in the infrapatellar fat pad: another source of cytokines in knee synovial fluids. Ann Rheum Dis. 2003 Feb; 62(2):108-112. doi: 10.1136/ard.62.2.108

Vailas AC, Tipton CM, Laughlin HL, Tcheng TK, Matthes RD. Physical activity and hypophysectomy on the aerobic capacity of ligaments and tendons. J Appl Physiol Respir Environ Exerc Physiol. 1978 Apr; 44(4):542-546. doi: 10.1152/jappl.1978.44.4.542

Van der Linden, P.D.; Sturkenboom, M.C.; Herings, R.M.; Leufkens, H.G.; Stricker, B.H. Fluoroquinolones and risk of Achilles tendon disorders: case-control study. BMJ. 2002 Jun; 324(7349):1306–1307. doi: 10.1136/bmj.324.7349.1306

Vandeweerd JM, Hontoir F, Kirschvink N, Clegg P, Nisolle JF, Antoine N, Gustin P. Prevalence of naturally occurring cartilage defects in the ovine knee. Osteoarthritis Cartilage. 2013b Aug; 21(8):1125-1131. doi: 10.1016/j.joca.2013.05.006

Vandeweerd JM, Kirschvink N, Muylkens B, Cintas C, Catsyne CV, Hontoir F, Clegg P, Coomer R, Nisolle JF. Magnetic resonance imaging (MRI) anatomy of the ovine stifle. Veterinary Surgery. 2013a; 42(5): 551-558. doi: 10.1111/j.1532-950X.2013.12026.x

Vandeweerd JM, Kirschvink N, Muylkens B, Depiereux E, Clegg P, Herteman N, Lamberts M, Bonnet P, Nisolle JF. A study of the anatomy and injection techniques of the ovine stifle by positive contrast arthrography, computed tomography arthrography and gross anatomical dissection. Vet J. 2012 Aug; 193(2):426-432. doi: 10.1016/j.tvjl.2011.12.011

Vaquero-Picado A, Rodriguez-Merchan EC. Isolated posterior cruciate ligament tears: An update of management. EFORT Open Rev. 2017 Apr; 2(4): 89–96. doi.org/10.1302/2058-5241.2.160009

Varlot Rémi, Martinot Paul. Prévalence des tendinopathies calcanéennes et patellaires de l'enfant en population générale. Médecine humaine et pathologie. 2020. dumas-03035350

Wang A, Mackie K, Breidahl W, Wang T, Zheng MH. Evidence for the Durability of Autologous Tenocyte Injection for Treatment of Chronic Resistant Lateral Epicondylitis: Mean 4.5-Year Clinical Follow-up. Am Sports Med. 2015 Jul; 43(7):1775–1783. doi: 10.1177/0363546515579185

Wang AW, Bauer S, Goonatillake M, Breidahl W, Zheng MH. Autologous tenocyte implantation, a novel treatment for partial-thickness rotator cuff tear and tendinopathy in an elite athlete. BMJ Case Rep. 2013 Jan; 2013: bcr2012007899. doi: 10.1136/bcr-2012-007899

Wang CZ, Li TJ, Zheng YP. Shear modulus estimation on vastus intermedius of elderly and young females over the entire range of isometric contraction. PLoS One. 2014 Jul; 9(7): e101769. doi: 10.1371/journal.pone.0101769

Wang JHC. Mechanobiology of tendon. J Biomech. 2006; 39(9): 1563-1582. doi: 10.1016/j.jbiomech.2005.05.011

Weinberg EP, Adams MJ, Hollenberg GM. Color Doppler sonography of patellar tendinosis. Am J Roentgenol. 1998 Sep; 171(3):743-744. doi: 10.2214/ajr.171.3.9725308

Whitehouse MR, Howells NR, Parry MC, Austin E, Kafienah W, Brady K, Goodship AE, Eldridge JD, Blom AW, Hollander AP. Repair of Torn Avascular Meniscal Cartilage Using Undifferentiated Autologous Mesenchymal Stem Cells: From in Vitro Optimization to a First-in-Human Study. Stem Cells Transl Med. 2017 Apr; 6(4): 1237–1248.
doi: 10.1002/ sctm.16-0199

Williams JG. Achilles tendon lesions in sport. Sports Med. 1986; 3(2):114-35.
doi: 10.2165/00007256-198603020-00003

Williams IF, McCullagh KG, Goodship AE, Silver IA. Studies on the pathogenesis of equine tendonitis following collagenase injury. Res Vet Sci. 1984 May; 36(3):326-338

Wood LK, Brooks SV. Ten weeks of treadmill running decreases stiffness and increases collagen turnover in tendons of old mice. J Orthop Res. 2016 Feb; 34(2): 346-353.
doi: 10.1002/jor.22824

Wu CH, Chen WS, Wang TG. Elasticity of the coracohumeral ligament in patients with adhesive capsulitis of the shoulder. Radiology. 2016 Feb;278(2):458–464.
doi: 10.1148/radiol.2015150888

Xu SY, Liu SY, Xu L, Deng SY, He YB, Li SF, Ni GX. Response of decorin to different intensity treadmill running. Molecular Medicine Reports. 2018 Mar; 17(6): 7911-7917.
doi: 10.3892/mmr.2018.8802

Yasuda K and Hayashi K. Changes in biomechanical properties of tendons and ligaments from joint disuse. Osteoarthritis Cartilage. 1999 Jan; 7(1): 122-129. doi: 10.1053/joca.1998.0167

Yeh CL, Kuo PL, Gennisson JL, Brum J, Tanter M, Li PC. Shear Wave Measurements for Evaluation of Tendon Diseases. IEEE Trans Ultrason Ferroelectr Freq Control. 2016 Nov; 63(11):1906-1921. doi: 10.1109/TUFFC.2016.2591963

Yoo SJ, Lee S, Song Y, Kim CK, Lee BG, Bae J. Elasticity of torn supraspinatus tendons measured by shear wave elastography: a potential surrogate marker of chronicity? Ultrasonography. 2020 Apr; 39(2):144-151. doi: 10.14366/usg.19035

Yu M, Wu J, Hou J, Tang Y, Li F, Zhou C, Li Q, Long Y, Zhang C, Zhang Y, Alike Y, Ou B, Yang R. Young's Modulus of Bilateral Infraspinatus Tendon Measured in Different Postures by Shear Wave Elastography Before and After Exercise. Orthop Surg. 2021 Jul; 13(5): 1570–1578. doi: 10.1111/os.12989

Zanetti M, Metzdorf A, Kundert HP, Zollinger H, Vienne P, Seifert B, Hodler J. Achilles tendons: clinical relevance of neovascularization diagnosed with power Doppler US. Radiology. 2003 May; 227(2):556-560. doi:10.1148/radiol.2272012069

Zhang C, Duan L, Liu Q, Zhang W. Application of shear wave elastography and B-mode ultrasound in patellar tendinopathy after extracorporeal shockwave therapy. J Med Ultrason. 2020 Jul; 47(3):469-476. doi: 10.1007/s10396-019-00979-7

Zhang ZJ, Fu SN. Shear Elastic Modulus on Patellar Tendon Captured from Supersonic Shear Imaging: Correlation with Tangent Traction Modulus Computed from Material Testing System and Test-Retest Reliability. PLoS ONE. 2013 Jun; 8(6): 1–9.
doi: 10.1371/journal.pone.0068216

Zhang ZJ, Ng GYF, Fu SN. Effects of habitual loading on patellar tendon mechanical and morphological properties in basketball and volleyball players. Eur J Appl Physiol. 2015 Nov; 115(11): 2263–2269. doi: 10.1007/s00421-015-3209-6

Zhang ZJ, Ng GYF, Lee WC, Fu SN. Changes in morphological and elastic properties of patellar tendon in athletes with unilateral patellar tendinopathy and their relationships with pain and functional disability. PLoS One 2014 Oct; 9(10):1–9. doi: 10.1371/journal.pone.0108337

Zhu B, You Y, Xiang X, Wang L, Qiu L. Assessment of common extensor tendon elasticity in patients with lateral epicondylitis using shear wave elastography. Quant Imaging Med Surg. 2020 Jan; 10(1):211-219. doi: 10.21037/qims.2019.10.07

ACKNOWLEDGEMENTS

This thesis was made possible thanks to several people whom I would like to thank sincerely.
I am particularly grateful to the Fondation Mont Godinne that made this thesis possible through a research grant.
I am also especially grateful to the University of Namur, URVI and NARILIS for providing funding, as well as to the firm Benetec for providing the ultrasound system.
I would particularly like to thank Professor Jean-Michel Vandeweerd for being so patient with me, providing me his explanations and valuable advices, teaching me how to dissect a sheep's knee, and helping me prepare my tendon samples. I am extremely grateful to Jean-Michel who supported me during the long journey of my thesis.
I am also extremely grateful to my co-promoters, Professor Bernardo Innocenti, Professor Ivo Lambrichts and Professor Peter Clegg for their insightful and constructive criticisms at different stages of my research, and carefully reading and commenting of this manuscript.
I am particularly thankful to Prof Fanny Hontoir for having been so patient with me, explaining me how to prepare histologic slides, and for the many hours of reading together the histologic slides, explaining statistics to me, providing me the descriptive anatomical drawings and all the valuable explanations and advices. I am extremely grateful to Fanny for her availability and support during the long journey of my thesis.
I am particularly grateful to Bernardo Innocenti and Edoardo Bori for familiarizing me with the biomechanical properties of the tendon and for helping me with the performance and interpretation of the biomechanical tests as well as the proofreading of my papers.
I am also very grateful to Nicola Armillotta for helping me with the performance of the biomechanical tests.
I am very thankful to Vincent Simon for helping me with the logistics in sheep and tendon handling, as well as to all the collaborators of the veterinary faculty of UNamur.
I am particularly grateful to Professor Marie-Cécile Nollevaux and her team from the pathology unit of the CHU UCL NAMUR site Godinne for helping me with the cartilage paraffin embedding and slide preparation, and to Professor Charles Nicaise for letting me use his histology laboratory at UNamur.
Many thanks to Alexandra Dugdale for proofreading my papers.
A huge thank to the staff of my hospital's scientific unit who assisted me with the layout of the final thesis.
I am also extremely grateful to my husband Stephane, my daughter Charlotte, my 3 sons Olivier, Victor and Arthur, my parents, my friends and my work colleagues for their patience and constant support throughout the ups and downs during this long journey.
All the people I had the chance to meet or work with during the achievement of my thesis have all my gratitude.
I also thank my dog Clovis for sticking to me for a good part of the writing of my thesis, and preventing me from becoming demoralized or insane.
In addition, I would like to thank all the sheep who gave their lives for my thesis.

ADDENDUM: PUBLISHED AND SUBMITTED PAPERS



"Ultrasound anatomy of the normal stifle in the sheep"

Kayser, Françoise ; Hontoir, Fanny ; Clegg, Peter ; Kirschvink, Nathalie ; Dugdale, Alex ; Vandeweerd, Jean Michel

Document type : *Article de périodique (Journal article)*

Référence bibliographique

Kayser, Françoise ; Hontoir, Fanny ; Clegg, Peter ; Kirschvink, Nathalie ; Dugdale, Alex ; et. al. *Ultrasound anatomy of the normal stifle in the sheep.* In: *Anatomia, Histologia, Embryologia*, (2018)

DOI : 10.1111/ahe.12414

Available at:
http://hdl.handle.net/2078.1/209916

[Downloaded 2019/01/10 at 20:10:36]

Received: 5 September 2018 | Accepted: 28 October 2018

DOI: 10.1111/ahe.12414

ORIGINAL ARTICLE

WILEY ANATOMIA HISTOLOGICA EMBRYOLOGICA

Ultrasound anatomy of the normal stifle in the sheep

Françoise Kayser[1] | Fanny Hontoir[2] | Peter Clegg[3] | Nathalie Kirschvink[2] | Alex Dugdale[4] | Jean Michel Vandeweerd[2]

[1]Centre Hospitalier Universitaire (CHU) UCL Namur-Mont Godinne, Université Catholique de Louvain, Yvoir, Belgium

[2]Department of Veterinary Medicine, Integrated Veterinary Research Unit-Namur Research Institute for Life Sciences (IRVU-NARILIS), University of Namur, Namur, Belgium

[3]Faculty of Health and Life Sciences, Department of Musculoskeletal Biology, University of Liverpool, Neston, UK

[4]Chester Gates Veterinary Specialists, Chester, UK

Correspondence
Jean Michel Vandeweerd, Department of Veterinary Medicine, Integrated Veterinary Research Unit-Namur Research Institute for Life Sciences (IRVU-NARILIS), University of Namur, Namur, Belgium.
Email: jean-michel.vandeweerd@fundp.ac.be

Funding Information
This study was supported by the University of Namur (UNamur), NARILIS (Namur Research Institute for Life Science).

Abstract

Though the ovine stifle is commonly used as a model in research, there is no description of its anatomy at ultrasonography (US). The objective of this study was to provide reference US images of the ovine stifle that are relevant in musculoskeletal research. Four pairs of hindlimbs were scanned, whilst four other pairs were frozen and cut in different planes to compare gross anatomy to US scans. In another pair, the synovial compartments of the stifle were injected and scanned. This study demonstrated that US could be used to assess the ovine stifle. Several structures of clinical interest could be identified with cranial, lateral and medial approaches, such as (a) the tendons of m. quadriceps femoris, m. gluteobiceps, m. popliteus, (b) the common tendon of m. peroneus tertius–extensor longus digitorum–extensor digiti III proprius, (c) the patellar ligament, (d) the medial and lateral collateral ligaments, (e) the cranial horn and middle segment of medial and lateral meniscus, and (f) the synovial recesses. However, the caudal approach was not successful to identify caudal anatomical structures of the joint, due to the muscular mass, that is the caudal aspects of the articular surfaces of the femoral and tibial condyles, the caudal horns of the menisci and the supracondylar synovial recesses. In addition, US remained challenging to assess the internal structures such as cruciate ligaments and articular surfaces. The feasibility of US needs to be tested in vivo.

KEYWORDS
animal model, ovine, sheep, stifle, ultrasound

1 | INTRODUCTION

Skeletally mature sheep are commonly used as large animal models in musculoskeletal research. The ovine stifle has often been the joint of choice to evaluate surgical and medical therapeutics for osteoarthritis (OA) (Aigner et al., 2010; Appleyard, Ghosh, & Swain, 1999; Ghosh et al., 1991; Little et al., 1997; Oakley, 2004), meniscal injuries (Chevrier, Nelea, Hurtig, Hoemann, & Buschmann, 2009; Kohn, 1997; McNickle, Wang, Shewman, Cole, & Williams, 2009), cruciate ligaments (Amis, Camburn, Kempson, Radford, & Stead, 1992; Hunt, Scheffler, Unterhauser, & Weiler, 2005) and collateral ligaments (Allen, Houlton, Adams, & Rushton, 1998). Knowledge of the anatomy of the joint is useful to plan surgical access and to assess the progress of the disease in research studies.

The anatomy of the ovine stifle has been described using radiography (Allen et al., 1998), computed tomography (Vandeweerd et al., 2012) and magnetic resonance imaging (Vandeweerd et al., 2013). Ultrasonography (US) is another useful imaging modality that is time- and cost-effective, non-invasive and dynamic (Alves, Girish, Kalume Brigido, & Jacobson, 2016; Bianchi, Martinoli, Bianchi-Zamorani, & Valle, 2002). Moreover, US is a useful tool for guiding injections and monitoring treatment effectiveness (Alves et al., 2016; Craig, 1999; Oo & Bo, 2016). High-frequency US is considered as an excellent modality to image normal ligaments, tendons, muscles and peripheral nerves as well as to diagnose a wide variety of

 © 2018 Blackwell Verlag GmbH

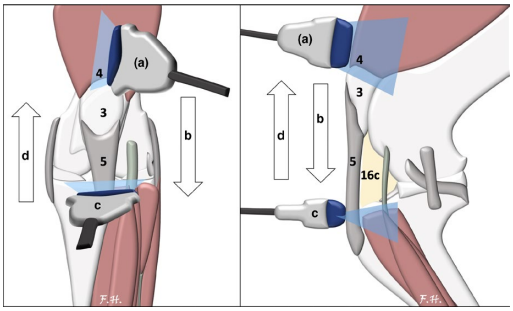


FIGURE 1 Description of the cranial approach (angle 95°). The examination started in the sagittal plane, proximally to the patella (3) (a). The 17.5 MHz linear transducer was placed longitudinally on the tendon of m. quadriceps (4), and the tendon was scanned from the musculo-tendinous junction to its attachment on the patella. The transducer was then moved further distally (b) to visualize the patellar ligament (5) from its patellar attachment to its tibial attachment. The transducer was then rotated through 90° (c), and moved proximally to scan the patellar ligament and the tendon of m. quadriceps in a transverse plane (d). The infrapatellar fat pad (16c) was identified in sagittal and transverse planes. For key, see Table 1

TABLE 1 Annotations in figures

1. Femur
   a Lateral femoral condyle
   b Medial femoral condyle
   c Trochlea
2. Tibia
   a Lateral plateau
   b Medial plateau
3. Patella
4. Tendon of m. quadriceps femoris
5. Patellar ligament
6. Common tendon of m. peroneus tertius–extensor longus digitorum–extensor digiti III proprius
7. Tendon of m. gluteobiceps
8. Medial meniscus
   a Cranial horn
   b Middle segment
9. Lateral meniscus
   a Cranial horn
   b Middle segment
10. Cranial cruciate ligament
11. Caudal cruciate ligament
12. Synovial recesses (Vandeweerd et al., 2012)
   a Suprapatellar
   b Medial femoro-tibial
   c Lateral femoro-tibial
   d Tendinous
   e Subpopliteus
13. Lateral collateral ligament
14. Medial collateral ligament
15. Tendon of m. popliteus
16. Adnexa
   a Skin
   b Fat
   c infrapatellar fat pad

pathological conditions affecting these structures. The US anatomy of the stifle has been described in horses (Hoegaerts et al., 2005) and cattle (Kofler, 1999). However, it has not been described so far in the sheep. US reference images are lacking and would be useful in research studies.

The objective of the current study was to describe the US anatomy of the ovine stifle and provide reference images that would be useful for veterinarians and researchers.

2 | MATERIALS AND METHODS

2.1 | Animals

The hindlimbs of nine Ile-de-France ewes (n = 18), euthanatized for reasons other than musculoskeletal diseases (mastitis), were disarticulated at the coxofemoral joint and collected within 12 hr of death. Sheep were 6–8 years old, weighed 50–85 kg and came from the Sheep Centre of the University of Namur. The experimental protocol (KI 10/148) was approved by the local ethical committee for animal welfare. Limb specimens were moistened, wrapped in gauze, sealed in plastic bags and stored at −20°C. Each limb was identified by a number. For all investigations, limbs were thawed to room temperature, clipped and cleaned.

2.2 | Ultrasonography and gross anatomy

Four pairs of limbs (n = 8) were scanned using an ultrasound iU22 machine (Philips, Eindhoven). Acoustic gel was used to improve transmission of US. Relevant scans were identified for optimal

visualization of anatomical structures of clinical interest: articular surfaces and margins, ligaments, articular capsule, synovial cavity, menisci and their attachments, and tendons. A 17–5 MHz linear transducer was used for all structures except for the cruciate ligaments that were scanned with a 5–1 MHz convex transducer. After scanning, all limbs were dissected, and relevant anatomical structures were identified.

In addition, four other pairs of limbs (n = 8) were frozen in the positions that had been used for scanning. Then, the stifle joints were cut into 3-mm slab sections in sagittal, parasagittal, coronal, transverse and oblique planes. Each gross section was photographed and compared to the corresponding US images for identification of anatomical structures.

One other pair of fresh limbs (n = 2) was used to visualize synovial compartments. Twenty millilitres of water was injected into the femoro-tibial joint with a paraligamentous technique (Vandeweerd et al., 2013). A 21 G 38 mm (11/2 in.) needle was inserted along the lateral aspect of the patellar ligament at mid-distance between its distal and proximal insertions. Immediately after injection, the joint was flexed and extended 30 times.

3 | RESULTS

Four approaches were tested to image the stifle by US: cranial, medial, lateral and caudal.

The caudal approach was not useful since articular structures could not be visualized accurately due to the presence of thigh muscles. Cranial scans were made with the tibia and femur forming an angle of 95°. An angle of 75° was used to better visualize cruciate ligaments. Medial and lateral scans were obtained with the tibia and femur forming an angle of 95° and of 110° to better straighten collateral ligaments.

We described the US scans obtained with each approach in the sagittal, transverse and coronal planes. An oblique plane was used for the cruciate ligaments. Images were captured on a left limb. Scanning planes and positions of the probe are shown in Figures 1, 3, 5, 8 and 10. Figure annotations are detailed in Table 1.

3.1 | Cranial approach

The examination started with a 17–5 MHz linear transducer in the sagittal plane (Figure 1), proximally to the patella, progressing distally, then in a transverse plane progressing proximally. The tendon of m. quadriceps, the patellar ligament and the infrapatellar fat pad were consistently visualized in both planes. The tendon of m. quadriceps and the patellar ligament were hyperechoic to muscle, with a fibrillar yet homogeneous pattern (Figure 2). The infrapatellar fat pad appeared isoechoic to muscle.

Then, the transducer was placed laterally to the patellar ligament, on the cranio-lateral aspect of the joint, to scan, in sagittal and transverse planes, the common tendon of m. peroneus tertius–extensor longus digitorum–extensor digiti III proprius and the tendon of m. gluteobiceps (Figure 3). Both tendons were hyperechoic, fibrillar, homogeneous and fully visualized (Figure 4).

The joint was then flexed (75°), and transverse scans of the articular surface of the trochlea of the femur were made proximally to the patella (Figure 5). Cartilage was seen on the whole surface of the trochlea, being somewhat thicker on the medial aspect. It was hypoechoic to muscle, whilst the cortical bone was hyperechoic (Figure 6). Then, the transducer was moved distally and placed in medial and lateral parasagittal planes to visualize the surfaces of

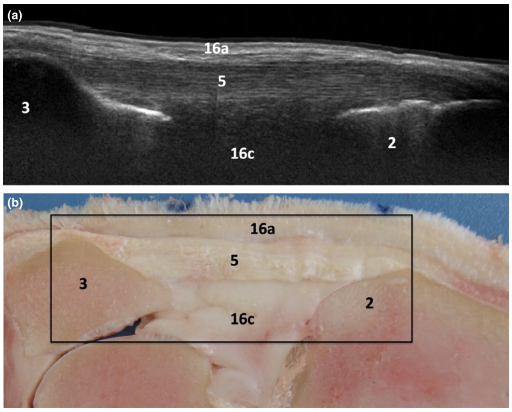


FIGURE 2 Cranio-sagittal US scan (panoramic reconstruction) (a) and corresponding gross anatomic section (angle 95°) (b). The black rectangle shows the scanning field. Note that the infrapatellar fat pad is not visualized on this US scan due to the reconstruction of the image for the manuscript. Tibia (2), patella (3), patellar ligament (5), skin (16a), infrapatellar fat pad (16c)

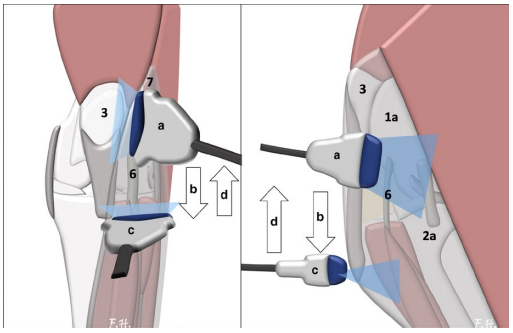


FIGURE 3 Description of the cranio-lateral approach (angle 95°). The transducer was placed on the cranio-lateral aspect of the joint (a) and moved distally (b), to scan the common tendon of m. peroneus tertius–extensor longus digitorum–extensor digiti III proprius (*6*) in a sagittal plane, from its femoral attachment, along the extensor groove, to 2 cm below the tibial plateau. Then, the structures were scanned in a transverse plane (c) from distal to proximal (d). The tendon of m. gluteobiceps (7) was also identified. Lateral femoral condyle (1a), lateral tibial plateau (2a), patella (3)

the femoral condyles. Only the abaxial part of the cartilage surface could be scanned. The margins of the tibial plateau and the cranial horns of the medial and lateral menisci were identified. However, the meniscus was less well visualized laterally than medially due to the interposition of the tendon of m. popliteus. Femoral cartilage was hypoechoic, with the cortical bone being hyperechoic, to muscle. The medial meniscus was hyperechoic to muscle. The lateral meniscus was mostly isoechoic to muscle, but its echogenicity varied due to the interposition of the tendon of m. popliteus. The cartilage of the medial and lateral tibial plateau was not visualized.

A convex 1 MHz transducer was then used in sagittal, oblique and transverse planes to image cruciate ligaments (Figures 5 and 7). The cranial and caudal cruciate ligaments were consistently but incompletely seen (Figure 7) due to their deep location and the necessity of using a 5–1 curvilinear transducer instead of a high-frequency linear transducer.

The cranial approach was suitable to scan several synovial recesses. After intraarticular injection of saline, the suprapatellar recess and the medial and lateral femoro-tibial compartments of the synovial cavity were consistently visualized cranially, respectively, sagittally and parasagittally (Figure 8). The tendinous recess extended distally on the cranio-lateral aspect of the proximal tibia in the extensor groove surrounding the common tendon of m. peroneus tertius–extensor longus digitorum–extensor digiti III proprius.

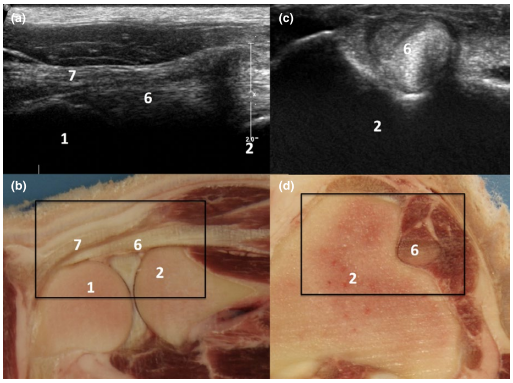


FIGURE 4 Cranio-lateral sagittal (a) and transverse (c) US scans and corresponding gross anatomic sections (b, d) (angle 95°). The black rectangle shows the scanning field. Femur (1), tibia (2), common tendon of m. peroneus tertius–extensor longus digitorum–extensor digiti III proprius (*6*), tendon of m. gluteobiceps (7)

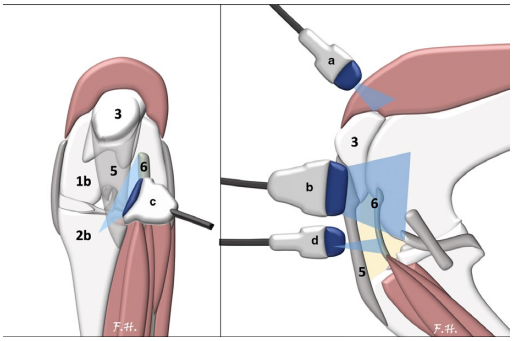


FIGURE 5 Description of the cranial approach (angle 75°). The transducer was placed proximally to the patella and moved distally, in a transverse plane (a), to visualize the trochlea of the femur and its overlying cartilage. Then, the transducer was rotated in parasagittal planes (b), medial and lateral, to visualize the femoral condyles and overlying cartilage, the margins of the tibial plateau, and the cranial horns of the medial and lateral menisci. A curvilinear 5–1 MHz transducer was then placed longitudinally on the patellar ligament and, from that landmark, rotated about 20° clockwise (for a left limb) (c) and anticlockwise (for a right limb), to visualize the cranial and caudal cruciate ligaments. The transducer was rotated further to a transverse plane, to identify the proximal attachment of the cranial cruciate ligament on the axial aspect of the lateral femoral condyle (d). Patella (3), patellar ligament (5), common tendon of m. peroneus tertius–extensor longus digitorum–extensor digiti III proprius (6)

All the recesses were anechoic due to the liquid content. The capsule appeared very thin and hyperechoic (Figure 9).

3.2 | Lateral approach

The lateral aspect of the stifle was evaluated with a linear 17–5 MHz transducer. The transducer was placed parallel to the lateral collateral ligament, the angle between femur and tibia being 110° (Figure 10). The lateral collateral ligament was identified with its attachments respectively on the lateral femoral tubercule and the fibular head (Figure 11). The lateral collateral ligament was hyperechoic to muscle and fibrillar. The middle body of the lateral meniscus was isoechoic to muscle. The peripheral margin of the lateral femoral condyle and its overlying hypoechoic cartilage, and the

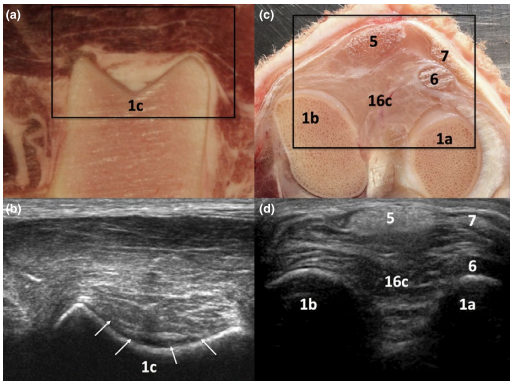


FIGURE 6 Cranio-transverse US scans (b, d) and corresponding gross anatomic sections (a, c) (angle 75°). The black rectangle shows the scanning field. Lateral femoral condyle (1a), medial femoral condyle (1b), trochlea (1c), patellar ligament (5), common tendon of m. peroneus tertius–extensor longus digitorum–extensor digiti III proprius (6), tendon of m. gluteobiceps (7)

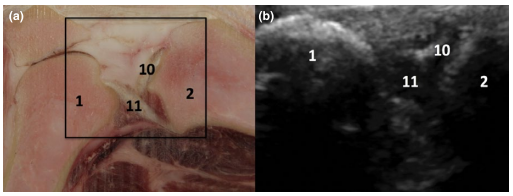


FIGURE 7 Cranio-sagittal US scans (a) and corresponding gross anatomic section (b) (angle 75°). The black rectangle shows the scanning field. Femur (1), tibia (2), cranial cruciate ligament (10), caudal cruciate ligament (11)

margins of the lateral tibial plateau, were consistently visualized. With the joint in a more flexed position (95°), the tendon of m. popliteus was identified. It was hyperechoic to muscle, fibrillar and lying within the groove in the femoral condyle. This tendon was subject to anisotropy because of its curved course. In injected limbs, the subpopliteus recess was visualized, was anechoic and was of small volume.

3.3 | Medial approach

The medial aspect of the stifle was evaluated with a linear 17–5 MHz transducer in coronal and transverse planes similarly to the lateral approach. The medial collateral ligament and its attachments, the middle body of the medial meniscus, the articular margins of the medial femoral condyle and its overlying cartilage, and the abaxial part of the tibial plateau were visualized. The medial collateral ligament was hyperechoic and fibrillar. The medial meniscus was hyperechoic and better visualized than the lateral meniscus (via the lateral approach).

4 | DISCUSSION

This study demonstrated that US can be used to assess the ovine stifle. The caudal approach was not successful to identify caudal anatomical structures of the joint that might be relevant clinically, such as the caudal aspects of the articular surfaces of the femoral and tibial plateau, the caudal horns of the menisci and the supracondylar synovial recesses. Nevertheless, several other relevant anatomical structures could be identified with cranial, lateral and medial approaches. This is of clinical interest for several pathologies that occur in humans and are the object of research in ovine models.

In the current study, the cranial and middle parts of the ovine menisci could be visualized, and especially well in the medial meniscus. Meniscal tear is a very common disease in humans. Different localizations of such tears within and between the menisci have been described (Beaufils & Pujol, 2018). Severe meniscal tears cause meniscal extrusion, mainly in the medial meniscus. Posterior tears are more common than middle or anterior tears (Chahla et al., 2016; Oei et al., 2010). Lesions of the posterior part of the medial meniscus

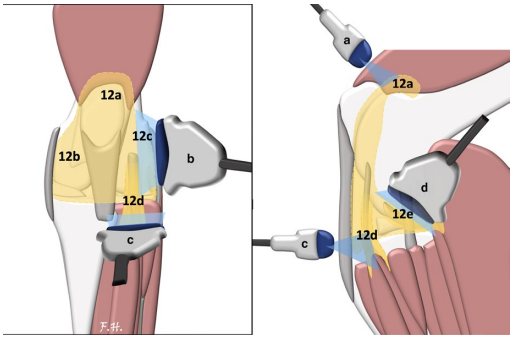


FIGURE 8 Description of the approach to scan synovial recesses (angle 95°). In a cranial approach, the transducer was placed proximally to the patella to identify the suprapatellar recess in a transverse plane (a). Then, it was turned in parasagittal planes to scan the femoro-tibial compartments, laterally and medially (b), and in a transverse plane to image the tendinous recess (c). In a lateral approach (d), the transducer was placed obliquely, in the same plane as the tendon of m. popliteus, to scan the subpopliteus recess. Suprapatellar recess (12a), medial femoro-tibial compartment (12b), lateral femoro-tibial compartment (12c), tendinous recess (12d), subpopliteus recess (12e)

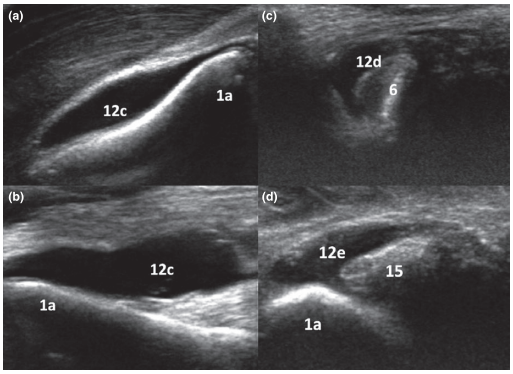


FIGURE 9 Cranio-sagittal (a), cranio-transverse (b, c) and latero-transverse (d) US scans of synovial recesses (angle 95°). Lateral femoral condyle (1a), common tendon of m. peroneus tertius–extensor longus digitorum–extensor digiti III proprius (6), lateral femoro-tibial compartment (12c), tendinous recess (12d), subpopliteus recess (12e), tendon of m. popliteus (15)

are described to occur generally in association with anterior cruciate ligament injuries (Seil et al., 2017). In humans, US has been reported to be a valid alternative to magnetic resonance imaging in the assessment of meniscal extrusion (Papalia et al., 2017). Ovine mesenchymal stem cells/collagen scaffold was tested in a sheep meniscal cartilage tear model (Whitehouse et al., 2017); different repair techniques have also been tested (Scotti, Hirschmann, Antinolfi, Martin, & Peretti, 2013) such as stem cells seeded into scaffolds, cell-free scaffolds, gene therapy, intraarticular delivery of progenitor cells, biological glues, and partial and total tissue engineered meniscus replacement. Meniscectomy and induction of meniscal tears can be performed on medial (Gruchenberg, Burkhardt, Read,

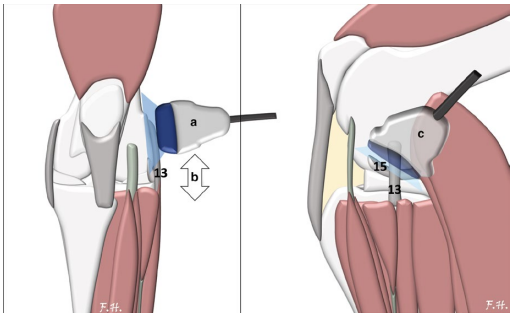


FIGURE 10 Description of the lateral approach. With an angle of 110° between femur and tibia, the transducer was placed longitudinally (a) on the lateral collateral ligament (13), and moved proximally and distally (b) to visualize its attachments on the lateral femoral tubercule and the fibular head. The limb was slightly flexed (angle of 95°), and the transducer was placed obliquely, cranio-proximally to caudo-distally, parallel to the fibres of the tendon of m. popliteus (15) (c)

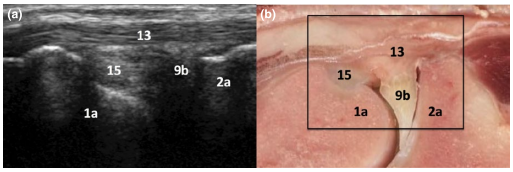


FIGURE 11 Latero-coronal US scans and corresponding gross anatomic section (110°). The black rectangle shows the scanning field. Lateral femoral condyle (1a), lateral tibial plateau (2a), middle segment of lateral meniscus (9b), lateral collateral ligament (13), tendon of m. popliteus (15)

& Bellenger, 2015) and lateral (Beveridge, Shrive, & Frank, 2011) meniscus in the sheep (Little et al., 2010). The current study suggested that, if US must be used to evaluate the efficacy of a treatment for meniscal tears, in a longitudinal research study using the ovine stifle, the initial lesion should be created in the cranial and middle body of the medial meniscus to optimize visualization. Laterally, menisci are also visible but cannot be assessed as accurately due to presence of the popliteus tendon. The echogenicity of the menisci appears similar to humans.

This study also demonstrated that US was able to identify the abaxial cortical surfaces of the femoral condyles and the abaxial overlying cartilage of the femur. The cartilage of the tibial plateau could not be identified, but the lateral, medial and cranial bony margins of the articular tibial surface could be visualized. In addition, the suprapatellar recess, the medial and lateral femoro-tibial compartments of the synovial cavity, the tendinous recess and the subpopliteus recess could be seen. All these anatomical structures can be useful to observe in an ovine model of induced OA. In sheep, OA is induced by medial (Cake et al., 2013) or lateral (Beveridge, Heard, Brown, Shrive, & Frank, 2014) meniscectomy or injuries to cranial cruciate ligament or medial collateral ligament (Beveridge et al., 2014). In OA, in humans, US is used to detect joint effusion, synovial hypertrophy and structural changes, including decrease in cartilage thickness, meniscus bulging and osteophyte formation (Oo & Bo, 2010). The current study indicated that those abnormalities are likely to be detected by US of the ovine stifle.

Cruciate ligament tears are frequent in humans (incidence of 68.6 per 100.000 person-years for the cranial cruciate ligament (Sanders et al., 2016); incidence unknown for caudal cruciate ligament). Caudal cruciate ligament tears are less common than cranial cruciate ligament tears and occur mainly in a multi-ligament-injured knee (Vaquero-Picado & Rodriguez-Merchan, 2017); it can be torn at its tibial or femoral attachments or more commonly through its substance. Isolated caudal cruciate ligament tears are uncommon and are often associated with meniscal tears and future symptomatic OA (Sanders et al., 2017). Research has been conducted in sheep with induced tears to test regeneration of cranial cruciate ligament, for example, after implantation of cell-seeded scaffold (Teuschl et al., 2016). Our study showed that the replacement of the linear transducer by a convex transducer made it possible to differentiate the cruciate ligaments, but a thorough examination of these structures by means of US remained difficult and would probably be not efficient in assessing healing in longitudinal trials.

This study also showed that the trochlea can be examined by US and is easily accessible by maximal flexion of the stifle. A trochlear defect repair method by allograft transplant has been described previously in the sheep (Cinque et al., 2017; Kitamura, Yokota, Kurokawa, Gong, & Yasuda, 2016), and therefore, US could potentially be useful in such studies. The medial and lateral collateral ligaments were also well identified. In humans, the medial collateral ligament is the most common injured ligament in the knee; it is a major stabilizer of the knee joint (Frank et al., 2012). In research sheep, damage to the medial collateral ligament can be induced (Beveridge et al., 2014; Funakoshi et al., 2007), and it is likely that US could be used to follow up healing. The patellar ligament was perfectly visualized in our study. In humans, injuries such as patellar tendinopathy, chronic tendinosis, enthesiopathy or patellar tendon tear or rupture are known (Pengas, Assiotis, Khan, & Spalding, 2016; Schwartz, Watson, & Hutchinson, 2015). US was shown to be a good tool to assess the patellar tendon in humans (Miller, 2013). Again US could be used in the sheep for the follow-up of induced lesions of the patellar ligament. The other tendons are less suited for US monitoring in longitudinal research studies in sheep. Though the quadriceps tendon is well identified by US in humans, it is less well visualized in sheep due to its shortness. The common tendon of m. peroneus tertius–extensor longus digitorum–extensor digiti III proprius is well visualized in sheep but does not exist in humans. Finally, our study showed that the ovine tendon of m. popliteus has a similar aspect as in humans, but is not well identified in its caudal part.

However, it is important to be aware of the limitations to the current study. It was performed in cadaveric limbs. We did not have to contend with animal movements and therefore probably obtained a higher image quality. Sedation or general anaesthesia would probably improve acquisition of images in live subjects. Furthermore, the posterior aspect of the stifle joint remained inaccessible by US.

In conclusion, US is likely to be an effective tool to monitor several structural changes associated with induced OA, with tears of the medial meniscus, and with injuries to the collateral and patellar ligaments. However, this needs to be assessed in in vivo research studies.

ACKNOWLEDGEMENTS

We acknowledge V. Simon and N. Legrand for their help.

COMPETING INTERESTS

None of the authors of this paper has a financial or personal relationship with people or organizations that could inappropriately influence or bias the content of the paper.

ORCID

Fanny Hontoir https://orcid.org/0000-0003-0847-8167

Jean Michel Vandeweerd https://orcid.org/0000-0002-2482-4878

REFERENCES

Aigner, T., Cook, J. L., Gerwin, N., Glasson, S. S., Laverty, S., Little, C. B., … Kraus, V. B. (2010). Histopathology atlas of animal model systems - overview of guiding principles. *Osteoarthritis Cartilage*, *18*, S2–S6. https://doi.org/10.1016/j.joca.2010.07.013.

Allen, M. J., Houlton, J. E., Adams, S. B., & Rushton, N. (1998). The surgical anatomy of the stifle joint in sheep. *Veterinary Surgery*, *27*, 596–605. https://doi.org/10.1111/j.1532-950X.1998.tb00536.x

Alves, T. I., Girish, G., Kalume Brigido, M., & Jacobson, J. A. (2016). US of the Knee: Scanning techniques, pitfalls, and pathologic conditions. *Radiographics*, *36*, 1759–1775. https://doi.org/10.1148/rg.2016160019

Amis, A., Camburn, M., Kempson, S., Radford, W., & Stead, A. (1992). Anterior cruciate ligament replacement with polyester fibre. A long-term study of tissue reactions and joint stability in sheep. *The Journal of Bone and Joint Surgery, British*, *74*, 605–613. https://doi.org/10.1302/0301-620X.74B4.1624524

Appleyard, R. C., Ghosh, P., & Swain, M. V. (1999). Biomechanical, histological and immunohistological studies of patellar cartilage in an ovine model of osteoarthritis induced by lateral meniscectomy. *Osteoarthritis and Cartilage*, *7*, 281–294. https://doi.org/10.1053/joca.1998.0202

Beaufils, P., & Pujol, N. (2018). Meniscal repair: Technique. *Orthopaedics & Traumatology Surgery & Research*, *104*, 137–S145. https://doi.org/10.1016/j.otsr.2017.04.016.

Beveridge, J. E., Heard, B. J., Brown, J. J., Shrive, N. G., & Frank, C. B. (2014). A new measure of tibia femoral subchondral bone interactions that correlates with early cartilage damage in injured sheep. *Journal of Orthopaedic Research*, *32*, 1371–1380. https://doi.org/10.1002/jor.22685.

Beveridge, J. E., Shrive, N. G., & Frank, C. B. (2011). Meniscectomy causes significant in vivo kinematic changes and mechanically induced focal chondral lesions in a sheep model. *Journal of Orthopaedic Research*, *29*, 1397–1405. https://doi.org/10.1002/jor.21395.

Bianchi, S., Martinoli, C., Bianchi-Zamorani, M. P., & Valle, M. (2002). Ultrasound of the joints. *European Radiology*, *12*, 56–61. https://doi.org/10.1007/s00330-001-1162-8.

Cake, M. A., Read, R. A., Corfield, G., Daniel, A., Burkhardt, D., Smith, M. M., & Little, C. B. (2013). Comparison of gait and pathology outcomes of three meniscal procedures for induction of knee osteoarthritis in sheep. *Osteoarthritis Cartilage*, *21*, 226–236. https://doi.org/10.1016/j.joca.2012.10.001

Chahla, J., Dean, C., Moatshe, G., Mitchell, J., Cram, T., Yacuzzi, C., & LaPrade, R. (2016). Meniscal ramp lesions. anatomy, incidence, diagnosis, and treatment. *Orthopaedic Journal of Sports Medicine*, *4*, 2325967116657815. https://doi.org/10.1177/2325967116657815.

Chevrier, A., Nelea, M., Hurtig, M., Hoemann, C. D., & Buschmann, M. D. (2009). Meniscus structure in human, sheep, and rabbit for animal models of meniscus repair. *Journal of Orthopaedic Research*, *27*, 1197–1203. https://doi.org/10.1002/jor.20869.

Cinque, M., Kennedy, N., Moatshe, G., Vinagre, G., Chahla, J., Hussain, Z., & LaPrade, R. (2017). Osteochondral allograft transplants for large trochlear defects. *Arthroscopy Techniques*, *6*, e1703–e1707. https://doi.org/10.1016/j.eats.2017.06.027.

Craig, J. G. (1999). Infection: Ultrasound-guided procedures. *Radiologic Clinics of North America*, *37*, 669–678. https://doi.org/10.1016/S0033-8389(05)70122-6

Frank, C. B., Beveridge, J. E., Huebner, K. D., Heard, B. J., Tapper, J. E., O'Brien, E. J., & Shrive, N. G. (2012). Complete ACL/MCL deficiency induces variable degrees of instability in sheep with specific kinematic abnormalities correlating with degrees of early osteoarthritis. *Journal of Orthopaedic Research*, *30*, 384–392. https://doi.org/10.1002/jor.21549.

Funakoshi, Y., Hariu, M., Tapper, J. E., Marchuk, L. L., Shrive, N. G., Kanaya, F., … Frank, C. B. (2007). Periarticular ligament changes following ACL/MCL transection in an ovine stifle joint model of osteoarthritis. *Journal of Orthopaedic Research*, *25*, 997–1006. https://doi.org/10.1002/jor.20370

Ghosh, P., Burkhardt, D., Read, R., & Bellenger, C. (1991). Recent advances in animal models for evaluating chondroprotective drugs. *The Journal of Rheumatology*, *27*, 143–146.

Gruchenberg, K., Ignatius, A., Friemert, B., von Lübken, F., Skaer, N., Gellynck, K., … Dürselen, L. (2015). In vivo performance of a novel silk fibroin scaffold for partial meniscal replacement in a sheep model. *Knee Surgery, Sports Traumatology, Arthroscopy*, *23*, 2218–2229. https://doi.org/10.1007/s00167-014-3009-2.

Hoegaerts, M., Nicaise, M., Van Bree, H., & Saunders, J. H. (2005). Cross-sectional anatomy and comparative ultrasonography of the equine medial femorotibial joint and its related structures. *Equine Veterinary Journal*, *37*, 520–529. https://doi.org/10.2746/042516405775314817

Hunt, P., Scheffler, S., Unterhauser, F., & Weiler, A. (2005). A model of soft-tissue graft anterior cruciate ligament reconstruction in sheep. *Archives of Orthopaedic and Trauma Surgery*, *125*, 238–248. https://doi.org/10.1007/s00402-004-0643-z

Kitamura, N., Yokota, M., Kurokawa, T., Gong, J. P., & Yasuda, K. (2016). In vivo cartilage regeneration induced by a double-network hydrogel: Evaluation of a novel therapeutic strategy for femoral articular cartilage defects in a sheep model. *Journal of Biomedical Materials Research Part A*, *104*, 2159–2165. https://doi.org/10.1002/jbm.a.35745.

Kofler, J. (1999). Ultrasonographic examination of the stifle region in cattle-normal appearance. *The Veterinary Journal*, *158*, 21–32. https://doi.org/10.1053/tvjl.1998.0329.

Kohn, D., Rudert, M., Wirth, C., Plitz, W., Reiss, G., & Maschek, H. (1997). Medial meniscus replacement by a fat pad autograft. An experimental study in sheep. *Internal Orthopaedics*, *21*, 232–238. https://doi.org/10.1007/s002640050157

Little, C., Smith, M., Cake, M., Read, R., Murphy, M., & Barry, F. (2010). The OARSI histopathology initiative-recommendations for assessments of osteoarthritis in sheep and goats. *Osteoarthritis and Cartilage*, *18*, 80–92. https://doi.org/10.1016/j.joca.2010.04.016.

Little, C., Smith, S., Ghosh, P., & Bellenger, C. (1997). Histomorphological and immunohistochemical evaluation of joint changes in a model of osteoarthritis induced by lateral meniscectomy in sheep. *The Journal of Rheumatology*, *24*, 2199–2209.

McNickle, A., Wang, V., Shewman, E., Cole, B., & Williams, J. (2009). Performance of a sterile meniscal allograft in an ovine model. *Clinical Orthopaedics and Related Research*, *467*, 1868–1876. https://doi.org/10.1007/s11999-008-0567-y.

Miller, T. T. (2013). The patellar tendon. *Seminars in Musculoskeletal Radiology*, *17*, 56–59. https://doi.org/10.1055/s-0033-1333915

Oakley, S. P., Lassere, M. N., Portek, I., Szomor, Z., Gosh, P., Kirkham, B. W., … Appleyard, R. C. (2004). Biomechanical, histologic and macroscopic assessment of articular cartilage in a sheep model of osteoarthritis. *Osteoarthritis and Cartilage*, *12*, 667–679. https://doi.org/10.1016/j.joca.2004.05.006.

Oei, E. H., Koster, I. M., Hensen, J. H., Boks, S. S., Wagemakers, H. P., Koes, B. W., … Hunink, M. G. (2010). MRI follow-up of conservatively treated meniscal knee lesions in general practice. *European Radiology*, *20*, 1242–1250. https://doi.org/10.1007/s00330-009-1648-3.

Oo, W. M., & Bo, M. T. (2016). Role of Ultrasonography in Knee Osteoarthritis. *Journal of Clinical Rheumatology*, *22*, 324–329. https://doi.org/10.1097/RHU.0000000000000436.

Papalia, R., Papalia, G., Russo, F., Diaz, L. A., Bressi, F., Sterzi, S., & Denaro, V. (2017). Meniscal extrusion as booster of osteoarthritis. *Journal of Biological Regulators & Homeostatic Agents*, *31*, 33–44.

Pengas, I. P., Assiotis, A., Khan, W., & Spalding, T. (2016). Adult native knee extensor mechanism ruptures. *Injury*, *47*, 2065–2070. https://doi.org/10.1016/j.injury.2016.06.032.

Sanders, T. L., Kremers, H. M., Bryan, A. J., Larson, D. R., Dahm, D. L., Levy, B. A., … Krych, A. J. (2016). Incidence of Anterior Cruciate Ligament Tears and Reconstruction: A 21-Year Population-Based Study. *The American Journal of Sports Medicine*, *44*, 1502–1507. https://doi.org/10.1177/0363546516629944.

Sanders, T. L., Pareek, A., Barrett, I. J., Kremers, H. M., Bryan, A. J., Stuart, M. J., … Krych, A. J. (2017). Incidence and long-term follow-up of isolated posterior cruciate ligament tears. *Knee Surgery, Sports Traumatology, Arthroscopy*, *25*, 3017–3023. https://doi.org/10.1007/s00167-016-4052-y.

Schwartz, A., Watson, J. N., & Hutchinson, M. R. (2015). Patellar tendinopathy. *Sports. Health*, *7*, 415–420. https://doi.org/10.1177/1941738114568775.

Scotti, C., Hirschmann, M. T., Antinolfi, P., Martin, I., & Peretti, G. M. (2013). Meniscus repair and regeneration: Review on current methods and research potential. *European Cells & Materials Journal*, *26*, 150–170. https://doi.org/10.22203/eCM.v026a11

Seil, R., Hoffmann, A., Scheffler, S., Theisen, D., Mouton, C., & Pape, D. (2017). Ramp lesions: Tips and tricks in diagnostics and therapy. *Der Orthopäde*, *46*, 846–854. https://doi.org/10.1007/s00132-017-3461-z.

Teuschl, A., Heimel, P., Nürnberger, S., van Griensven, M., Redl, H., & Nau, T. (2016). A Novel Silk Fiber-Based Scaffold for Regeneration of the Anterior Cruciate Ligament: Histological Results From a Study in Sheep. *The American Journal of Sports Medicine*, *44*, 1547–1557. https://doi.org/10.1177/0363546516631954.

Vandeweerd, J. M., Kirschvink, N., Muylkens, B., Cintas, C., Catsyne, C., Hontoir, F., … Nisolle, J. F. (2013). Magnetic resonance imaging (MRI) anatomy of the ovine stifle. *Veterinary Surgery*, *42*, 551–558. https://doi.org/10.1111/j.1532-950X.2013.12026.x.

Vandeweerd, J. M., Kirschvink, N., Muylkens, B., Depiereux, E., Clegg, P., Herteman, N., … Nisolle, J. F. (2012). A study of the anatomy and injection techniques of the ovine stifle by positive contrast arthrography, computed tomography arthrography and gross anatomical dissection. *The Veterinary Journal*, *193*, 426–432. https://doi.org/10.1016/j.tvjl.2011.12.011.

Vaquero-Picado, A., & Rodriguez-Merchan, E. C. (2017). Isolated posterior cruciate ligament tears: An update of management. *EFORT Open Reviews*, *2*, 89–96. https://doi.org/10.1302/2058-5241.2.160009.

Whitehouse, M. R., Howells, N. R., Parry, M. C., Austin, E., Kafienah, W., Brady, K., … Hollander, A. P. (2017). Repair of Torn Avascular Meniscal Cartilage Using Undifferentiated Autologous Mesenchymal Stem Cells: From in Vitro Optimization to a First-in-Human Study. *Stem Cells Translational Medicine*, *6*, 1237–1248. https://doi.org/10.1002/sctm.16-0199.

How to cite this article: Kayser F, Hontoir F, Clegg P, Kirschvink N, Dugdale A, Vandeweerd JM. Ultrasound anatomy of the normal stifle in the sheep. *Anat Histol Embryol*. 2018;00:1–10. https://doi.org/10.1111/ahe.12414

Ex vivo study correlating the stiffness of the ovine patellar tendon to age and weight

Françoise Kayser[1], Edoardo Bori[2], Sophie Fourny[3], Fanny Hontoir[4], Bernardo Innocenti[5], Peter Clegg[6], Alexandra Dugdale[7], Jean-Michel Vandeweerd[8]

[1]CHU UCL NAMUR (Centre Hospitalier Universitaire-Université Catholique de Louvain-NAMUR) site Godinne, Avenue Gaston Thérasse 1, 5530 Yvoir, Belgium, francoise.kayser@uclouvain.be;
ORCID: 0000-0002-2151-9253

[2]BEAMS Department (Bio-Electro and Mechanical System)- ULB (Université Libre de Bruxelles)-Ecole Polytechnique de Bruxelles, Avenue Franklin Roosevelt 50, 1000 Bruxelles, Belgium, edoardo.bori@gmail.com; ORCID: 0000-0002-1670-8359

[3]Department of Veterinary Medicine, University of Namur, Rue de Bruxelles 61, 5000 Namur, Belgium, sophiefourny@hotmail.com; ORCID: 0000-0001-9639-0952

[4]NaRILiS (Namur Research Institute for Life Sciences)-IRVU (Integrated Veterinary Research Unit), Department of Veterinary Medicine, University of Namur, Rue de Bruxelles 61, 5000 Namur, Belgium, fanny.hontoir@unamur.be;
ORCID: 0000-0003-0847-8167

[5]BEAMS Department (Bio-Electro and Mechanical System)- ULB (Université Libre de Bruxelles)-Ecole Polytechnique de Bruxelles, Avenue Franklin Roosevelt 50, 1000 Bruxelles, Belgium, bernardo.innocenti@ulb.ac.be;
ORCID: 0000-0001-8992-8865

[6]Faculty of Health and Life Sciences, Department of Musculoskeletal Biology, University of Liverpool, Neston, Liverpool L69 7TX, UK, p.d.clegg@liverpool.ac.uk/
ORCID: 0000-0003-0632-0032

[7]Chester Gates Veterinary Specialists CVS (UK) Ltd., Units E & F, Telford Court, Dunkirk Trading Estate, Gates Lane, Chester, CH1 6LT, UK, alexdugdale@btinternet.com;
ORCID: 0000-0002-6577-968X

[8] NaRILiS (Namur Research Institute for Life Sciences)-IRVU (Integrated Veterinary Research Unit), Department of Veterinary Medicine, University of Namur, Rue de Bruxelles 61, 5000 Namur, Belgium, jean-michel.vandeweerd@unamur.be.
ORCID: 0000-0002-2482-4878

Corresponding author: Françoise Kayser CHU UCL NAMUR site Godinne, Avenue Gaston Thérasse 1, 5530 Yvoir, Belgium, francoise.kayser@uclouvain.be

Abstract

Tendons play a crucial role in the musculoskeletal system. In humans, tendon injuries, especially chronic tendinopathy, are very common and the patellar tendon is a frequent location for tendinopathy or injuries. The biomechanical characteristics of the patellar tendon, such as elasticity and stiffness, are of paramount importance and constitute major outcome measures in research studies. We aimed to assess whether the stiffness of the healthy ovine patellar tendon changes with age and weight in a population of normal animals. Sixty-eight "patella-patellar tendon-tibial tuberosity" units from thirty-four Ile-de-France ewes of body mass 65 to 95 kg, euthanized for reasons other than musculoskeletal diseases, underwent a tensile test providing a measure of the tendon stiffness. Animals were sorted into three categories of age (1-2 yo, 3-5 yo, 6-10 yo). We found a positive but not significant correlation between age category and stiffness ($r=0.22$, $p=0.27$). There was a significantly positive correlation between weight and stiffness ($r=0.39$, $p=0.04$). In conclusion, the study characterized biomechanical properties of healthy tendons, provided useful reference values, and established the basis for future biomechanical tests on healing tendons in sheep. The most appropriate sheep population for those future studies would be non-overweight young adults presenting with no lameness.

Keywords: age, ovine, patellar tendon, stiffness, weight

Introduction

Tendons play a crucial role in the musculoskeletal system. In humans, tendon injuries, especially chronic tendinopathy, are very common in occupational and athletic settings, and in the elderly population. They may be associated with significant morbidity and abnormal joint movement, and are an important cause of musculoskeletal disabilities or pain.

In particular, patellar tendon injuries occur either naturally as chronic tendinosis, partial/full-thickness tendon tears, acute avulsion fractures [Peace et al. 2006], or as artificially-created lesions when the patellar tendon is used as a donor site for tendon autograft in anterior cruciate ligament [Benner et al. 2012] and medial patellofemoral ligament reconstruction [Witoński et al. 2013].

Because of the restricted self-restoring capacity of tendon, spontaneous tendon healing often results in fibrous adhesions and inferior fibrotic scar tissue which is both mechanically- and functionally inferior [Sharma and Maffulli 2005]. The tendon is also prone to re-injury.

Functional recovery of tendon injuries is challenging. Currently, treatment solutions are disappointing and healed tendons do not recuperate the biomechanical properties of intact tendons. There is, therefore, a need for an improved therapeutic approach [Gaida and Cook 2011; Charousset et al. 2014; Nanos and Malanga 2015; Ode and al. 2016].

In orthopaedic research, to develop new technologies, preclinical studies using animal models are needed [Cook and al. 2014]. The need to mimic the dimensions and loading experienced by an adult human joint requires that large animal models of disease are employed. The use of the sheep as an animal model enables larger sampling populations, lameness assessment and scoring, and the use of non-invasive imaging in longitudinal studies. One of the advantages of the sheep over other large animal models is the human-like size of joints such as the knee [Little and Smith 2008]. The anatomy of the ovine knee (stifle) has been well-characterized [Proffen and al. 2012]. Ultrasonographic, CT and MRI anatomy of the stifle have been

described [Vandeweerd and al. 2012; Vandeweerd and al. 2013; Kayser and al. 2019].

Since the patellar tendon covers a key-role in extension of the knee joint, the biomechanical characteristics of the patellar tendon, such as elasticity and stiffness, are of paramount importance and constitute major outcome measures in research studies. However, to date, these patellar tendon properties have not been described in sheep, and there is therefore a need to document them in a population of research animals.

The aim of this study was therefore to document the properties of the healthy patellar tendon in research sheep, assessing eventual changes with age and weight; the result was sought in terms of stiffness, addressing in this way the whole tendon system and not only the material it is composed by.

Material and methods

Animals

Thirty-four ewes (Ile de France; n= 34), from the Ovine Research Center of the University of Namur, were used. Their age ranged from 2 to 10 years, and their weight from 65 to 95 kg. The experimental protocol 10150MU was approved by the local ethical committee for animal welfare. All animals had no history of hindlimb lameness. They were assessed by palpation and observation. No swelling or pain of the stifle was observed. Animals were not lame before euthanasia.

Animal were sorted into three categories of age (1-2yo, 3-5yo, 6-10yo).

Gross anatomy

Animals were sacrificed by intravenous administration of pentobarbital (150 mg/kg). Both hind limbs were transected at the level of the mid-femur within 1 hour of death. Soft tissue, including skin and muscles were removed. The patellar tendon and its attachments on the patella and the tibial tuberosity were carefully dissected and observed to confirm the absence of lesions or abnormalities.

The joint capsule, collateral ligaments and cruciate ligaments were transected. The knee joint was disarticulated, and the tibial tuberosity and patella were transected at 1.5 cm from their respective tendon attachments. Bone attachments were preserved so as not to affect the tendon insertion areas that are fundamental for mechanical load-transfer.

Each harvested specimen consisting of an intact "patella-patellar tendon-tibial tuberosity" unit was individually wrapped in moistened gauze (with 0.9 % w/v NaCl), sealed in plastic bags, individually identified by a number and stored at -20°C.
Four-mm thick osteochondral slabs in a coronal plane were obtained (medial femoral condyle, lateral femoral condyle, medial tibial condyle, lateral tibial condyle), before being processed for histology.

Histopathology of cartilage

Histology is used as the gold standard to assess the articular cartilage of a joint, joint deterioration and joint ageing [Little and al. 2010; Vandeweerd and al. 2013b]. Articular cartilage changes are associated with ageing and diseases such as osteoarthritis. In the current study, histology was performed to assess joint deterioration and confirm the sample was representative of a normal ageing population of sheep by comparison to results of previously published studies [Vandeweerd and al. 2013a].
The osteochondral slabs were fixed in a 10% w/v neutral buffered formalin for 48 hours. The specimen was decalcified in 10% w/v formic acid/ 5% w/v formalin during 8 to 10 days, depending on softening of the slabs. After paraffin embedding, 7µm sections were cut and mounted on Superfrost Ultraplus® slides that improve cartilage adhesion. The sections were thoroughly deparaffinized in several xylene washes and graded alcohols to 70% w/v ethanol, then stained in 0.04% w/v toluidine blue and counterstained in 0.1% w/v aqueous fast green FCF. Finally, the slides were dehydrated in two changes of 99% isopropyl alcohol and two changes of xylene before mounting in DPX (DPX mounting media for histology).

The OARSI recommendations were used for histological scoring of the cartilage [Little and al. 2010]. Histological abnormalities included: structural defects (0-10), chondrocyte density (0-4), cell cloning (0-4), interterritorial Toluidine blue (0-4), tidemark (0-3), extent of the defect (0-5) with a total scoring of 0-30 (Figure 1). The histological grade per limb was determined by the summation of the total scores of the 4 anatomical regions in that limb.

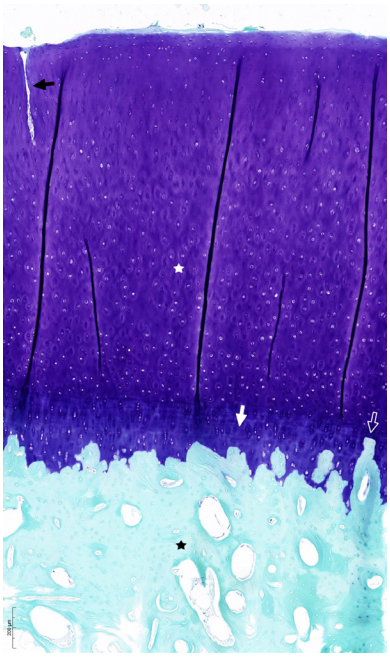


Fig.1. Toluidine blue/fast green stained section of cartilage scored as follows: Structure 4 (fissures to transitional zone 1/3 depth (black arrow)), Chondrocyte density 0, Cell cloning 0, Interterritorial toluidine blue 0, Tidemark 2 (duplicated tidemark (white arrow) with blood vessel penetrating through the subchondral bone plate (white open arrow)), with a total score of 6. Cartilage (white star). Subchondral bone (black star). Scale in lower left corner.

Biomechanical tests

In thirty-four matched pairs of limbs (n=68), a uni-axial tensile test was performed on patellar tendons following an in-house validated procedure [Innocenti and al. 2018]. For all investigations, frozen "patella-patellar tendon-tibial tuberosity" units were thawed to room temperature, cleaned thoroughly with 0.9 % w/v of NaCl and placed

on a metal frame. The osseous parts of the specimen were cut with pliers to fit the clamp size. Four black ink dot markers were directly drawn onto each specimen in order to measure the displacement of the tendon tissue during the tensile test (Figure 2).

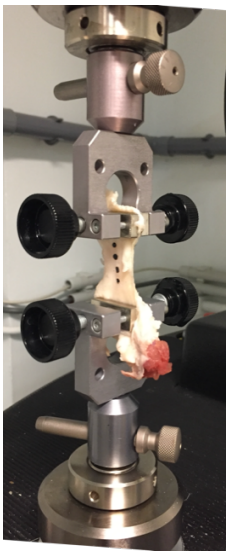


Fig.2. Patella-patellar tendon-tibial tuberosity unit fixed by two clamps. Four black ink dot markers were directly drawn onto the tendon specimen.

The camera was set to 100 fps. Force outputs were obtained via a dedicated 1 kN load cell (Lloyd Instruments Ltd). As the tendons had been manipulated and then stored at -20° C before the biomechanical tests, a series of 10 pre-conditioning stress-relaxation procedures was performed to ensure fibers alignment before the tensile testing. As recommended in the ASTM D638 standard [ASTM International 2018], a crosshead speed of 5 mm/min was applied for the tensile test. The axial force was recorded and paired with the relative displacement during the tests. The tensile test was performed until failure and the resulting force-displacement curve was analyzed: after the initial toe-region, the linear region of the curve (corresponding to the elastic region, i.e. the elongation of the helical structure of collagen [Kirkendall and Garrett 1997]) was defined thanks to the dedicated software: a linear fitting process was used to determine the boundaries of the linear region and this latter was studied to obtain the relative stiffness of the tissue (obtained from the slope of the curve in the selected region).

Statistical analysis

In order to examine the normality of data (patellar tendon stiffness and histological scores of articular cartilage), Kolmogorov-Smirnov and Shapiro-Wilk tests were applied. Non-parametric tests were used, due to the non-normality of the data. The Wilcoxon signed-rank test was used to compare observations that were not independent (difference in patellar tendon stiffness between left and right hindlimbs). One limb was randomly chosen within each pair and data obtained from that limb (tendon stiffness, articular cartilage histological grades) were used for analysis. Correlations between patellar tendon stiffness and other variables (age, weight, histological grades) were assessed by Spearman correlation coefficient. Data were collected in Microsoft Excel and analysed using Graph Pad Prism 8. A p-value below 0.05 was considered to indicate a statistically significant difference.

Results

Cartilage histopathology

Among the 272 (4x68) histological slices, none presented artefacts or inadequate coloration that may have prevented correct interpretation. We found no significant difference in limb histological total scores between left and right limbs ($p=0.93$).

The histological scores (median, minimum, maximum) were, however, different between regions of interest: medial tibial condyle (7, 2, 17), lateral tibial condyle (6, 2, 18), medial femoral condyle (6, 2, 21) and lateral femoral condyle (5.5, 1, 13). Among the total number of lesions, we found 36.2% in the medial femoral condyle, 6.8% in the lateral femoral condyle, 37.9% in the medial tibial condyle and 15.5% in the lateral tibial condyle. Among the histological abnormalities, beside the total score, structural defects and tidemark increased the most with age and weight.

There was a significant positive correlation between body weight and histological score ($r=0.51$; $p=0.002$), and between age and histological score ($r= 0.67$; $p<0.0001$).

Tendon stiffness

Our tests confirmed that the patellar tendon has the typical "region" behavior, with a non-linear one (toe-region) followed by a linear region preceding the eventual damaging of the fibers and consequent failure of the tendon (Figure 3).
The mean stiffness value of the 68 tendons was 52.44N/mm (SD 35.62, SD = standard deviation).

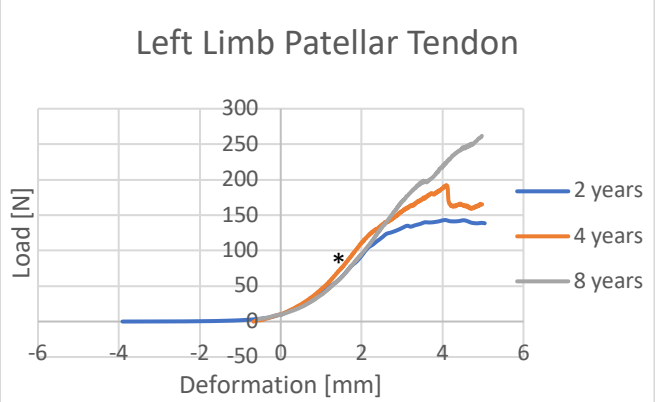


Fig.3. Stiffness curve of the left patellar tendons related to three different age groups: 2 yo (year old), 4 yo) and 8 yo. * = linear region of the curve.

We found a positive but not significant correlation between stiffness and age (r=0.22, p=0.27). We also found a statistically-significant positive correlation between body weight and tendon stiffness (r=0.39, p=0.04) and between articular cartilage histological scores and tendon stiffness (r=0.47, p=0.02) (Table 1).

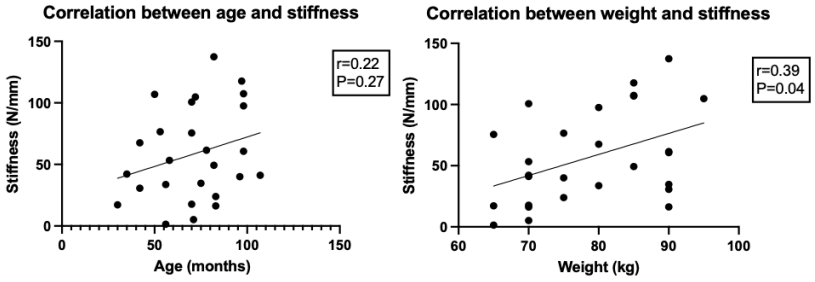


Figure 4: Correlation plot between age and stiffness (left) and between weight and stiffness (right). Correlation was positive but not significant between stiffness and age and statistically-significant positive between body weight and stiffness.

	A1(1-2yo)	A2(3-5yo)	A3(6-10yo)
Weight (kg, mean+/-SD)	74.47+/-8.8	77.79+/-9.23	77.63+/-8 .44
Histological score (median, minimum, maximum)	4(0,4)	9(4,47)	22.5(6,69)
Stiffness (N/mm, mean+/SD)	25.51+/-14.57	53.14+/-35.6	47.2+/-30.11

Table 1: Weight, histological scores and stiffness related to three different age groups: A1 (1-2 yo (year old)), A2 (3-5 yo) and A3 (6-10 yo).

Discussion

In research studies, the biomechanical characteristics of the tendon, like elasticity and stiffness, represent major outcome measures. Due to the biomechanical similarity of the ovine stifle joint and the human knee [Herfat and al. 2012], the patellar tendon of the sheep can be adopted as a large animal model for human tendon disease investigation.

In our study, as previously described in a population of normal sheep [Vandeweerd and al. 2013a], the histological changes of the stifle articular cartilage differed between anatomical regions of the joint, and the proportions of defects were around 30 % of lesions identified at the medial femoral condyle and 30 % at the medial tibial condyle. In addition, a significant positive correlation between age and histological grade was identified. This indicated that our sample could be considered

representative of a normal ageing population of sheep. We also found a significant positive correlation between body weight and histological grade of cartilage. Overweight has previously been described in man as a risk factor for articular joint deterioration [Zhang and Jordan 2010; Vidal-Bralo and al.2016; Valdes and Stocks 2018].

The mean value of stiffness was 52.44N/mm (SD35.62) in our patellar tendons. Our results are quite similar to those found in a previous ex-vivo study (46-65-80 N/mm) performed in ovine patellar tendon [Kasperczyk and al. 1991].
Our study showed a positive but not significant correlation between age and tendon stiffness. A study on canine patellar tendons demonstrated progressive stiffening of connective tissues with ageing [Haut and al. 1992]. A study performed in rats showed that normal ageing altered the passive biomechanical properties of the muscle-tendon unit in Achilles tendons, with a decreased relaxation response and increased stiffness in the tendons of middle-aged animals [Plate and al. 2013].
A study conducted in New Zealand White rabbits, however, showed no evidence of age-related decline in the biomechanics of healing tendons [Dressler and al. 2006].

The association between increased tendon stiffness and ageing may have different explanations. Tendons contain tenocytes that secrete matrix components such as elastin, proteoglycans and collagen (90% collagen type I). Several of these components may be involved in tendon stiffness changes with ageing.

Two different studies hypothesized that tensile stiffness changes in tissue are most likely due to changes in higher collagen structures rather than stiffness increasing at the fibril level [Li and al. 2013; Fessel and al. 2014]. The difference in biomechanical properties between energy-storing tendons (i.e. the patellar tendon) and positional ones could also originate from a difference in the geometrical disposition of collagen within the fascicles [Shearer and al. 2017]. The compliance of energy-storing tendons may be due to the helicoidal fibril disposition of their fascicles rather than differences in their fibril Young's modulus or crimp angle. Energy-storing tendons present a less stiff interface between the tendon fascicles enabling a greater fascicle sliding. This may account eventually for increased failure strain [Thorpe et al. 2015].

Concomitantly fascicle sliding has been described to decrease with ageing [Thorpe et al. 2013]. Even if no decrease in collagen content was noted in ageing tendons, less organized collagen fibers containing an increased number of larger fibrils were observed [Gehwolf et al. 2016].

In mice, older tendons were stiffer than young tendons. It was suggested that the consequences of ageing on mechanical properties could be due to advanced glycation end products (AGEs). The level of AGEs was higher in aged mice compared to younger ones [Wood and Brooks 2016]. Denaturation and crosslinking of collagen result from the formation of AGEs. These collagen crosslinks limit fiber-fiber and fibril-fibril sliding, reduce the viscoelasticity of the tendon and increase the tendon stiffness. This may explain the increase in tendon stiffness with ageing as observed in another study conducted in rats [Gautieri et al. 2017]. Some in vitro studies [Reddy 2004] showed an association between AGEs and tendon mechanical properties. However, a clinical study conducted in man failed to associate tendon AGEs and in vivo patellar tendon mechanical properties [Eriksen and al. 2019].

Proteoglycans also are involved in viscoelastic changes in aged tendons. Decorin is the most abundant proteoglycan in the small leucine-rich proteoglycan family (SLRP) in tendons. Decorin regulates the assembly of collagen I which is the primary structural unit and transmits mechanical force [Xu and al. 2018]. The absence of decorin leads to an abnormal collagen fibrillogenesis, decreased tendon strength and stiffness [Danielson and al. 1997]. Decorin and biglycan are essential regulators of collagen fibril and matrix assembly and provide overlapping functions rather than single deficiency-related abnormalities. A study in a both decorin and biglycan gene expression knockout mouse model showed changes in structural properties as a shift to larger diameter fibrils with increased heterogeneity, and altered mechanical properties as decreased stiffness [Robinson and al. 2017]. A study carried out on old rats found decreased proteoglycan 4 and elastin mRNA expression in tendons was responsible for the increased tendon stiffness observed with ageing through reduced gliding properties of fascicular sheets [Kostrominova and Brooks 2013].

An age-associated reduction in the functional fitness and metabolism of tendon stem cells may be partially responsible for an ageing induced deterioration of the structure,

composition and mechanical properties of tendon. Some authors described ageing as an “anarchy of stem cells”, with a decrease in the number and the functional fitness of tissue-specific stem cells [Fukada and al. 2014].

A former study showed a higher stiffness in aged rat tendon-derived stem cells (TDSCs) than that of young TDSCs [Kiderlen and al. 2019].

In the current study, we observed a significant positive correlation between tendon stiffness and increasing weight in sheep. In man, higher tendon injury incidence [Kelly and al. 2001; Savarese and al. 2010] and lower patellar tendon stiffness [Tas and al. 2017] were reported in overweight and obese human individuals. Another study showed that patellar tendon stiffness was higher in males than in females, and obesity decreased patellar tendon stiffness in females contrary to males [Tas and al. 2018]. A different study reported instead that higher BMI was likely to be associated with greater tendon stiffness particularly in young men [Tomlinson and al. 2021].

Despite the possible correlations, strict comparison between species is complicated because lipid metabolism seems to be involved in tendon stiffness and this factor is different between omnivores and ruminants. A positive association between increased adiposity and tendinopathies was shown in man [Gaida and al. 2009]. A study conducted in mice observed an accumulation of lipid droplets in aged Achilles and tail tendons, with an increased expression of adipogenic markers and reduced expression of beta-catenin, the latter being a regulator of adipogenesis [Gehwolf and al. 2016].

Tendolipomatosis, may lead to tendolipomatosis-tendinopathy by lipid cell deposition in the tendon tissue [Jozsa and al. 1984; Kannus and Jozsa 1991]. Tendolipomatosis was predominantly reported in the quadriceps or patellar tendons. The lipid cells deposit in the tendon among the collagen fibers and may disrupt the cohesion of the collagen framework, thus weakening the tendon and increasing the risk of its mechanical failure. Tendon-weakening is further exacerbated in overweight or obese individuals where the larger body mass increases the mechanical loading of the tendons.

Beside the effect of local lipid cells, the metabolic effects of increased adipose tissue might be responsible for lower tendon stiffness in man. The profile of adipokines (cytokines released by adipose tissue), and other cytokines expressed in obese individuals generally indicates a pro-inflammatory state [Battery and Maffulli 2011]. Cytokines may originate from the infrapatellar fat pad [Ushiyama and al. 2003]. There is a relation between cytokines released by infrapatellar fat pad (Hoffa's fat pad) and knee osteoarthritis [Pottie and al. 2006]. A larger infrapatellar fat pad [Culvenor and al. 2011] and systemic adiposity [Gaida and al. 2009] was associated with tendinopathy [Culvenor and al. 2011].

Recently, shear wave ultrasound elastography has been evaluated to assess the mechanical properties of muscles and tendons, including stiffness, based on the speed with which induced shear waves propagate in the tissue of interest. The effect of hyperlipidemia on the patellar tendon stiffness has been investigated by this method; and a moderate positive statistically significant correlation was found between patellar tendon shear wave velocity and low-density lipoprotein independently of body mass index [Torgutalp and al. 2020].

Those various and contradictory results indicate that different variables should be considered to assess the effect of weight in a species, such as the sheep, including biomarkers of lipid metabolism. This should be taken into account in future studies. One other limitation of the current study is that we measured the stiffness over the entire bone-tendon-bone unit whilst regional variations in stiffness may occur.
However, in the scope of an ovine model of patellar tendon, this study showed that the stiffness of the healthy ovine patellar tendon increases significantly with weight. It also increases, but not significantly, with age.
Even if the parameters taken into consideration were only a part of the huge amount to address when dealing with soft tissues, this study achieved promising results in terms of characterization of biomechanical properties of healthy tendons, providing useful reference values and establishing the basis for future biomechanical tests on healing tendons in sheep. The most appropriate sheep population for those future studies would be young, non-overweight adults presenting with no lameness. Non-

invasive techniques such as shear wave ultrasound elastography warrant investigation.

CRediT author statement:

Françoise Kayser: Conceptualization, Methodology, Investigation, Formal Analysis, Validation, Writing Original Draft. **Edoardo Bori:** Investigation, Formal analysis, Validation. **Sophie Fourny:** Investigation. **Fanny Hontoir:** Investigation, Formal Analysis, Validation. **Bernardo Innocenti:** Conceptualization, Methodology, Formal analysis, Validation. **Peter Clegg:** Methodology, Validation. **Alexandra Dugdale:** Writing, Review and Editing. **Jean-Michel Vandeweerd:** Conceptualization, Methodology, Investigation, Formal analysis, Validation, Supervision

Acknowledgments: We acknowledge Vincent Simon for his help in ovine manipulation.

Disclosure of Interest: The authors report no conflict of interest.

Funding: This work was supported by the Fondation Mont Godinne; and the University of Namur (UNamur), NARILIS (Namur Research Institute for Life Science).

Ethical Approval: The experimental protocol 10150MU was approved by the local ethical committee for animal welfare in accordance with our institution guidelines and in accordance with the EU Directive 2010/63/EU.

References

ASTM International. 2003. Standard test method for tensile properties of plastics. ASTM Int. 8: 46-58

Battery L, Maffulli N. 2011. Inflammation in overuse tendon injuries. Sports Med Arthrosc Rev. 19(3):213-217. doi:10.1097/JSA.0b013e31820e6a92

Benner RW, Shelbourne KD, Urch SE, Lazarus D. 2012. Tear patterns, surgical repair, and clinical outcomes of patellar tendon ruptures after anterior

cruciate ligament reconstruction with a bone-patellar tendon-bone autograft. Am J Sports Med. 40(8):1834-1841. doi:10.1177/0363546512449815

Charousset C, Zaoui A, Bellaiche L, Bouyer B. 2014. Are multiple platelet-rich plasma injections useful for treatment of chronic patellar tendinopathy in athletes? a prospective study.Am J Sports Med. 42(4):906-911. doi:10.1177/0363546513519964

Cook JL, Hung CT, Kuroki K, Stoker AM, Cook CR, Pfeiffer FM, Sherman SL, Stannard JP. 2014. Animal models of cartilage repair. Bone Joint Res. 3(4):89-94. doi:10.1302/2046-3758.34.2000238

Culvenor AG, Cook JL, Warden SJ, Crossley KM. 2011. Infrapatellar fat pad size, but not patellar alignment, is associated with patellar tendinopathy. Scand J Med Sci Sports. 21(6)e405-411. doi:10.1111/j.1600-0838.2011.01334.x

Danielson KG, Baribault H, Holmes DF, Graham H, Kadler KE, Iozzo RV. 1997. Targeted disruption of decorin leads to abnormal collagen fibril morphology and skin fragility. J Cell Biol. 136(3):729-743. doi:10.1083/jcb.136.3.729

Dressler MR, Butler DL, Boivin GP. 2006. Age-related changes in the biomechanics of healing patellar tendon. J Biomech. 39(12):2205-2212.

doi:10.1016/j.jbiomech.2005.07.003

Eriksen CS, Svensson RB, Gylling AT, Couppé C, Magnusson SP, Kjaer M. 2019. Load magnitude affects patellar tendon mechanical properties but not collagen or collagen cross-linking after long-term strength training in older patients. BMC Geriatr. 19(1):30. doi:10.1186/s12877-019-1043-0

Fukada SI, Ma Y, Uezumi A. 2014. Adult stem cell and mesenchymal progenitor theories of aging. Front Cell Dev Biol. 2: 10. doi:10.3389/fcell.2014.00010

Fessel G, Li Y, Diederich V, Guizar-Sicairos M, Schneider P, Sell DR, Monnier VM, Snedeker JG. 2014. Advanced glycation end-products reduce collagen molecular sliding to affect collagen fibril damage mechanisms but not stiffness. PLoS One. 9(11):e110948. doi:10.1371/journal.pone.0110948

Gaida JE, Ashe MC, Bass SL, Cook JL. 2009. Is adiposity an under-recognized risk factor for tendinopathy? A systematic review. Arthritis Rheum. 61(6):840–849.

doi:10.1002/art.24518

Gaida JE, Cook J. 2011. Treatment options for patellar tendinopathy: critical review. Curr Sports Med Rep. 10(5):255-270. doi:10.1249/JSR.0b013e31822d4016

Gautieri A, Passini FS, Silvan U, Guizar-Sicairos M, Carimati , Volpi, P, Moretti M, Schoenhuber H, Redaelli A, Berli M, et al. 2017. Advanced glycation end-products: mechanics of aged collagen from molecule to tissue. Matrix Biol. 59:95-108.

doi:10.1016/j.matbio.2016.09.001

Gehwolf R, Wagner A, Lehner C, Bradshaw AD, Scharler C, Niestrawska JA, Holzapfel GA, Bauer HC, Tempfer H, Traweger A. 2016. Pleiotropic roles of the matricellular protein Sparc in tendon maturation and ageing. Sci. Rep. 6, 32635. doi 10.1038/srep32635

Haut RC, Lancaster RL, DeCamp CE. 1992. Mechanical properties of the canine patellar tendon: some correlations with age and the content of collagen. J Biomech. 25(2):163-173. doi:10.1016/0021-9290(92)90273-4

Herfat ST, Boguszewski DV, Shearn JT. 2012. Applying Simulated in vivo motions to measure human knee and ACL kinetics. Ann Biomed Eng. 40(7): 1545-1553. doi:10.1007/s10439-011-0500-5

Innocenti B, Larrieu JC, Lambert P, Pianigiani S. 2018. Automatic characterization of soft tissues material properties during mechanical tests. Muscles, Ligaments Tendons J. 7(4):529-537. doi:10.11138/mltj/2017.7.4.529

Jozsa L, Réffy A, Bálint JB. 1984. The pathogenesis of tendolipomatosis: an electron microscopical study. Int Orthop. 7(4):251–255. doi:10.1007/BF00266836

Kannus P, Jozsa L. 1991. Histopathological changes preceding spontaneous rupture of a tendon: a controlled study of 891 patients. J Bone Joint Surg Am. 73(10):1507–1525

Kasperczyk W J, Bosch U, Oestern HJ, Tscherne H. 1991. Influence of immobilization on autograft healing in the knee joint: a preliminary study in a sheep knee PCL model. Arch Orthop Trauma Surg. 110:158-161

Kayser F, Hontoir F, Clegg P, Kirschvink N, Dugdale A, Vandeweerd JM. 2019. Ultrasound anatomy of the normal stifle in the sheep. Anat Histol Embryol. 48(1):87-96. doi:10.1111/ahe.12414

Kelly BM, Rao N, Louis SS, Kostes BT, Smith RM. 2001. Bilateral, simultaneous, spontaneous rupture of quadriceps tendons without trauma in an obese patient: a case report. Arch Phys Med Rehabil. 82(3):415-418. doi:10.1053/apmr.2001.19784

Kiderlen S, Polzer C, Rädler JO, Docheva D, Clausen-Schaumann H, Sudhop S. 2019. Age related changes in cell stiffness of tendon stem/progenitor cells and a rejuvenating effect of ROCK-inhibition. Biochem Biophys Res Commun. 509 (3): 839-844.

doi:10.1016/j.bbrc.2019.01.027

Kirkendall DT, Garrett WE. 1997. Function and biomechanics of tendons. Scand J Med Sci Sports. 7:62-66. doi:10.1111/j.1600-0838.1997.tb00120.x

Kostrominova T Y, Brooks S V. 2013. Age-related changes in structure and extracellular matrix protein expression levels in rat tendons. Age (Dordr). 35(6):2203-2214. doi:10.1007/s11357-013-9514-2

Li Y, Fessel G, Georgiadis M, Snedeker JG. 2013. Advanced glycation end-products diminish tendon collagen fiber gliding. Matrix Biol. 32(3-4): 169-177.

doi:10.1016/j.matbio.2013.01.003

Little CB, Smith MM. 2008. Animal models of osteoarthritis. Current Rheumatology Reviews. 4(3):175-182. doi:10.2174/157339708785133523

Little CB, Smith MM, Cake MA, Read RA, Murphy MJ, Barry FP. 2010. The OARSI histopathology initiative - recommendations for histological assessments of osteoarthritis in sheep and goats. Osteoarthritis Cartilage. 18 Suppl 3:S80-92. doi:10.1016/j.joca.2010.04.016

Nanos KN, Malanga GA. 2015. Treatment of patellar tendinopathy refractory to surgical management using percutaneous ultrasonic tenotomy and platelet-rich plasma injection: a case presentation. PM R. 7(12):1300-1305. doi:10.1016/j.pmrj.2015.06.439

Ode GE, Piasecki DP, Habet NA, Peindl RD. 2016. Cortical button fixation: A better patellar tendon repair? Am J Sports Med. 44(10):2622-2628. doi:10.1177/0363546516651614

Peace KA, Lee JC, Healy J. 2006. Imaging the infrapatellar tendon in the elite athlete. Clin Radiol. 61(7):570-578. doi:10.1016/j.crad.2006.02.005

Plate JF, Wiggins WF, Haubruck P, Scott AT, Smith TL, Saul KR, Mannava S. 2013. Normal aging alters in vivo passive biomechanical response of the rat gastrocnemius-Achilles muscle-tendon unit. J Biomech. 46(3):450-455.

doi:10.1016/j.jbiomech.2012.11.007

Pottie P, Presle N, Terlain B, Netter P, Mainard D, Berenbaum F. 2006. Obesity and osteoarthritis: more complex than predicted! Ann Rheum Dis. 65(11):1403-1405. doi:10.1136/ard.2006.061994

Proffen BL, McElfresh M, Fleming BC, Murray MM. 2012. A comparative anatomical study of the human knee and six animal species. Knee. 19(4):493-499. doi:10.1016/j.knee.2011.07.005

Reddy GK. 2004. Cross-linking in collagen by nonenzymatic glycation increases the matrix stiffness in rabbit Achilles tendon. Exp Diabesity Res. 5(2):143-153.

doi:10.1080/15438600490277860

Robinson KA, Sun M, Barnum CE, Weiss SN, Huegel J, Shetye SS, Lin L, Saez D, Adams SM, Iozzo RV, et al. 2017. Decorin and biglycan are necessary for maintaining collagen fibril structure, fiber realignment and mechanical properties of mature tendons. Matrix Biol. 64:81-93. doi:10.1016/j.matbio.2017.08.004

Savarese E, Bisicchia S, Amendola A. 2010. Bilateral spontaneous concurrent rupture of the patellar tendon in a healthy man: case report and review of the literature. Musculoskelet Surg. 94(2):81-88. doi:10.1007/s12306-010-0077-4

Sharma P, Maffulli N. 2005. Tendon injury and tendinopathy: healing and repair. J Bone Joint Surg Am. 87(1): 187-202. doi:10.2106/JBJS.D.01850

Shearer T, Thorpe CT, Screen HRC. 2017. The relative compliance of energy-storing tendons may be due to the helical fibril arrangement of their fascicles. J R Soc Interface. 14(133):20170261. doi:10.1098/rsif.2017.0261

Tas S, Yılmaz S, Onur MR, Soylu AR, Altuntas O,Korkusuz F. 2017. Patellar tendon mechanical properties change with gender, body mass index and quadriceps femoris muscle strength. Acta Orthop Traumatol Turc. 51 (1): 54-59.
doi:10.1016/j.aott.2016.12.003

Tas S, Yilmaz S, Onur MR, Korkusuz F. 2018. Obesity decreases patellar tendon stiffness in females but not males. Orthopaedic Proceedings Vol. 99-B, No. SUPP_1.

Thorpe CT, Udeze CP, Birch HL, Clegg PD, Screen HR. 2013. Capacity for sliding between tendon fascicles decreases with ageing in injury prone equine tendons: a possible mechanism for age-related tendinopathy? Eur Cell Mater. 25: 48-60.

doi:10.22203/ecm.v025a04

Thorpe CT, Godinho MSC, Riley GP, Birch HL, Clegg PD, Screen HRC. 2015. The interfascicular matrix enables fascicle sliding and recovery in tendon, and behaves more elastically in energy storing tendons. J Mech Behav Biomed Mater. 52:85-94. doi:10.1016/j.jmbbm.2015.04.009

Tomlinson DJ, Erskine RM, Morse CI, Pappachan JM, Sanderson-Gillard E, Onambélé-Pearson GL. 2021. The combined effects of obesity and ageing on skeletal muscle function and tendon properties in vivo in men. Endocrine. 72:411-422.

doi:10.1007/s12020-020-02601-0

Torgutalp SS, Babayeva N, Tas S, Dönmez G, Korkusuz F. 2020. Effects of hyperlipidemia on patellar tendon stiffness: a shear wave elastography study. Clinical Biomechanics 75. doi:10.1016/j.clinbiomech.2020.104998

Ushiyama T, Chano T, Inoue K, Matsusue Y. 2003. Cytokine production in the infrapatellar fat pad: another source of cytokines in knee synovial fluids. Ann Rheum Dis. 62(2):108-112. doi:10.1136/ard.62.2.108

Valdes AM, Stocks J. 2018. Osteoarthritis and ageing. EMJ. 3(1):116-123.

Vandeweerd JM, Kirschvink N, Muylkens B, Depiereux E, Clegg P, Herteman N, Lamberts M, Bonnet P, Nisolle JF. 2012. A study of the anatomy and injection techniques of the ovine stifle by positive contrast arthrography, computed tomography arthrography and gross anatomical dissection. Vet J. 193(2):426-432. doi:10.1016/j.tvjl.2011.12.011

Vandeweerd JM, Hontoir F, Kirschvink N, Clegg P, Nisolle JF, Antoine N, Gustin P. 2013a. Prevalence of naturally occurring cartilage defects in the ovine knee. Osteoarthritis Cartilage. 21(8):1125-1131. doi:10.1016/j.joca.2013.05.006

Vandeweerd JM, Kirschvink N, Muylkens B, Cintas C, Catsyne CV, Hontoir F, Clegg P, Coomer R, Nisolle JF. 2013b. Magnetic resonance imaging(MRI) anatomy of the ovine stifle. Veterinary Surgery. 42(5): 551-558. doi:10.1111/j.1532-950X.2013.12026.x

Vidal-Bralo L, Lopez-Golan Y, Mera-Varela A, Rego-Perez I, Horvath S, Zhang Y, del Real A, Zhai G, Blanco FJ, Riancho JA, et al. 2016. Specific premature epigenetic aging of cartilage in osteoarthritis. Aging. 8(9):2222-2230. doi:10.18632/aging.101053

Witonski D, Keska R, Synder M, Sibinski M. 2013. An isolated medial patellofemoral ligament reconstruction with patellar tendon autograft. Biomed Res Int. 2013:637678. doi:10.1155/2013/637678

Wood LK, Brooks SV. 2016. Ten weeks of treadmill running decreases stiffness and increases collagen turnover in tendons of old mice. J Orthop Res. 34 (2): 346-353.

doi:10.1002/jor.22824

Xu SY, Liu SY, Xu L, Deng SY, He YB, Li SF, Ni GX. 2018. Response of decorin to different intensity treadmill running. Molecular Medicine Reports. 17(6): 7911-7917. doi:10.3892/mmr.2018.8802

Zhang Y, Jordan JM. 2010. Epidemiology of osteoarthritis. Clin Geriatr Med. 26(3):355-369. doi:10.1016/j.cger.2010.03.001

Arch Clin Biomed Res 2022; 6 (1): 248-259 *DOI: 10.26502/acbr.50170240*

Research Article

Correlation between Shear Wave Velocity Assessed by Elastography and Stiffness given by Tensile Test in the Ovine Patellar Tendon

Kayser F[1*], Bori E[2], Armillotta N[2], Innocenti B[3], Hontoir F[4], Vandeweerd JM[5]

[1]Centre Hospitalier Universitaire, Université Catholique de Louvain, NAMUR, site Godinne, Yvoir, Belgium
[2]Bio-Electro and Mechanical System, Université Libre de Bruxelles, Ecole Polytechnique de Bruxelles, Belgium
[3]Department of Bio-Electro and Mechanical System, Université Libre de Bruxelles, Ecole Polytechnique de Bruxelles, Belgium
[4]Namur Research Institute for Life Sciences, Integrated Veterinary Research Unit, Department of Veterinary Medicine, University of Namur, Belgium
[5]Namur Research Institute for Life Sciences, Integrated Veterinary Research Unit, Department of Veterinary Medicine, University of Namur, Belgium

***Corresponding author:** Françoise Kayser, Centre Hospitalier Universitaire, Université Catholique de Louvain, NAMUR, site Godinne, Yvoir, Belgium.

Received: 08 February 2022; **Accepted:** 15 February 2022; **Published:** 18 February 2022

Citation: Kayser F, Bori E, Armillotta N, Innocenti B, Hontoir F, Vandeweerd JM. Correlation between Shear Wave Velocity Assessed by Elastography and Stiffness given by Tensile Test in the Ovine Patellar Tendon. Archives of Clinical and Biomedical Research 6 (2022): 248-259.

Abstract

Background: Tendon injuries are very common in man, healing process often slow and incomplete, and available treatment options unsatisfactory. Mechanical properties such as stiffness can reflect the progress of tissue healing over time. Unfortunately, these measures cannot be recorded *in vivo* due to the invasive nature of the available conventional biomechanical testing methods. SWE can be used *in vivo* to investigate mechanical properties of tendons. Before clinical acceptance, SWE must be compared to tensile test values. The aim of our *ex vivo* study was to investigate whether SWE performed in vivo was correlated to stiffness assessed by an *ex vivo* uniaxial tensile test considered as gold standard.

Material and methods: Twelve patellar tendons in six healthy ewes underwent conventional ultrasound, color Doppler ultrasound and SWE *in vivo* followed by uniaxial testing performed *ex vivo*.

Results: The mean stiffness value of the 12 tendons was 45.69 N/mm (SD+/- 14.56). The mean shear wave velocity was 6.27 m/s (SD+/-0.6). There was a not statistically significant positive correlation between shear wave velocity and age (r=0.137, p=0.79), and a significant positive correlation between stiffness and SWV (r=0.87; p=0.02). Conclusion: SWE can be a surrogate to biomechanical properties of the tendon with the advantage that it can be performed *in vivo*. It could be a useful imaging tool in the context of disease progression and healing follow-up. The SWV values obtained in our study could be considered as baseline values for further research studies on patellar tendons in the ovine model.

Keywords: Patellar tendon; Sheep; Shear wave elastography; Shear wave velocity; Stiffness; Uniaxial tensile test

Abbreviations: CDUS: Color Doppler-Ultrasound; MRI: Magnetic resonance imaging; ROI: Region of interest; SE: Strain elastography; SWE: Shear wave elastography; SWV: Shear wave velocity; US: Ultrasound

1. Introduction

Tendon injuries and chronic tendinopathies occur commonly in man and are usually related to musculoskeletal pain and disability, significant morbidity and abnormal joint movement. The patellar tendon, besides the Achilles tendon and rotator cuff tendons, is often subject to tendinopathies [1]. To date, tendons are mainly evaluated clinically, by conventional Ultrasound (US), Color Doppler-ultrasound (CDUS) and Magnetic Resonance Imaging (MRI). Morphological changes of tendons such as echogenicity, homogeneity or thickness are well described by US [2]. Neovascularization in chronic tendinopathies can be documented by CDUS [3]. Inconveniently neither US and CDUS nor MRI inform on the mechanical properties of tendons. Tendon mechanical properties such as stiffness and elasticity are useful to quantify the progress of tissue healing over time. Stiffness is the ratio between the force applied to the tendon and its change in length. Elasticity, or Young's modulus, is the ratio between the stress (ratio between the force applied and the cross-sectional area) and the strain (the ratio between the change in length and the initial length). Unfortunately, these measures cannot be recorded *in vivo* due to the invasive nature of the available conventional biomechanical testing methods. Ultrasound elastography, a more recent non-invasive technique, allows the investigation of those mechanical properties by applying a force either manually (Strain Elastography, SE) or mechanically (Shear Wave Elastography, SWE). SWE enables quantitative analysis of the tendon mechanical properties by measuring the shear elastic modulus and the Shear Wave Velocity (SWV) related to tissue elasticity. Unlike SE, SWE does not require a manual intervention by the ultrasonographer to produce strain, hence limiting operator biases [4-7]. To date sonoelastography has been widely used in diagnosis and follow-up of several diseases such as breast neoplasm [8, 9], liver fibrosis [10] and thyroid neoplasm [11]. Patellar tendon [12], Achilles tendon [12] and rotator cuff tendon [2] have also been explored by SWE [13]. It is reported to be an accessible, non-invasive, easy- to-use, fast, cost-

effective, reproducible and reliable tool in clinical and research work providing quantitative data, with a high level of inter-operator agreement [4, 14]and minimal operator training. However, there is still a lack in standardization of elastography and there is no consensus about its application in tendon pathology. Animal models are required to transfer new technologies from research to clinical application [15]. The humanlike size of joints such as the knee (stifle) represents an advantage of the sheep compared to small animal models [16]. Sheep could be used to elucidate the clinical relevance and potential applications of SWE. The patellar tendon is a superficial easily accessible structure in living animals. The mechanical characteristics of the patellar tendon, such as elasticity and stiffness, are of capital importance and constitute major outcome measures in research studies.

Ultrasonographic, CT and MRI anatomy of the stifle have been described [17-19]. To date, the patellar tendon SWE properties have not been described in sheep, and there is therefore a need to document them in a population of research animals. Moreover, before clinical acceptance, the validation of SWE requires correlation to tensile test values. It is of paramount importance to establish the SWV values in normal ovine patellar tendons before using SWE in injured tendons. The aim of our *ex vivo* study was to investigate whether SWV in healthy ovine patellar tendons, determined by SWE tested *in vivo*, was correlated to stiffness assessed by an *ex vivo* uniaxial tensile test considered as gold standard.

2. Material and Methods

2.1. Animals

Six ewes (Ile de France; n= 6), from the Ovine Research Center of the University of Namur, were used. Their age ranged from 2 to 8 years. Previously to testing, the animals were kept free of movement in an outside paddock. Palpation of their stifle and locomotion were normal. No swelling, pain or lameness was observed. The experimental protocol 19006 VA was approved by the local ethical committee for animal welfare.

2.2. Ultrasound examination

Animals were hold in a sitting position, in a chair specifically designed for sheep studies (Figure 1). Before ultrasound assessment, both left and right stifles were clipped, cleaned with water and soap, and shaved. The ultrasound examinations were performed with a high- resolution US scan (RS 85 Ultrasound System, Samsung Medison Co., Ltd Seoul Korea). A generous amount of coupling gel was used to improve transmission of US waves. The ultrasound transducer was hold manually for all examinations. All investigations were made at room temperature, with the tibia and femur forming an angle of approximately 95°. The examinations were performed by a radiologist with more than 20 years of experience in musculoskeletal ultrasound. All the data were acquired on the same day.

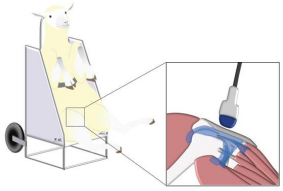


Figure 1: Study conducted with the sheep in a sitting position, hold by an abdominal strap in a dedicated chair.

2.3. 2D Ultrasound

US examination included the evaluation of the entire patellar tendon, the patellar and tibial tuberosity attachments, the adjacent cranial soft tissues and the patellar fat pad using a L3- 12A and LA4-18B linear-array transducer. Tendon echogenicity and homogeneity were assessed in transverse and longitudinal planes. Abnormalities were searched and recorded if present.

2.4. Color doppler ultrasound

Potential neovascularization, that could be a sign of tendon disorder, was assessed by CDUS, using the LA4-18B linear-array transducer, in transverse and longitudinal planes. The entire patellar tendon and the adjacent soft tissues were explored.

2.5. Shear wave elastography

2D ultrasound was used to locate the patellar tendon and align the transducer longitudinally with the tendon fibers. When a correct image of the patellar tendon, without artefacts, was obtained, the shear wave mode was activated to obtain a color-coded elastogram. Through a dual display, the fiber-transducer alignment was constantly verified. The size of the rectangular acquisition box was defined previously to the data acquisition, to maximize the amount of tissue analyzed, avoiding the tendon extremities. The diameter of the circular ROI (Region of Interest) was held constant at 0.3 cm throughout the measurements in all the limbs. The ROI was set manually and was centered on the targeted patellar tendon. SWE was assessed in a longitudinal plane, parallel to the fiber orientation, with light pressure on the skin, basically in the mid portion of the tendon, avoiding the tendon extremities, using a LA2-9A linear-array transducer. The transducer was kept motionless during 8-12 seconds to acquire the color-coded elastogram. When the color in the color- coded elastogram was uniform, the image was frozen enabling an off-line analysis through the captured images (Figure 2). Three images were captured, with 6 measurements on each. For each PT, the SWV was assessed, expressed in m/s, as well as the shear elastic modulus expressed in kPa. In our study, we considered the SWV for correlations.

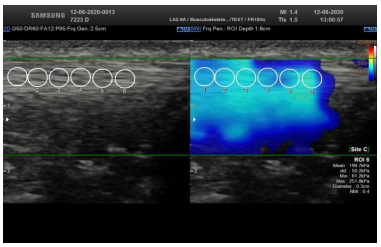


Figure 2: Dual display (left) showing a 2D ultrasound image used to locate the patellar tendon and align the tendon fibers longitudinally with the transducer. When a correct image of the patellar tendon was obtained (right), the shear wave mode was activated to obtain a color-coded elastogram. Three images were captured, with 6 measurements on each.

2.6. Gross anatomy

Animals were sacrificed by intravenous administration of pentobarbital (150 mg/kg). Both hind limbs were transected at the level of the mid-femur, immediately after death. The patellar tendon and its attachments on the patella and the tibial tuberosity were carefully dissected. The patella and tibial tuberosity were sawed at 1.5 cm from their tendon attachment in order to not affect the tendon insertion areas that are fundamental for transferring loads. Each harvested specimen consisting of an intact "patella-patellar tendon-tibial tuberosity" unit was individually wrapped in moistened gauze (with 0.9 % w/v NaCl), sealed in plastic bags, individually identified by a number and stored at -20°C until processed for biomechanical tests.

2.7. Biomechanical tests

All specimens were submitted to biomechanical tests on a same day. In six matched pairs of limbs (n=12), a uniaxial tensile test was performed on patellar tendons following a procedure described previously [20]. The frozen "patella-patellar tendon- proximal tibial" units were thawed to room temperature, cleaned thoroughly with 0.9 % w/v of NaCl solution and placed on a metal frame. The osseous parts of the specimen were cut with pliers to fit the clamp size (Figure 3). The camera was set to 100 fps. Force outputs were obtained via a dedicated 1 kN load cell (Lloyd Instruments Ltd). A series of 10 preconditioning stress-relaxation procedures were performed to obtain a good alignment of fibers prior to tensile testing since tendons had been previously manipulated and then stored at -20°C. As suggested in the ASTM D638 standard [21], the tensile test was performed with a crosshead speed of 5 mm/min. The axial force was recorded and paired with the relative displacement during the tests. The tensile test was performed until failure. The resulting force-displacement curve was analyzed. The linear region of the curve, corresponding to the elastic region, i.e., the elongation of the helical structure of collagen [22], was determined thanks to a dedicated software: a linear fitting process was used to determine the boundaries of the linear region and this latter was studied to obtain the relative stiffness of the tissue

(obtained from the slope of the curve in the selected region). Tendon stiffness, expressed in N/mm, is defined as the ratio between the force applied on the tendon and the change of the tendon length.

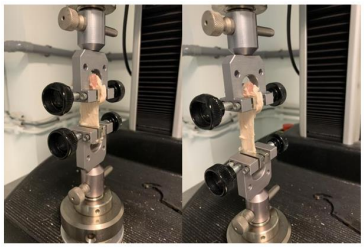


Figure 3: Patella-patellar tendon-tibial tuberosity unit fixed by two clamps. A: at the beginning of the uniaxial tensile test. B: at a more advanced phase of the uniaxial tensile test.

3. Statistical Analysis

Kolmogorov-Smirnov and Shapiro-Wilk tests were used to examine the normality of data (stiffness). Due to the normality of data, parametric tests were used. The Paired T test was used to compare observations that were not independent (difference in stiffness between left and right hindlimbs). Since there was no difference, one limb was randomly chosen within each pair and data obtained from that limb (SWV, tendon stiffness) was used for analysis. Correlations between mechanically measured SWV and tendon stiffness and age were assessed by Pearson correlation coefficient. Data were collected in Microsoft Excel and were analysed using Graph Pad Prism 8. A p-value less than 0.05 was considered to indicate a statistically significant difference.

4. Results

On ultrasound all tendons presented a homogeneous fibrillar structure. We noted no focal or global abnormal thickening. We found no abnormalities in the patellar and tibial tuberosity attachments. The cranial soft tissues adjacent to the patellar tendon and the patellar fat pad were homogeneous in all cases. No neovascularization was observed by CDUS nor in the patellar tendon neither in the adjacent soft tissues. The mean stiffness value of the 12 tendons was 45.69 N/mm (SD+/- 14.56). The tendon stiffness increased until failure. Since there was no difference in patellar tendon stiffness between left and right hindlimbs, one limb was randomly chosen within each pair and data obtained from that limb (Tendon stiffness) was used for analysis. Our tests confirmed that the patellar tendon had a typical non-linear behavior (Figure 4).

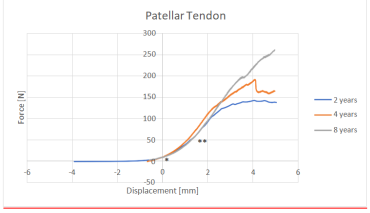


Figure 4: Force-Displacement curve in three different legs showing the initial toe region (*) and the linear region (**).

On SWE, the mean SWV value within the ROI was 6.27 m/s (SD+/-0.6).

We found a statistically not significant positive correlation between SWV and age (r=0.137, p=0.79).

Our data showed a significant positive correlation (r=0.87; p=0.02) between stiffness and SWV (Figure 5).

Correlation between shear wave velocity and stiffness

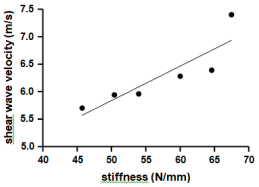


Figure 5: Correlation plot between shear wave velocity (m/s) and stiffness (N/mm). Correlation was significantly positive between shear wave velocity and stiffness.

5. Discussion

In this study the mean stiffness of patellar tendons was 45.69 N/mm (SD+/- 14.56). As previous studies were conducted in other animal models and reported only Young's modulus, our data constitute, to the best of our knowledge, the first reference values for patellar tendon stiffness in sheep. With soft tissue structures, as they are quite irregular, the estimation of the cross-sectional area during the test may be quite difficult and could induce some measure errors in the determination of the stress (ratio between the force applied and the cross-sectional area) and therefore of the Elastic Modulus. For that reason, we decided to measure the stiffness as our technique is

accurate in evaluating force and displacement. Moreover, stiffness is a structural property, i.e., a property of the tendon as a whole, while elasticity is a material property (related to the material that constitutes a structure), meaning that it could change locally and not be homogeneous along the tendon length. We found a statistically not significant positive correlation between SWV and age (r=0.137, p=0.79). This may be explained by progressive stiffening of connective tissues with ageing as shown in a study performed in canine patellar tendons [23]. Similarly, a former study showed altered passive biomechanical properties of the muscle-tendon unit in normal ageing rats, with increased stiffness and decreased relaxation response in the Achilles tendons of middle-aged animals [24]. The association between ageing and increased tendon stiffness may have different explanations. Collagen crosslinks, resulting from the formation of advanced glycation end products, limit fiber-fiber and fibril- fibril sliding, reduce the viscoelasticity of the tendon and increase the tendon stiffness [25]. Concomitantly fascicle sliding has been described to decrease with ageing [26]. The reduced gliding properties of fascicular sheets may be explained by decreased proteoglycan 4 and elastin mRNA expression in tendons [27].

In the current study, a mean value of SWV of 6.27 m/s (SD+/-0.6) was found and there was a significant positive correlation (r=0.87; p=0.02) between stiffness and SWV. A former study performed *ex vivo* in human Achilles tendon by Haen et al. demonstrated a statistical correlation between shear modulus given by SWE and elastic modulus given by tensile test [28]. Feng et al. showed a significant correlation between shear wave modulus and stiffness index obtained from a hand-held Myoton PRO device in healthy human Achilles tendon [29]. Several *ex vivo* studies performed in swine [5, 30], New Zealand white rabbits [31] and bovines [32] showed a linear correlation between SWV measured by SWE and Young's modulus given by biomechanical tests. Most studies have correlated *ex vivo* measurement of SWE to *ex vivo* biomechanical testing of dissected tendons [5, 28-32]. The originality of our study was to investigate, *in vivo*, the patellar tendon biomechanical properties and to correlate them directly to the *ex vivo* biomechanical testing of dissected bone-tendon-bone units, creating a baseline database for further research use in testing therapeutics for tendon healing.

By connecting bone to bone, the patellar tendon is different from other tendons. A greater portion of the tendon is in proximity to bony insertion sites that may result in a tendon with a greater range of stiffness values. Therefore, the tendon may be more susceptible to subtle changes in the imaging area that occur between testing sessions or trials as pointed out by Peltz et al. [6]. In the present study, the ultrasonographer was aware of ultrasonography anatomy of the ovine stifle and dedicated time to adequately position the transducer at mid-tendon, to avoid bias in measurement of the tendon SWE. However, our study has some limitations. First, though the position of the animal in the chair and the position of the limbs and instruments were held constant, since we performed the SWE in living non-sedated animals knee joint movement control was not always optimal and eventually muscle contracture may have changed slightly the flexion angle of the stifle and therefore the SWV values. Former studies reported variations of SWE measurements with knee flexion. Shear elastic modulus [33] and shear wave velocity [34] were shown to be higher in the flexed

knee. It is important to consider the conditions of measurement techniques well before any study in order to allow comparison of the results [35]. In our study we controlled the testing position as much as possible to avoid this influence, but minimal limb movement cannot be excluded. In upcoming studies, a custom-designed mold with straps to keep the limb in a fixed position could be developed. Unfortunately, all sheep do not support being constrained and sedation might be required, what could induce another bias.

Second, SWE was performed *in vivo*, in a relative static condition, opposed to the force- displacement test conducted *ex vivo*, in a non-static manner, with progressive force application. But that was precisely the objective of this study to compare non-invasive *in vivo* techniques to post-mortem *ex vivo* methods. We showed that SWV obtained in clinical condition i.e., in living animals, is correlated to SWV values obtained *ex vivo*. Similarly, Haen et al. reported that shear wave modulus in clinical-like condition was significantly correlated to shear modulus in harvested, not yet elongated Achilles tendon [28]. Third, although bone insertions were preserved for optimal tendon fixation during tensile test, a minimal slipping in the clamps may have occurred. Fourth, our study included a small number of limbs. The known wide range of normal patellar tendon shear modulus [7, 36, 37], and hence shear wave velocities, may require a larger sample to be tested in order to obtain more reliable reference values. To date, due to the subjective nature of the available common clinical evaluation methods, the success of conservative, non-conservative and rehabilitative treatments remains still controversial. Assessing healing as outcomes is important. The ovine patellar tendon could be used as a research model by creating injury either by surgery or by collagenase technique. SWE would allow a quantitative manner to track tendon stiffness changing in the healing process and assess the efficacy of novel therapies. The improved tendon mechanical properties, as measured by SWE, may be considered as an objective evaluation in tendon recovery.

Another future challenge for clinicians and researchers is the early detection of the disease that would allow effective strategies to attenuate the disease process before its chronic development. We can speculate that SWE may detect early changes in biomechanical properties related to tendinopathy, even before any changing may be diagnosed on US or CDUS. Currently, the effects of those novel management strategies on shortening or improving the healing process are based on some animal studies, as New Zealand white rabbits [38], but none have been conducted in sheep. Even if our study showed that age does not seem to have a major impact on biomechanical results, the most appropriate sheep population for those future studies would be young adults since there are indications in the scientific literature that degradation of the biomechanical properties can occur with age [25,39].

6. Conclusion

In conclusion, by assessing tendon properties, SWE may be a promising technique to improve tendon disease diagnosis and to assess progress, tendon healing and efficacy of treatments or interventions. Shear wave modulus values obtained in our study could be considered as preliminary reference values in ovine patellar tendon for further research studies.

Acknowledgments

We acknowledge V. Simon for his help. This study did benefit from a grant of the Fondation Mont Godinne and was supported by the University of Namur (UNamur), NARILIS (Namur Research Institute for Life Science) and Benetec (providing the SAMSUNG ultrasound device).

Competing interests

None of the authors of this paper has a financial or personal relationship with people or organizations that could inappropriately influence or bias the content of the paper.

References

1. Maffulli N, Wong J, Almekinders LC. Types and epidemiology of tendinopathy. Clinics in Sports Medicine 22 (2003): 675-692.
2. Davies SG, Baudouin CJ, King JB, et al. Ultrasound, computed tomography and magnetic resonance imaging in patellar tendinitis. Clinical Radiology 43 (1991): 52-56.
3. Weinberg EP, Adams MJ, Hollenberg GM. Color Doppler sonography of patellar tendinosis. American Journal of Roentgenology 171 (1998):743-744.
4. Hsiao MY, Chen YC, Lin CY, et al. Reduced patellar tendon elasticity with aging: *in vivo* assessment by Shear Wave Elastography. Ultrasound in Medicine & Biology 41 (2015): 2899-2905.
5. Zhang ZJ, Fu SN. Shear elastic modulus on patellar tendon captured from Supersonic Shear Imaging: correlation with tangent traction modulus computed from Material Testing System and test-retest reliability. PLoS One 8 (2013): 68216.
6. Peltz CD, Haladik JA, Divine G, et al. Shearwave elastography: repeatability for measurement of tendon stiffness. Skeletal Radiology 42 (2013):1151-1156.
7. Kot BCW, Zhang ZJ, Lee AWC, et al. Elastic modulus of muscle and tendon with shear wave ultrasound elastography: variations with different technical settings. PLoS One 7 (2012): 44348.
8. Song EJ, Sohn Y-M, Seo M. Tumor stiffness measured by quantitative and qualitative shear wave elastography of breast cancer. The British Journal of Radiology 91 (2018): 20170830.
9. Pesce K, Binder F, Chico MJ, et al. Diagnostic performance of shear wave elastography in discriminating malignant and benign breast lesions: Our experience with QelaXtoTM software. Journal of Ultrasound 23 (2020): 575-583.
10. Trebicka J, Gu W, de Ledinghen V, et al. Two-dimensional shear wave elastography predicts survival in advanced chronic liver disease. GUT Journal gutjnl 2020 (2021): 323419.
11. Tuan PA, Duc NM, An M, et al. The Role of Shear Wave Elastography in the Discrimination Between Malignant and Benign Thyroid Nodules. Acta Informatica Medica 28 (2020): 248-253.
12. Coombes BK, Tucker K, Vicenzino B, et al. Achilles and patellar tendinopathy display opposite changes in elastic properties: a shear wave elastography study. Scandinavian Journal of Medicine & Science in Sports 28 (2018): 1201- 1208.

13. Dirrichs T, Quack V, Gatz M, et al. Shear Wave Elastography (SWE) for the evaluation of patients with Tendinopathies. Academic Radiology 23 (2016): 1204- 1213.
14. Payne C, Watt P, Cercignani M, et al. Reproducibility of shear wave elastography measures of the Achilles tendon. Skeletal Radiology 47 (2018): 779-784.
15. Cook JL, Hung CT, Kuroki K, et al. Animal models of cartilage repair. Bone & Joint Research 3 (2014): 89-94.
16. Little CB, Smith MM. Animal models of osteoarthritis. Current Rheumatology Reviews 4 (2008): 175-182.
17. Kayser F, Hontoir F, Clegg P, et al. Ultrasound anatomy of the normal stifle in the sheep. Anatomia, Histologia, Embryologia 48 (2019): 87-96.
18. Vandeweerd JM, Kirschvink N, Muylkens B, et al. A study of the anatomy and injection techniques of the ovine stifle by positive contrast arthrography, computed tomography arthrography and gross anatomical dissection. The Veterinary Journal 193 (2012): 426-432.
19. Vandeweerd JM, Kirschvink N, Muylkens B, et al. Magnetic resonance imaging (MRI) anatomy of the ovine stifle. Veterinary Surgery 42 (2013): 551-558.
20. Innocenti B, Larrieu JC, Lambert P, et al. Automatic characterization of soft tissues material properties during mechanical tests. Muscles, Ligaments and Tendons Journal 7 (2018): 529-537.
21. ASTM D638. Standard Test Method for Tensile Properties of Plastics. ASTM Int 2014.
22. Kirkendall DT, Garrett WE. Function and biomechanics of tendons. Scandinavian Journal of Medicine & Science in Sports 7 (1997): 62-66.
23. Haut RC, Lancaster RL, DeCamp CE. Mechanical properties of the canine patellar tendon: some correlations with age and the content of collagen. Journal of Biomechanics 25 (1992): 163-173.
24. Plate JF, Wiggins WF, Haubruck P, et al. Normal aging alters *in vivo* passive biomechanical response of the rat gastrocnemius-Achilles muscle-tendon unit. Journal of Biomechanics 46 (2013): 450-455.
25. Gautieri A, Passini FS, Silvan U, et al. Advanced glycation end-products: Mechanics of aged collagen from molecule to tissue. Matrix Biology 59 (2017): 95-108.
26. Thorpe CT, Udeze CP, Birch HL, et al. Capacity for sliding between tendon fascicles decreases with ageing in injury prone equine tendons: a possible mechanism for age- related tendinopathy? European Cells & Materials 25 (2013): 48-60.
27. Kostrominova TY, Brooks SV. Age-related changes in structure and extracellular matrix protein expression levels in rat tendons. Age 35 (2013): 2203-2214.
28. HaenT-X, Roux A, Soubeyrand M, et al. Shear waves elastography for assessing of human Achilles tendon's biomechanical properties: an experimental study. Journal of the Mechanical Behavior of Biomedical Materials 69 (2017): 178-184.
29. Feng YN, Li YP, Liu CL, et al. Assessing the elastic properties of skeletal muscle and tendon using shearwave ultrasound

elastography and MyotonPRO. Scientific Reports 8 (2018): 17064.

30. Hsiao YY, Yang TH, Chen PY, et al. Characterization of the extensor digitorum communis tendon using high-frequency ultrasound shear wave elastography. Medical Physics 47 (2020): 1609-1618.
31. Martin JA, Biedrzycki AH, Lee KS, et al. *In vivo* measures of shear wave speed as a predictor of tendon elasticity and strength. Ultrasound in Medicine & Biology 41 (2015): 2722-2710.
32. Rosskopf AB, Bachmann E, Snedeker JG, et al. Comparison of shear wave velocity measurements assessed with two different ultrasound systems in an *ex-vivo* tendon strain phantom. Skeletal Radiology 45 (2016): 1541-1551.
33. Hardy A, Rodaix C, Vergari C, et al. Normal range of patellar tendon elasticity using the sharewave elastography technique: an *in vivo* study in normal volunteers. Surgical Technology International 31 (2017): 227-230.
34. Kuervers EJ, Firminger CR, Edwards WB. Effect of knee angle and Quadriceps muscle force on Shear-Wave Elastography measurements at the Patellar Tendon. Ultrasound in Medicine & Biology 47 (2021): 2167-2175.
35. Yu M, Wu J, Hou J, et al. Young's Modulus of Bilateral Infraspinatus Tendon Measured in Different Postures by Shear Wave Elastography Before and After Exercise. Journal of Orthopaedic Surgery 13 (2021): 1570–1578.
36. Zhang ZJ, Ng GYF, Fu SN. Effects of habitual loading on patellar tendon mechanical and morphological properties in basketball and volleyball players. European Journal of Applied Physiology 115 (2015): 2263-2269.
37. Mannarino P, Lima KMM, Fontenelle CRC, et al. Analysis of the correlation between knee extension torque and patellar tendon elastic property. Clinical Physiology and Functional Imaging 38 (2018): 378-383.
38. Chiu YH, Chang KV, Chen IJ, et al. Utility of sonoelastography for the evaluation of rotator cuff tendon and pertinent disorders: a systematic review and meta-analysis. European Radiology 30 (2020): 6663-6672.

This article is an open access article distributed under the terms and conditions of the Creative Commons Attribution (CC-BY) license 4.0